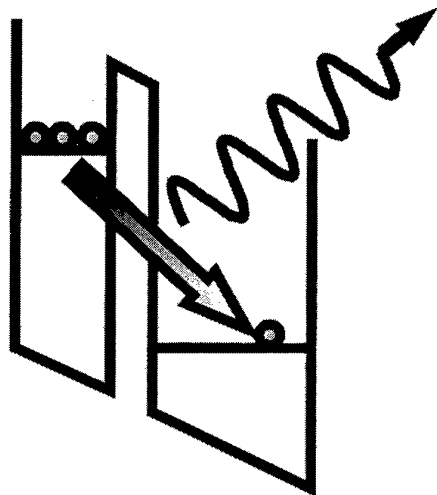


# **5th International Conference on Intersubband Transitions in Quantum Wells**

## **ITQW'99**

### **Program and Abstracts**



**7 - 11 September 1999**

**Bad Ischl, Austria**

#### **Sponsors:**

OÖ Landesregierung

GMe

ONRIFO

European Research Office, US Army

Bruker Optik

20010430 054

**REPORT DOCUMENTATION PAGE**

Form Approved OMB No. 0704-0188

Public reporting burden for this collection of information is estimated to average 1 hour per response, including the time for reviewing instructions, searching existing data sources, gathering and maintaining the data needed, and completing and reviewing the collection of information. Send comments regarding this burden estimate or any other aspect of this collection of information, including suggestions for reducing this burden to Washington Headquarters Services, Directorate for Information Operations and Reports, 1215 Jefferson Davis Highway, Suite 1204, Arlington, VA 22202-4302, and to the Office of Management and Budget, Paperwork Reduction Project (0704-0188), Washington, DC 20503.

1. AGENCY USE ONLY (Leave blank)		2. REPORT DATE  1999	3. REPORT TYPE AND DATES COVERED  Conference Proceeding
4. TITLE AND SUBTITLE  5 <sup>th</sup> International Conference on Intersubband Transitions in Quantum Wells. ITWQW'99. Program and Abstracts. 7-11 September 1999, Bad Ischl, Austria.			5. FUNDING NUMBERS  N00014-99-1-1049
6. AUTHOR(S)  Multiple			
7. PERFORMING ORGANIZATION NAME(S) AND ADDRESS(ES)			8. PERFORMING ORGANIZATION REPORT NUMBER
9. SPONSORING/MONITORING AGENCY NAME(S) AND ADDRESS(ES)  Office of Naval Research International Field Office PSC 802 Box 39 FPO AE 09499-0039			10. SPONSORING/MONITORING AGENCY REPORT NUMBER
11. SUPPLEMENTARY NOTES  This work relates to Department of Navy Grant N00014-99-1-1049 issued by the Office of Naval Research-Europe. The United States has a royalty free license to exercise all rights under the Copyright claimed herein for Government Purposes.			
12a. DISTRIBUTION/AVAILABILITY STATEMENT  Approved for Public Release; Distribution Unlimited. Government Purpose Rights License. All other rights reserved by the copyright holders.			12b. DISTRIBUTION CODE  A
12. ABSTRACT (Maximum 200 words)  5 <sup>th</sup> International Conference on Intersubband Transitions in Quantum Wells. ITWQW'99. Program and Abstracts. 7-11 September 1999, Bad Ischl, Austria. The scope of the conference will cover all phenomena related to intersubband transitions in quantum wells, wires and dots, both basic and applied, the relevant spectral range thus extending from 2 to 200 um. Special emphasis is put on the recent developments in mid-infrared intersubband lasers. In a addition, a session on Bloch oscillations in superlattices and other THz phenomena is included.  Conference Topics are: Intersubband emission and lasers; Quantum well infrared detectors (QWIPs); Nonlinear and coherent optical effects; Collective and many-body effects; Intersubband relaxation; Intersubband transitions in quantum wires and dots; Bloch oscillations in superlattices and other THz phenomena; Intersubband transitions in novel materials.			
14. SUBJECT TERMS  Abstracts, lasers, infrared detectors			15. NUMBER OF PAGES
			16. PRICE CODE
17. SECURITY CLASSIFICATION OF REPORT  UNCLASSIFIED	18. SECURITY CLASSIFICATION OF THIS PAGE  UNCLASSIFIED	19. SECURITY CLASSIFICATION OF ABSTRACT  UNCLASSIFIED	20. LIMITATION OF ABSTRACT  UL

NSN 7540-01-280-5500

Standard Form 298 (Rev. 2-89)  
Prescribed by ANSI Std. Z39-18  
298-102

**5th International Conference  
on  
Intersubband Transitions in Quantum Wells**

**ITQW'99**

**Conference Chairs:**

**Manfred Helm, *University of Linz, Austria***  
**Karl Unterrainer, *Technical University Vienna, Austria***

**CONFERENCE VENUE:**

Kurhotel Bad Ischl  
Vogelhuberstrasse 10  
A-4820 Bad Ischl, Austria  
Tel: ++43 6132 204  
Fax: ++43 6132 27682  
E-mail:  
kurhotel.badischl@tourism.co.at

**CONFERENCE CONTACT:**

Klaus Rabeder  
Institut für Halbleiterphysik  
Universität Linz  
A-4040 Linz, Austria  
Fax: ++43 732 2468-650  
E-mail:  
k.rabeder@hlphys.uni-linz.ac.at

**CONFERENCE HOMEPAGE:**

<http://www.hlphys.uni-linz.ac.at/hl/itqw1999.htm>

**The organizers gratefully acknowledge substantial financial support  
by:**

Province Government of Upper Austria (Amt der OÖ Landesregierung), Linz, Austria  
Society for Microelectronics (Gesellschaft für Mikroelektronik), Wien, Austria  
Office of Naval Research International Field Office (ONRIFO) - Europe, London, U.K.  
European Research Office of the US Army (USARDSG), London, U.K.  
Bruker Optik GmbH, Karlsruhe, Germany  
Upper Austrian Tourism Board (Tourismusverband OÖ), Austria

This work relates to Department of the Navy Grant N00014-99-1-1049 issued by the Office of Naval Research International Field Office - Europe. The United States has a royalty-free license throughout the world in all copyrightable material contained herein.  
The content does not necessarily reflect the position or the policy of the United States Government.

AQ FOI-07-1421

**PROGRAM COMMITTEE:**

M. Helm, University of Linz, Austria (chair)  
K. Unterrainer, TU Vienna, Austria (co-chair)  
J. Faist, Université de Neuchâtel, Switzerland  
F. Julien, Université de Paris-Sud, Orsay, France  
H. C. Liu, NRC, Ottawa, Canada  
A. Sa'ar, Hebrew University, Jerusalem, Israel  
M. S. Sherwin, UCSB, Santa Barbara, CA, USA

**ADVISORY COMMITTEE:**

F. Capasso, Lucent Technologies, Murray Hill, USA  
E. Ehrenfreund, Technion, Haifa, Israel  
S. Gunapala, JPL, Pasadena, CA, USA  
S. S. Li, University of Florida, USA  
H. Ohno, Tohoku University, Sendai, Japan  
H. Schneider, IAF, Freiburg, Germany  
Y. K. Su, National Cheng-Kung University, Tainan, Taiwan

**ORGANIZING COMMITTEE:**

M. Helm, University of Linz, Austria  
K. Unterrainer, TU Vienna, Austria

**LOCAL ORGANIZATION:**

Klaus Rabeder, University of Linz, Austria  
Karin Hammerschmid, University of Linz, Austria  
Eva Scharber, TU Vienna, Austria

## GENERAL INFORMATION

### INTRODUCTION AND SCOPE:

The ITQW'99 is the 5th in a series which started in Cargese, Corsica, France in 1991 and has been successfully continued in Whistler, Canada (1993), Ginosar, Israel (1995) and Tainan, Taiwan (1997). Its scope will cover all phenomena related to intersubband transitions in quantum wells, wires and dots, both basic and applied, the relevant spectral range thus extending from 2 to 200  $\mu\text{m}$ . Special emphasis is put on the recent developments in mid-infrared intersubband lasers. In addition, a session on Bloch oscillations in superlattices and other THz phenomena is included.

### TOPICS:

- Intersubband emission and lasers
- Quantum well infrared detectors (QWIPs)
- Nonlinear and coherent optical effects
- Collective and many-body effects
- Intersubband relaxation
- Intersubband transitions in quantum wires and dots
- Bloch oscillations in superlattices and other THz phenomena
- Intersubband transitions in novel materials.

### LOCATION:

The conference takes place in the Kurhotel Bad Ischl in the province of Upper Austria. Bad Ischl is a small town in the heart of the Salzkammergut in the province Upper Austria, an area with lakes and mountains which is famous for its scenic beauty. Bad Ischl is known for having been the summer residence of the Habsburg emperor Franz-Joseph, whose villa can still be visited today. Bad Ischl has a nice town center with a promenade along the river Traun. If you enjoy eating cakes, we recommend you a visit in the traditional Café-Konditorei Zauner right downtown. If the weather is warm enough you can enjoy having a drink or dinner in one of the many outside cafés and restaurants in town.

The area offers possibilities for many activities such as mountain hiking or swimming in the nearby lakes. (If you go hiking, we advise you to wear proper shoes). If you have some extra time before or after the conference, we recommend you to visit some of the nearby sightseeing spots as there are the salt mines in Bad Ischl or Hallstatt (the site of the conference excursion), the Dachstein mountain with its famous caves (an ice cave among others) or the city of Salzburg (60 km from Bad Ischl). Hallstatt and Salzburg have been declared to World Cultural Heritage by UNESCO. In Linz (100 km) there is the classical music "Bruckner Festival" being held, starting with a spectacular open-air "sound cloud" (Bruckner's 3rd symphony) at the banks of the river Danube on Sept., 12. Before and during the conference (4 - 10 Sept.) the "Ars Electronica" festival takes place in Linz, devoted to connecting modern technology with the arts.

### TRAVEL:

The closest international airports are Salzburg (60 km), Linz (100 km), Munich (200 km), and Vienna (300 km). From Salzburg and Linz there are several daily scheduled flights to Frankfurt and Zurich, from Munich and Vienna to many other international destinations. From all four cities there are train connections to Bad Ischl, but you may have to change trains in Salzburg, Linz, or Attnang-Puchheim. There is a regular bus service from Bad Ischl to Salzburg (90 minutes). The conference hotel is within walking distance from the Bad Ischl railway station.

### CLIMATE:

The weather in Austria in early September is very changeable, with rain or sunshine. The daytime high temperature can lie anywhere between 15 and 25 degrees C (59 to 77 degrees Fahrenheit), with night-time lows down to 10 C (50 F). To bring a sweater and raincoat is thus recommended.

### REGISTRATION:

The registration fee was ATS 3500 before August 1, 1999, and is ATS 4000 after this date or on site. No personal checks or credit cards are accepted. The fee includes the abstract booklet, welcome reception, coffee breaks, conference dinner, excursion, and the proceedings. Please pick up your conference materials at the registration desk on Tuesday between 4 and 8 p.m. or Wednesday morning. Please notify us upon arrival, whether you will take part in the conference banquet.

**ACCOMMODATION:**

More than half of the participants stay in the "Kurhotel" at a rate of ATS 770 (single) or 620 (double) per person and night including breakfast. Most of the other hotels and pensions are within walking distance of the conference site. Guests of the Kurhotel can enjoy swimming in the indoor and outdoor pools (partly salt water) or use the sauna free of charge.

**LUNCH:**

We have arranged that all participants can have lunch together at the "Kurhotel" Wednesday and Friday. On Thursday, before the departure for the conference excursion, lunch boxes will be handed out.

**MANUSCRIPTS:**

Please submit your manuscript (3 copies plus original figures plus floppy disk) when you register on Tuesday or Wednesday morning at the conference desk. Please don't forget to fill in the "length calculation form" and submit it together with your paper. 4 printed pages are allowed for contributed talks and posters, 8 pages for invited talks. On Wednesday afternoon manuscripts will be handed out to the referees, who are asked to return them until Friday. The proceedings will be published as a special issue of the journal "Physica E (Low-Dimensional Systems & Nanostructures)" by Elsevier in May 2000.

**TALKS:**

A total of 20 minutes (15 min talk plus 5 min discussion) is allotted to each contributed talk, and 30 minutes (25 + 5 min) for the invited talks. If you need equipment other than an overhead projector, please contact the organizers.

**POSTERS:**

There will be two poster sessions, on Wednesday afternoon and Friday afternoon. The available space for each poster is 120 (width) × 150 cm (height). Please mount your poster already Wednesday morning or Friday morning, respectively, to allow for discussion also during the coffee breaks.

**CONFERENCE EXCURSION:**

We intend to visit the village of Hallstatt, a UNESCO world cultural heritage. Main attractions are a salt mine located some 500 m above the village on the mountain slope (accessible by ropeway plus 30 min walk), from where a marvellous view of the surrounding lakes and mountains can be enjoyed. Also we will pass by a prehistoric burial ground, dating from 800 to 400 BC, a time when Hallstatt was an eminent settlement.

There will be two buses for the excursion leaving in front of the Kurhotel on Thursday at 1:30 p.m. We will return in time to give enough time for dinner before the evening session.

**CONFERENCE BANQUET:**

The conference banquet will take place on Friday in the famous Hotel-Restaurant "Weisses Rössl" in the center of St. Wolfgang, directly at the waterfront of the "Wolfgangsee". This restaurant actually gave the name to an operetta by the composer Ralph Benatzky. Two buses will leave for St. Wolfgang on Friday at 17:15. After arrival there, you will have some time to enjoy a walk through the village (in particular, we recommend you to visit the church of St. Wolfgang with the marvelous wood-carved altar by Michael Pacher from the 15th century), before the banquet starts at 7 p.m. The two buses will bring us back to Bad Ischl at 10 p.m.

Please notify us upon your arrival, whether or not you will take part in the conference banquet.

**CURRENCY EXCHANGE:**

There are several banks in downtown Bad Ischl (opening hours mostly 8 a.m. - 12 p.m. and 2 p.m. - 4 p.m., Monday to Friday) You also might be able to change at the hotel reception of the Kurhotel. Some cash machines in the town may accept international bank cards or credit cards.

# SCIENTIFIC PROGRAM

**Tuesday, 7 Sept. 1999**

16:00 - 20:00 **Registration**

18:00 - 20:00 **Welcome reception**

**Wednesday, 8 Sept. 1999**

## **Wednesday morning 1: Quantum cascade lasers**

8:45 - 9:00 **Conference Opening, Welcome Address**

9:00 - 9:30 **Quantum cascade microdisk lasers (invited)**

W1 Claire Gmachl, F. Capasso, E. E. Narimanov, D. L. Sivco, J. N. Baillargeon, A. Y. Cho, J. Faist, J. U. Nöckel, A. D. Stone, *Lucent Technologies, USA*

9:30 - 9:50 **Superlattice quantum cascade lasers**

W2 A. Tredicucci, F. Capasso, C. Gmachl, D. L. Sivco, A. L. Hutchinson, A. Y. Cho, *Lucent Technologies, USA*

9:50 - 10:10 **Theoretical study of SL quantum cascade lasers**

W3 F. Compagnone, S. Tortora, A. Di Carlo, P. Lugli, *Univ. Roma, Italy*

10:10 - 10:30 **High-power, long-wavelength ( $\lambda=10.2\ \mu\text{m}$ ) distributed feedback quantum cascade laser fabricated without epitaxial re-growth**

W4 D. Hofstetter, J. Faist, M. Beck, U. Oesterle, A. Müller, *Univ. Neuchatel, Switzerland*

10:30 - 11:00 **Coffee Break**

## **Wednesday morning 2: Quantum dots**

11:00 - 11:30 **Quantum dot infrared photodetectors in new material systems (invited)**

W5 E. Finkman, S. Maimon, V. Immer, G. Bahir, S. E. Schacham, *Technion, Israel*, O. Gauthier-Lafaye, S. Herriot, F. H. Julien, *Univ. Paris-Sud, France*, M. Gendry, J. Brault, *Ecole Central Lyon, France*

11:30 - 11:50 **Bound-to-continuum intersubband transition in self-assembled InAs quantum dots and its application to mid-infrared photodetectors**

W6 S.-W. Lee, K. Hirakawa, Y. Shimada, *IIS, Univ. Tokyo, Japan*

11:50 - 12:10 **Optically detected intraband resonances in InGaAs/GaAs quantum wells and dots**

W7 B. N. Murdin, A. R. Hollingworth, *Univ. Surrey, U.K.*, C. R. Pidgeon, P. C. Findlay, *Heriot-Watt-Univ., U.K.*, J.-P. Wells, I. V. Bradley, G. M. H. Knippels, *FOM Inst. Rijnhuizen, The Netherlands*, R. Murray, *Imperial College, U.K.*

12:10 - 12:30 **Femtosecond mid-infrared study of carrier dynamics in self-organized InAs/InAlAs quantum dots**

W8 E. Peronne, J. F. Lampin, A. Alexandrou, *ENSTA - Ecole Polytechnique*, O. Gauthier-Lafaye, F. H. Julien, *IEF, Univ. Paris-Sud*, J. Brault, M. Gendry, *Ecole Centrale Lyon, France*

12:30 - 12:50 **Intersubband photocurrent spectroscopy on self-assembled Ge quantum dots on Si**

W9 C. Miesner, O. Röthig, K. Brunner, G. Abstreiter, *WSI, TU München, Germany*

13:00 Lunch

15:00 - 16:00 **Poster session 1**

### **Wednesday afternoon: THz emission, intersubband relaxation**

16:00 - 16:20 **Temperature dependence of THz GaAs and InGaAs quantum cascade light emitting diodes**  
W10 M. Rochat, J. Faist, M. Beck, *Univ. Neuchatel, Switzerland*, U. Oesterle, M. Illegems, *EPFL, Switzerland*

16:20 - 16:40 **Narrow linewidth THz intersubband emission from three-level multiple QW structures**  
W11 B. S. Williams, B. Xu, Q. Hu, *MIT*, M. R. Melloch, *Purdue Univ., USA*

16:40 - 17:00 **Parabolic quantum wells and quantum cascade structures as electrically driven THz-sources**  
W12 J. Ulrich, R. Zobl, K. Unterrainer, G. Strasser, E. Gornik, *TU Wien, Austria*

17:00 - 17:20 **Resonant tunneling and intersubband population inversion effects in asymmetric wide quantum well structures**  
W13 V.N. Murzin, Yu.A. Mityagin, V.A. Chuenkov, A.L. Karuzskii, A.V. Perestotinin, L.Yu. Shchurova, *Lebedev Inst., Russia*

17:20 - 17:40 Short break

17:40 - 18:00 **Intersubband relaxation due to electron-electron scattering in quantum well structures**  
W14 K. Kempa, P. Bakshi, *Boston College, USA*

18:00 - 18:20 **The intra- and inter-subband relaxation of nonequilibrium electron populations in wide semiconductor quantum wells**  
W15 S.-C. Lee, I. Galbraith, *Heriot-Watt University, U.K.*

18:20 - 18:40 **Monte Carlo modeling of far-infrared intersubband lasers**  
W16 R. W. Kelsall, P. Kinsler, P. Harrison, *Univ. Leeds, U.K.*

### **Thursday, 9 Sept. 1999**

#### **Thursday morning 1: Bloch oscillations**

8:30 - 9:00 **Coherent dynamics of photoexcited semiconductor superlattices with applied homogeneous electric fields (invited)**  
T1 T. Meier, P. Thomas, S. W. Koch, *Philipps University Marburg, Germany*

9:00 - 9:30 **Terahertz conductance of electrically biased Bloch oscillating superlattices: towards a solid state Terahertz oscillator (invited)**  
T2 J. S. Scott, M. C. Wanke, S. J. Allen, K. Maranowski, A. C. Gossard, *UC Santa Barbara*, D. H. Chow, *HRL Labs, USA*

9:30 - 9:50 **Interminiband spectroscopy of biased superlattices**  
T3 M. Helm, W. Hilber, *Univ. Linz, Austria*, G. Strasser, *TU Wien, Austria*, R. DeMeester, F. M. Peeters, *UIA, Belgium*, A. Wacker, *TU Berlin, Germany*



9:50 - 10:10 **Coherent Bloch oscillations in GaAs/AlGaAs superlattices**  
T4 T. Dekorsy, M. Först, G. Segschneider, A. Bartels, H. Kurz, *RWTH Aachen, Germany*,  
A. Ghosh, L. Jönsson, J. W. Wilkins, *Ohio State Univ., USA*, K. Köhler, *IAF, Germany*,  
R. Hey, K. Ploog, *PDI, Germany*

10:10 - 10:30 **Generation and manipulation of Bloch wave packets**  
T5 F. Löser, M. Sudzius, C. P. Hofeld, V. G. Lyssenko, K. Leo, *TU Dresden, Germany*,  
Y. Kosevich, *MPI-PKS, Germany*, M. M. Dignam, *Lakehead Univ., Canada*, K. Köhler,  
*IAF, Germany*

10:30 - 11:00 Coffee Break

## Thursday morning 2: QWIPs

11:00 - 11:30 **QWIP FPAs for high-performance thermal imaging (invited)**  
T6 H. Schneider, M. Walther, J. Fleißner, C. Schönbein, R. Rehm, W. Pletschen, E. Diwo,  
K. Schwarz, J. Braunstein, P. Koidl, *Fraunhofer-Institut für Angewandte*  
*Festkörperphysik*, J. Ziegler, W. Cabanski, *AEG, Germany*

11:30 - 11:50 **Recent developments and applications of quantum well infrared**  
T7 **photodetector focal plane arrays**  
S.D. Gunapala, S.V. Bandara, *Jet Propulsion Lab, USA*

11:50 - 12:10 **New designs and applications of corrugated QWIPs**  
T8 K. K. Choi, A. C. Goldberg, *US Army Research Lab, USA*, C. J. Chen, L. P. Rokhinson,  
D. C. Tsui, *Princeton Univ. USA*, N. C. Das, A. La, *NASA Goddard Space Flight Center,*  
*USA*

12:10 - 12:30 **Optical interference and nonlinearities in quantum well infrared**  
T9 **photodetectors**  
M. Ershov, A. G. U. Perera, V. Letov, S. G. Matsik, W. Z. Shen, *Georgia State Univ.,*  
*USA*, H. C. Liu, M. Buchanan, Z. R. Wasilewski, *NRC, Canada*

12:30 - 12:50 **Monte Carlo particle modeling of electron transport and capture**  
T10 **processes in AlGaAs/GaAs MQW photodetectors**  
M. Ryzhii, V. Ryzhii, *Univ. Aizu, Japan*

13:30 - 18:30 Conference excursion (with lunch boxes)

## Thursday Evening: Coherent and nonlinear effects

20:00 - 20:30 **Quantum interference phenomena in electron intersubband transitions**  
T11 W. Pötz, *University of Illinois at Chicago, USA*

20:30 - 21:00 **Observation of electromagnetically induced transparency in a three-**  
T12 **subband semiconductor quantum well (invited)**  
C. C. Phillips, E. Paspalakis, G. B. Serapiglia, C. Sirtori, K. L. Vodpyanov, *Imperial*  
*College, U.K.*

21:00 - 21:20 **Quantum computation with quantum dots and THz cavity quantum**  
T13 **electrodynamics**  
M. S. Sherwin, A. Imamoglu, *UC Santa Barbara, USA*

21:20 - 21:40 **Second-harmonic generation in InAs/GaAs self-assembled quantum**  
T14 **dots**  
T. Brunhes, P. Boucaud, S. Sauvage, I. F. Glotin, R. Prazeres, J.-M. Ortega, *Univ.*  
*Paris-Sud*, A. Lemaître, J.-M. Gérard, *CNET*, V. Thierry-Mieg, *CNRS, France*

21:40 - 22:00 **Intersubband electro-absorption and retardation in coupled quantum wells: the role of interface scattering**  
T15 R. Kapon, N. Cohen, V. Thierry-Mieg, R. Planel, A. Sa'ar, *Hebrew Univ., Israel & CNRS, France*

## Friday, 10 Sept. 1999

### Friday morning 1: GaAs quantum cascade lasers

- 9:00 - 9:30 **GaAs quantum cascade lasers (invited)**  
F1 C. Sirtori, P. Kruck, S. Barbieri, M. Beck, P. Collot, J. Faist, J. Nagle, *Thomson-CSF, France*
- 9:30 - 10:00 **Intersubband and interminiband GaAs/AlGaAs quantum cascade lasers (invited)**  
F2 G. Strasser, S. Gianordoli, L. Hvozda, W. Schrenk, K. Unterrainer, E. Gornik, *TU Vienna, Austria*
- 10:00 - 10:20 **Spectroscopic studies of GaAs/AlGaAs quantum cascade structures**  
F3 L. R. Wilson, P. T. Keightley, J. W. Cockburn, J. P. Duck, M. S. Skolnick, *Univ. Sheffield, U.K.*
- 10:20 - 10:50 Coffee Break

### Friday morning 2: Antimonides, new materials

- 10:50 - 11:20 **Interband cascade lasers (invited)**  
F4 Rui Q. Yang, J. D. Bruno, J. L. Bradshaw, J. T. Pham, D. E. Wortman, *US Army Research Lab, USA*
- 11:20 - 11:40 **Antimonide interband and intersubband mid-IR and THz lasers**  
F5 I. Vurgaftman, C. L. Felix, W. W. Bewley, E. H. Aifer, L. J. Olafson, D. W. Stokes, J. R. Meyer, M. J. Yang, *Naval Research Lab, H. Lee, Sarnoff, USA*
- 11:40 - 12:00 **Mid-infrared intersubband electroluminescence in InAs/GaSb/AlSb type-II cascade structures**  
F6 K. Ohtani, H. Ohno, *Tohoku University, Sendai, Japan*
- 12:00 - 12:20 **Intersubband transitions for optical communication devices in novel InGaAs-AlAsSb quantum well structures**  
F7 A. Neogi, H. Yoshida, T. Mozume, N. Georgiev, O. Wada, *FESTA, Japan*
- 12:20 - 12:40 **Investigation of mid-infrared intersubband transitions in modulation doped CdS/ZnSe quantum wells**  
F8 M. Göppert, R. Becker, A. Dinger, S. Petillon, C. Maier, M. Grün, C. F. Klingshirn, *Univ. Karlsruhe, Germany*
- 12:50 Lunch
- 14:00 - 15:00 **Poster session 2**

## Friday afternoon: Many-body effects

- 15:00 - 15:30 **Intersubband excitations in low dimensional semiconductor structures (invited)**  
F9 S. Das Sarma, *University of Maryland, USA*
- 15:30 - 16:00 **Collective effects in intersubband transitions (invited)**  
F10 R. J. Warburton, C. Jabs, K. Weillhammer, J. P. Kotthaus, M. Thomas, H. Kroemer, *LMU Munich, Germany*
- 16:00 - 16:20 **Direct observation of dynamical screening of the intersubband resonance**  
F11 S. Graf, H. Sigg, *PSI, Switzerland*, K. Köhler, *IAF, Germany*, W. Bächtold, *ETH, Switzerland*
- 16:20 - 16:40 **Many-body effects in the intersubband resonance of in-plane localized electron systems**  
F12 C. Metzner, G. H. Döhler, *Universität Erlangen, Germany*
- 17:15 **Departure for St. Wolfgang**
- 19:00 - 22:00 **Conference banquet at the "Weisses Rössl", St. Wolfgang**

## Saturday, 11 Sept. 1999

### Saturday morning 1: Optical excitation

- 9:00 - 9:30 **High-power tunable quantum fountain unipolar lasers (invited)**  
S1 O. Gauthier-Lafaye, B. Seguin-Roa, F. H. Julien, P. Collot, *Univ. Paris-Sud, France*, C. Sirtori, J. Y. Duboz, *Thomson-CSF, France*, G. Strasser, *TU Wien, Austria*
- 9:30 - 9:50 **Emission of mid-infrared radiation and intersubband population inversion in near-infrared laser QW structures**  
S2 L. E. Vorobjev, D. A. Firsov, V. A. Shalygin, *St. Petersburg State Tech. Univ., Russia*, Zh. I. Alferov, N. N. Ledentsov, V. M. Ustinov, Yu. M. Shernyakov, *Ioffe Inst., Russia*, V. N. Tulupenko, *Donbass State Eng. Acad., Ukraine*
- 9:50 - 10:10 **Modulated resonant Raman and photoluminescence spectroscopy of Bragg confined asymmetric quantum wells**  
S3 M. Levy, R. Kapon, A. Sa'ar, R. Beserman, *Technion & Hebrew Univ., Israel*, V. Thierry-Mieg, R. Planel, *CNRS, France*
- 10:10- 10:40 Coffee Break

### Saturday morning 2: Ultrafast phenomena

- 10:40 - 11:10 **Ultrafast dynamics of intersubband excitations (invited)**  
S4 T. Elsaesser, R. A. Kaindl, S. Lutgen, M. Woerner, *Max-Born-Institut, Germany*
- 11:10 - 11:30 **Hole-burning in inhomogeneously broadened intersubband absorption bands of quantum well structures**  
S5 A. Seilmeier, S. R. Schmidt, J. Kaiser, *Universität Bayreuth, Germany*

- 11:30 - 11:50 **Time resolved intersubband optical transitions in resonantly optically pumped semiconductor lasers - gain from correlated electron and hole plasmas**  
S6  
I. Shtrichman, U. Mizrahi, D. Gershoni, E. Ehrenfreund, *Technion, Israel*,  
K. Maranowski, A. C. Gossard, *UCSB, USA*
- 11:50 - 12:10 **Time-resolved intersubband spectroscopy of semiconductor nanostructures**  
S7  
R. Bratschitsch, R. Kersting, T. Müller, G. Strasser, K. Unterrainer, W. Fischler,  
J. N. Heyman, *TU Vienna, Austria*
- 12:10 - 12:20 **Conference closing**

## POSTERS

### Poster session 1 (Wednesday, 8 Sept., 15:00 - 16:00)

#### QWIPs:

- PW1 **Noise current investigations of g-r-noise limited and shot-noise limited QWIPs**  
R. Rehm, H. Schneider, C. Schönbein, M. Walther, *Fraunhofer Institut für Angewandte Festkörperphysik, Germany*
- PW2 **Trap effects on dark current transients in GaAs/AlGaAs quantum well infrared photodetectors**  
A. G. U. Perera, S. G. Matsik, Y. W. Yi, M. Ershov, *Georgia State Univ., USA*, H. C. Liu, M. Buchanan, Z. R. Wasilewski, *NRC, Canada*
- PW3 **Effects of electron and photon transport in integrated QWIP-LED pixelless images**  
V. Ryzhii, I. Khmyrova, *Univ. Aizu, Japan*, Ph. Bois, *Thomson-CSF, France*
- PW4 **Circuit model for quantum well infrared photodetectors and its comparison with experiments**  
Y. H. Chee, G. Karunasiri, *National University of Singapore*
- PW5 **Quantum grid infrared photodetectors**  
L. P. Rokhinson, C. J. Chen, D. C. Tsui, *Princeton University*, G. A. Vawter, *Sandia National Labs*, K. K. Choi, *US Army Research Lab, USA*

#### QCLs etc.:

- PW6 **GaAs/AlGaAs microresonator quantum cascade lasers**  
S. Gianordoli, L. Hvozda, G. Strasser, T. Maier, N. Finger, K. Unterrainer, E. Gornik, *TU Wien, Austria*
- PW7 **GaAs/AlGaAs quantum cascade laser - a source for gas absorption spectroscopy**  
L. Hvozda, S. Gianordoli, G. Strasser, W. Schrenk, K. Unterrainer, E. Gornik, V. Pustogow, Ch. S. S. S. Murthy, M. Kraft, B. Mizaikoff, *TU Wien, Austria*
- PW8 **Long-wavelength ( $\lambda=10.5 \mu\text{m}$ ) quantum cascade lasers based on photon-assisted tunneling transitions in strong magnetic field**  
S. Blaser, L. Diehl, J. Faist, M. Beck, *Université de Neuchâtel, Switzerland*
- PW9 **Designs for a quantum cascade laser using interband carrier extraction**  
V. J. Hales, A. J. L. Poulter, R. J. Nicholas, *Oxford University, U.K.*

- PW10 **The nature of the electron distribution function in quantum cascade lasers**  
P. Harrison, *University of Leeds, U.K.*
- PW11 **High-confinement waveguides for mid-IR devices**  
P. Holmström, *Royal Inst. of Technology (KTH), Sweden*
- PW12 **Waveguide design optimization for a quantum cascade laser emitting at 77  $\mu\text{m}$**   
V. M. Menon, W. D. Goodhue, A. S. Karakashian, *Univ. Mass Lowell, USA*, L. S. Ram-Mohan, *Worcester Polytechnic Inst., USA*
- PW13 **Intersubband plasmon emission based THz lasers**  
P. Bakshi, K. Kempa, *Boston College, USA*
- PW14 **Investigation of electric-field dependent population properties in a GaAs/AlGaAs multiple, asymmetric double quantum well structure by photoluminescence spectroscopy**  
L. Schrottke, R. Hey, H. T. Grahn, *Paul Drude Institut, Germany*
- PW15 **Pico- and femtosecond non-linear transmission/reflectance of an asymmetric triple quantum well structure**  
N. Sawaki, H. S. Ahn, K. Mizutani, M. Yamaguchi, *Nagoya University, Japan*
- PW16 **Population inversion and amplification under intersubband transitions of 2D-holes in GaAs/AlGaAs heterostructures**  
N. A. Bekin, V. N. Shastin, *Inst. Phys. Microstruct. RAS, Russia*
- PW17 **Intersubband lasing under lateral electron transport in GaAs/AlAs multi-quantum-well heterostructures**  
V. Ya. Aleshkin, A. A. Andronov, E. V. Demidov, *Inst. Phys. Microstruct. RAS, Russia*
- PW18 **Intraband population inversion of hot holes in MQW InGaAs/GaAs heterostructures excited at lateral charge transport**  
V. Aleshkin, A. Andronov, A. Antonov, N. Bekin, A. Gavrilenko, V. Gavrilenko, A. Korotkov, D. Revin, *Inst. Phys. Microstruct. RAS, Russia*, E. Uskova, B. Zvonkov, N. Zvonkov, *Nizhny Novgorod State Univ., Russia*

## **Poster session 2 (Friday, 10 Sept., 14:00 - 15:00)**

- PF1 **Nonlinear intersubband optical response of multiple quantum well structures**  
M. Zaluzny, C. Nalewajko, *M. Curie-Skłodowska Univ., Poland*
- PF2 **Second-harmonic generation in quantum wells: the role of many-body effects**  
V. Bondarenko, *Nat. Acad. of Sciences, Ukraine*, M. Zaluzny, *M. Curie-Skłodowska Univ., Poland*
- PF3 **Subband selective disorder in a quasi-2D system and its effect on the intersubband spectrum / Absorption of in-plane polarized light in quasi-2D systems enabled by strong potential fluctuations**  
M. Hackenberg, C. Steen, C. Metzner, M. Hofmann, G. H. Döhler, *Univ. Erlangen, Germany*
- PF4 **Linewidth and dephasing of THz-frequency collective intersubband excitations in a GaAs/AlGaAs square quantum well**  
J. B. Williams, M. S. Sherwin, K. Maranowski, A. C. Gossard, *University of California, Santa Barbara, USA*
- PF5 **First-order coherent THz optical sideband generation from asymmetric QW intersubband transitions**  
C. C. Phillips, *Imperial College, U.K.*, M. Y. Su, J. Ko, L. Coldren, M. S. Sherwin, *UC Santa Barbara, USA*

- PF6 **Theoretical study of intersubband transitions in InAs/GaSb semimetallic superlattices in a parallel magnetic field**  
R. DeMeester, F. M. Peeters, *UIA, Belgium*, A. J. L. Poulter, M. Lakrimi, R. J. Nicholas, N. J. Mason, P. J. Walker, *Univ. Oxford, U.K.*
- PF7 **Intersubband transitions in InGaAs/AlGaAs multiple quantum wells and their behavior under proton and electron irradiation**  
M.O. Manasreh, *Air Force Research Lab, USA*, P. Ballet, J.B. Smathers, G.J. Salamo, *Univ. Arkansas, USA*, Ch. Jagadish, *Australian National Univ., Australia*, H.J. von Bardeleben, *Univ. Paris, France*
- PF8 **Thermal relaxation processes in SiGe/Si quantum wells studied by intersubband and inter-valence band optical spectroscopy**  
B. Adoram, D. Krapf, M. Levy, R. Beserman, W. Wu, K. L. Wang, J. Shappir, A. Sa'ar, *Hebrew University & Technion, Israel; UCLA, USA*
- PF9 **Electron energy relaxation in silicon quantum dots by acoustic and optical phonon scattering**  
M. Dür, S. M. Goodnick, *Arizona State Univ., USA*
- PF10 **Fano profile in intersubband transitions in self-assembled InAs quantum dots**  
Ph. Lelong, S.-W. Lee, K. Hirakawa, H. Sakaki, *IIS, Tokyo University, Japan*
- PF11 **ErAs islands in GaAs for THz applications**  
Ch. Kadow, A. W. Jackson, A. C. Gossard, J. E. Bowers, *UC Santa Barbara, USA*, S. Matsuura, G. A. Blake, *California Institute of Technology, USA*

#### **Superlattices:**

- PF12 **Field-induced delocalization and Zener breakdown in semiconductor superlattices**  
B. Rosam, F. Löser, D. Meinhold, V. G. Lyssenko, K. Leo, *TU Dresden*, S. Glutsch, F. Bechstedt, *Univ. Jena*, K. Köhler, *IAF, Germany*
- PF13 **A semiconductor superlattice in strong magnetic fields**  
T. Bauer, A. B. Hummel, H. G. Roskos, *Universität Frankfurt, Germany*, K. Köhler, *IAF, Germany*
- PF14 **Negative differential resistance in a superlattice with overlapping minibands**  
R. A. Deutschmann, W. Wegscheider, M. Rother, M. Bichler, G. Abstreiter, *Walter Schottky Institut, Germany*
- PF15 **Dynamics of electric field domain walls in semiconductor superlattices**  
D. Sanchez, M. Moscoso, L.L. Bonilla, G. Platero, R. Aguado, *Inst. de Ciencia de Materiales & Universidad Carlos III, Madrid, Spain*
- PF16 **Mechanisms of absolute negative conductivity of semiconductor superlattices**  
Yu. A. Romanov, Ju. Yu. Romanova, E. V. Demidov, *Inst. Phys. Microstruct. RAS, Russia*,

## QUANTUM CASCADE MICRODISK LASERS

Claire Gmachl,<sup>\*</sup> Federico Capasso,<sup>\*</sup> E. E. Narimanov,<sup>\*,†</sup> Deborah L. Sivco,<sup>\*</sup> James N. Baillargeon,<sup>\*</sup>  
 Alfred Y. Cho,<sup>\*</sup> Jérôme Faist,<sup>\*,||</sup> Jens U. Nöckel,<sup>§</sup> A. Douglas Stone,<sup>‡</sup>

<sup>\*</sup> Bell Laboratories, Lucent Technologies, Murray Hill, NJ 07974, USA

<sup>‡</sup> Yale University, New Haven, CT 06520, USA

<sup>||</sup> present address: Université de Neuchâtel, rue Bréguet 1, CH-2000 Neuchâtel, Switzerland

<sup>§</sup> Max-Planck-Institut f. Physik komplexer Systeme, D-01187 Dresden, Germany

Quantum Cascade (QC) lasers with tailorable emission wavelength in the mid-infrared offer a great opportunity for studying microcavity-effects in semiconductor structures. Amongst the various microcavity designs, the QC laser is especially suited for “whispering gallery” type resonators due to its inherent lack of surface recombination and TM mode emission. We report first on long wavelength (5 – 11.5  $\mu\text{m}$ ) infrared QC disk lasers, with disk diameters of 20 – 200  $\mu\text{m}$ . The most important feature accompanying the size-reduction of the laser cavity is the reduction of the mode density, described by the so-called beta-factor ( $\beta$ ). The measured free spectral range of QC disk lasers ( $\lambda_{\text{em}} \approx 9.5 \mu\text{m}$ ) increases rapidly with decreasing disk radius. This is a clear indication of the decreased mode density. We obtain  $\beta = 0.05$  for the smallest long wavelength disk laser with 20  $\mu\text{m}$  diameter and  $\lambda_{\text{em}} \approx 9.5 \mu\text{m}$ .

Second, we report on *deformed* disk (cylinder) lasers with significantly improved laser performance as they overcome the low output power and lack of directionality of conventional disk lasers. Micro-cylinder lasers with quadrupolar cross section – from circular to quasi stadium-shaped – have been fabricated, emitting at mid-infrared (5 – 8  $\mu\text{m}$ ) wavelengths. In the low-deformation regime whispering gallery modes dominate and show an increase in output power with increasing deformation and weak directionality. This behavior is understood from the ray dynamics in deformed resonators, which is either partially or fully chaotic. At higher deformations a different type of laser resonance emerges and is responsible for highly directional and high power emission. These bow-tie shaped resonances are stable resonator modes surrounded (in phase space) by chaotic motion. In the favorable directions of the far-field, these lasers show a power increase of up to *three orders of magnitude* over the conventional circular symmetric laser. Recent work on (circular and deformed) annular disk resonators and near-infrared semiconductor lasers will also be discussed. The work has been supported in part by DARPA/US ARO under contract No. DAAG55-98-C-0050.

## Superlattice Quantum Cascade Lasers

Alessandro Tredicucci, Federico Capasso, Claire Gmachl,  
Deborah L. Sivco, Albert L. Hutchinson, and Alfred Y. Cho

*Bell Laboratories, Lucent Technologies, 600 Mountain Avenue, Murray Hill, NJ 07974*

Quantum cascade (QC) lasers based on interminiband transitions in semiconductor superlattices (SL) [1] have experienced a tremendous progress, marked also by the possibility of realizing new sophisticated device concepts, like simultaneous multiple wavelength laser emission [2].

The introduction of graded superlattices (SL), with varying period and duty-cycle, as a way to compensate the applied electric field in the active region has freed SL QC lasers from the constraint of high doping levels, leading to the highest performance (0.5 W peak and 14 mW average powers at room temperature, 175 K as maximum temperature for continuous wave (cw) operation) intraband lasers to date [3]. Although first demonstrated at  $\lambda \sim 7\text{--}8\text{ }\mu\text{m}$ , chirped SL's are even better suited for longer wavelengths, where they do not suffer from having the upper state of the lasing transition close to the continuum. A new device operating pulsed at  $\lambda \sim 11\text{ }\mu\text{m}$  up to 300 K displays hundreds of mW of peak power at cryogenic temperatures and is also the first QC laser at wavelengths  $> 9\text{ }\mu\text{m}$  capable of cw operation at liquid nitrogen temperature.

The large dipole matrix element of interminiband transitions, together with the intrinsic strong population inversion, offers a natural elegant solution to the reduction of radiative efficiency and increase in absorption losses which one has to face with decreasing transition energy. In this respect we have demonstrated the first QC lasers operating at wavelengths beyond the two atmospheric windows with devices lasing at  $\sim 17\text{ }\mu\text{m}$  (17 THz) up to 175 K with several mW of output power [4]. To extend this approach to even longer wavelengths, a key issue to be addressed is the design of the waveguide. The necessity of achieving large confinement factors minimizing at the same time absorption losses makes metallic waveguides promising candidates. Laser emission is achieved at  $\lambda \sim 16.2\text{ }\mu\text{m}$  from a QC structure  $< 4\text{ }\mu\text{m}$  thick with no cladding layers exploiting a surface plasmon Ag waveguide of the type described in [5], with performances not far from the above  $17\text{ }\mu\text{m}$  laser with conventional semiconductor waveguide.

### References:

- 1 G. Scamarcio, F. Capasso, C. Sirtori, J. Faist, A. L. Hutchinson, D. L. Sivco, and A. Y. Cho, *Science* **276**, 773 (1997); A. Tredicucci, F. Capasso, C. Gmachl, D. L. Sivco, A. L. Hutchinson, A. Y. Cho, J. Faist, and G. Scamarcio, *Appl. Phys. Lett.*, **72**, 2388 (1998).
- 2 A. Tredicucci, C. Gmachl, F. Capasso, D. L. Sivco, A. L. Hutchinson, and A. Y. Cho, *Nature* **396**, 350 (1998).
- 3 A. Tredicucci, F. Capasso, C. Gmachl, D. L. Sivco, A. L. Hutchinson, and A. Y. Cho, *Appl. Phys. Lett.*, **73**, 2101 (1998).
- 4 A. Tredicucci, C. Gmachl, F. Capasso, D. L. Sivco, A. L. Hutchinson, and A. Y. Cho, *Appl. Phys. Lett.*, **74**, 638 (1999).
- 5 C. Sirtori, C. Gmachl, F. Capasso, J. Faist, D. L. Sivco, A. L. Hutchinson, and A. Y. Cho, *Opt. Lett.* **23**, 1366 (1998).



# Theoretical study, modeling and simulation of SL quantum cascade lasers

Fabio Compagnone\*, Sergio Tortora, Aldo Di Carlo, Paolo Lugli\*\*

INFN and Dept. Electronic Engineering University of Roma "Tor Vergata", I-00133 Roma, Italy

Quantum Cascade Lasers (QCL) have been demonstrated to be the only valuable semiconductor light source for far-infrared application in the range 4-11  $\mu\text{m}$  [1,2]. The outstanding achievements obtained for such device have been pushed mainly by technology, with scarce support from theoretical investigations and modeling. Among the various realizations of QCL, the most promising one is based on the periodic repetition of superlattice (SL) stages. Each one comprises two different regions: the first one acting as an relaxation/injection region, the second as active layer, where radiative recombination occurs. We have performed extensive theoretical investigation of electron dynamics in such superlattice QCL, both for the InGaAs/AlInAs and for the GaAs/AlGaAs systems. Our approach is the following:

(i) We first determine the miniband dispersion and electron wavefunctions for the SL using a Kronig-Penney non parabolic model; (ii) We then calculate the scattering rates for electron-phonon (acoustic and optical phonons) and electron-electron interactions; (iii) we choose the optimal SL (in terms of barrier and well width, and material compositions) on the basis of various parameters: the miniband width must be large to assure better facing of electronic levels; intraminiband and interminiband phonon scattering rates have to be respectively largest and smallest as possible for the proper operation of the laser; (iv) we calculate the injector carrier energies and injection/extraction rates into the active region from a transfer matrix technique; (v) we perform Monte Carlo simulations of electron dynamics based on all previous ingredients, extracting the non equilibrium electron and phonon distribution functions; (vi) by using the calculated optical matrix elements between the two lowest (usually the two only existing) minibands, we finally calculate the emission spectra at the chosen injection condition.

Preliminary results for the InGaAs/AlInAs QCL are shown in figs. 1 and 2. We have found that the optimal structure has wells and barriers of respectively 60 and 18 Å (at the composition for lattice matched layers on a InP substrate). For electron densities above  $10^{17} \text{ cm}^{-3}$  electron-electron collisions play a major role in disrupting population inversion at the miniband edge, which in turn is the necessary condition for lasing action. A detailed analysis of the differences between InGaAs/AlInAs and GaAs/AlGaAs QCL will be presented, pointing out in particular the role of non equilibrium phonons and of intervalley transfer.

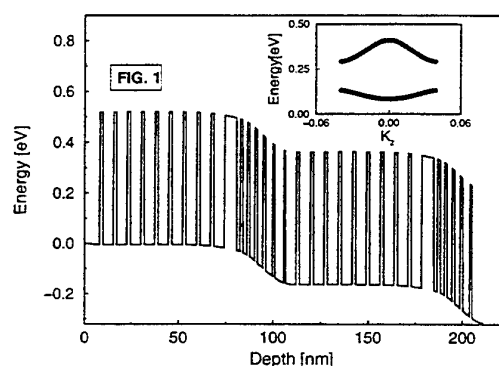


Fig.1 Self-consistent band edge profile of the cascade structure. Insert: I and II miniband dispersion.

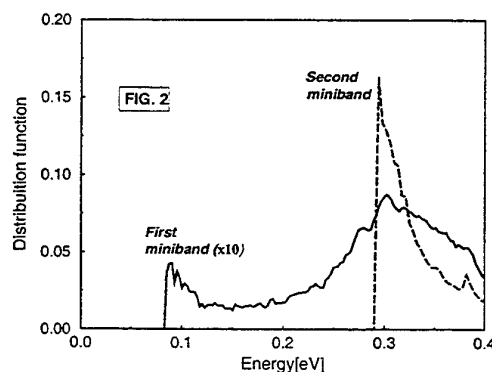


Fig.2 Distribution functions for the first two minibands

[1] J. Faist et al. Science, **264**, 553, (1994)

[2] G. Scamarcio et al. Applied Phys Lett. **70**, 1797 (1997)

[\*] E-mail: fabio@venere.eln.uniroma2.it

[\*\*] Corresponding author. E-mail: lugli@uniroma2.it Tel: +39 (6) 72597372 Fax: +39 (6) 2020519

# High-power, long wavelength ( $\lambda=10.2\ \mu\text{m}$ ) distributed feedback quantum cascade lasers fabricated without epitaxial re-growth

Daniel Hofstetter\*, Jérôme Faist, Mattias Beck, Ursula Oesterle,  
and Antoine Müller

University of Neuchâtel, CH-2000 Neuchâtel, Switzerland

\*email: Daniel.Hofstetter@iph.unine.ch

Distributed feedback (DFB) QC lasers have already shown excellent performance for spectroscopy applications in the mid-infrared at room temperatures [1]. When trying to develop such devices for long wavelength applications, the problem arises that only devices manufactured with a grating in the active region followed by an epitaxial regrowth will allow the strong coupling needed for high performance. We demonstrate here a completely new approach that allows extremely high single frequency performance to be reached together with a much better degree of device manufacturability. The quantum cascade laser active region is placed between high refractive index InGaAs confining layers in a waveguide bounded by the substrate on one side and air on the other. A heavily n-doped, and thus highly conducting, InGaAs cap layer, which serves as host layer for the grating, allows uniform current distribution throughout the device.

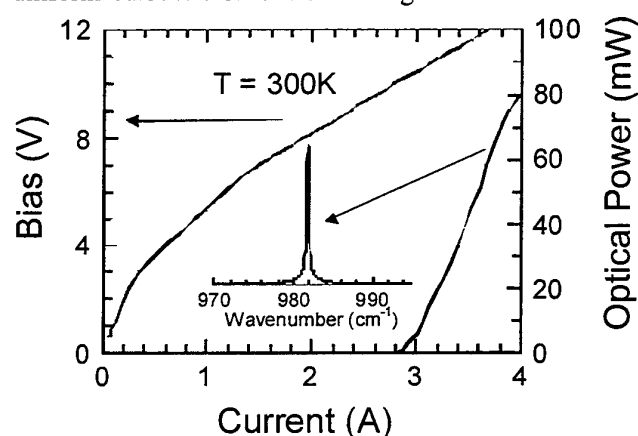


Fig. 1 - Light and voltage versus current characteristics of a  $45\ \mu\text{m}$  wide and  $1.2\ \text{mm}$  long DFB QC laser. The inset shows a spectrum measured of the laser close to the maximum power, as indicated by the arrow.

measure the peak power during operation. At 300 K, we obtained a record 80 mW optical output power with a slope efficiency of 80 mW/A. The threshold current was 2.9 A, which corresponded to a threshold current density of only  $5.5\ \text{kA}/\text{cm}^2$ . This low value shows that the waveguide losses are kept to a very low value. As shown in the inset of Fig. 1, the device operated in single frequency up to the largest power. The linewidth of the laser emission,  $0.3\ \text{cm}^{-1}$ , is limited by our experimental set up and by thermal drifts during the pulse. The device operates monomode over the whole temperature range from 80 K to 300 K.

This work was supported by the Swiss National Science foundation and the Science Foundation of the European community.

In this manner, a very strong grating coupling can be obtained (with a calculated  $\Delta n = 2\%$ ) while maintaining a very low waveguide loss, whose calculated value (neglecting the effect of the lateral contacts) at the lasing wavelength of  $10.2\ \mu\text{m}$  is only  $11\ \text{cm}^{-1}$ .

A diffraction grating is manufactured by holographic exposure and wet chemical etching. A low loss ZnSe insulating layer is then deposited. Non-alloyed Ti/Au metallic contacts are then evaporated on the mesa edges.

Typical L-I- and I-V-curves of a  $45\ \mu\text{m}$  wide and  $1.2\ \text{mm}$  long device are shown in figure 1. The current pulses were 100 ns long, and a pulse repetition frequency of 5 kHz was used for all temperatures. A room temperature HgCdTe detector calibrated with a thermopile detector was used to

## Quantum dot infrared photodetectors in new material systems

E. Finkman, S. Maimon, V. Immer, G. Bahir, and S.E. Schacham  
Department of Electrical Engineering and Solid State Institute, Technion,  
Haifa 32000, Israel

O. Gauthier-Lafaye, S. Herriot, F.H. Julien  
Institut d'Electronique Fondamentale, URA CNRS 22, Universite Paris-XI, 91405 Orsay,  
France

M. Gendry and J. Brault  
Laboratoire d'Electronique-LEOM, UMR CNRS 5512, Ecole Centrale de Lyon, 69131 Ecully,  
France

We report the advancements in implementing quantum dot infrared photodetectors (QDIPs) using the photoconductive effect in order to study the nature of the intraband transitions. The polarization selection rules, the symmetry of the energy states, and their dependence on the dot shape were studied. In this work, we concentrate on a new structure of InAs self-assembled quantum dots fabricated using Stranski-Krastanov growth mode on InAlAs matrix lattice matched to InP (001) substrates<sup>(1)</sup>. These dots grow with a shape of small boxes, of around 500 Å long, 300 Å wide and 20 Å high, with their long axis along the [-110] direction, and with a high concentration of  $7 \times 10^{10} \text{ cm}^{-2}$ . A single, strong in-plane intraband absorption in such dots peaked around 90 meV (14 μm), polarized perpendicular to the box long axis has been observed<sup>(2)</sup>. This was ascribed to a transition from the ground electron state to an excited state confined in the layer plane along the [110] direction. Present QDIP photoconductive measurements on similar structure, were performed in all 3 polarizations. Rich spectra of 6 transitions, in the range of 90-280 meV, with different polarization selection rules were observed. The bias dependence of peak intensity of the intraband transitions serves as an additional tool to identify their origin. The 90 meV band which was previously reported<sup>(2)</sup>, for example, does not appear at low applied voltage, and increases sharply with increasing bias. This indicates a strong tunneling out of the dots, which rules out the possibility that this transition is excited to the continuum in the layer plane. All the infrared bands are identified and assigned. The combination of photoconductivity and photo-induced absorption gives a complementary information. It is easier to identify bound-to-bound transitions and estimate their oscillator strengths using IR transmission. On the other hand, photoconductivity spectrum is usually richer, by giving easier access to bound-to-continuum transitions as well. The responsivity at normal-incidence is identical to that obtained for polarization normal to the layers, and is comparable to that achieved in QWIPs. A detector based on ten layers of n-doped quantum dots had reached, at normal incidence, a responsivity of 0.15 A/W with BLIP conditions at a temperature of 90K for integral photocurrent response. Results on InAs/GaAs dot system<sup>(3)</sup> will also be reviewed and extended. Such detectors have achieved operation in BLIP conditions at 77K with F/# 2 at 6 μm.

1. J Brault, M. Gendry, G. Grenet, G. Hollinger, Y. Desieres, and T. Benyatou, *Appl. Phys. Letters* **73**, 2932 (1998).
2. A. Weber, O. Gauthier-Lafaye, F.H. Julien, J Brault, M. Gendry, Y. Desieres, and T. Benyatou, *Appl. Phys. Letters* **74**, 413 (1999).
3. S. Maimon, E. Finkman, G. Bahir, S.E. Schacham, J.M. Garcia, and P.M. Petroff *Appl. Phys. Letters* **73**, 2003 (1998); S. Maimon, E. Finkman, G. Bahir, S.E. Schacham, L. Fonseca, J. Shumway, J.P. Leburton, J.M. Garcia, and P.M. Petroff, ICPS-24, Jerusalem, August, 1998.

Contact : E. Finkman: finkman@ee.technion.ac.il, Tel: 972 4 829 4686, Fax: 832 3041.

## Bound-to-Continuum Intersubband Transition in Self-Assembled InAs Quantum Dots and Its Application to Mid-Infrared Photodetectors

S. -W. Lee<sup>1</sup>, K. Hirakawa<sup>1,2</sup>, and Y. Shimada<sup>1</sup>

<sup>1</sup>*Institute of Industrial Science, University of Tokyo, Roppongi, Minato-ku, Tokyo 106-8558, Japan  
Phone: +81-3-3402-6231 ext. 2363, Fax: +81-3-3479-4634, E-mail: swlee@nano.iis.u-tokyo.ac.jp*

<sup>2</sup>*CREST, Japan Science and Technology Corporation*

The quantum dot infrared photodetectors (QDIPs) using InAs self-assembled quantum dots (QDs) have been proposed and successful operation in the mid-infrared range has been demonstrated [1,2]. Most of the structures reported so far utilize a vertical transport through stacked self-assembled QDs, simulating the operation of quantum well infrared photodetectors. However, because of unavoidable inhomogeneity in size and spatial alignment of the self-assembled QDs, the tunneling transport through multiple self-assembled QDs is strongly affected by the disorder. As a result, it seems to be difficult to obtain high photoconductive gains in the vertical transport structures.

In this work, we have designed and fabricated a QDIP which utilizes the bound-to-continuum intersubband transition in the self-assembled InAs QDs and subsequent lateral transport of photoexcited carriers in the modulation-doped AlGaAs/GaAs two-dimensional (2D) channel. The samples were grown on (001) semi-insulating GaAs substrates by molecular beam epitaxy. 10 InAs SAQD layers were grown at 470 °C. Each layer was embedded in the middle of 100 nm-thick GaAs quantum wells. The density of the QDs was approximately  $4 \times 10^{10} \text{ cm}^{-2}$ . The 30 nm-thick AlGaAs barriers were  $\delta$ -doped with Si up to  $1 \times 10^{11} \text{ cm}^{-2}$ . The essential points of the structure are ; 1) the size of the InAs QDs is made small to accommodate only one bound state in the QDs by adopting low temperature growth, 2) high-mobility modulation-doped AlGaAs/GaAs heterointerfaces are used as the conducting channels for photoexcited carriers, and 3) a long carrier lifetime is achieved by using a large distance between the QDs and the heterointerfaces. The electrons are photoexcited from the ground state in the QDs to the virtual excited state above the conduction band of GaAs (bound-to-continuum operation), relax to the heterointerface, and drift laterally along the interface due to the applied electric field, thereby producing a photocurrent.

The photocurrent spectra of the QDIP were measured in a single-pass normal incidence geometry by using a Fourier transform spectrometer. A broad photosignal is observed for the normal incidence radiation in a photon energy range of 100-300 meV and even above 400 meV. A peak responsivity as high as 4.7 A/W was obtained at  $h\nu = 160 \text{ meV}$  at  $T = 10 \text{ K}$ . This value is approximately two orders of magnitude larger than the values for the QDIPS reported so far [1]. The high responsivity is realized mainly by a high mobility and a long lifetime of photoexcited carriers in the modulation-doped 2D channels. Furthermore, it is found that the observed photosensitivity survives up to 190 K.

### References

- [1] S.J. Xu et al, Appl. Phys. Lett. **73**, 3153 (1998). [2] S. Maimon et al, Appl. Phys. Lett. **73**, 2003 (1998).

## Optically Detected Intraband Resonances In InGaAs/GaAs Quantum Wells and Dots

B. N. Murdin and A.R. Hollingworth,

*Department of Physics, University of Surrey, Guildford GU2 5XH, U.K.,*

*[tel: +44 -1483-259328; fax: +44 - 1483 876728; email: b.murdin@surrey.ac.uk]*

C. R. Pidgeon and P. C. Findlay,

*Department of Physics, Heriot Watt University, Edinburgh EH14 4AS, U.K.,*

J-P. Wells, I. V. Bradley and G.M.H. Knippels,

*FOM Institute 'Rijnhuizen', P.O.Box 1207, NL-3430BE Nieuwegein, The Netherlands,*

R. Murray

*IRC for Semiconductor Materials, The Blackett Lab., Imperial College, London SW7 2BZ, U.K.*

We have used a two-colour pump-probe technique to measure directly relaxation times associated with intraband absorption processes in low dimensional systems (the pump is a fs-pulsed Ti:sapphire laser and the probe is a tunable, far-infrared free electron laser, FELIX). The FIR radiation resonantly excites the *intraband* absorption and reduces the *interband* photoluminescence (PL) efficiency. The use of pulsed lasers allows extraction of the lifetime associated with the intraband process.

In particular we have studied low growth rate InAs/GaAs self-assembled quantum dots. The PL from these dots under high laser power shows a ground state transition at 1028meV, and higher energy peaks at 1102meV and 1164meV (all  $\sim 17$ meV wide). The infrared modulation of the PL is resonant at an FIR photon energy which corresponds closely with the predicted intersublevel energy at around 75 meV. The FIR resonance is unambiguously related to the quantum dots, since the modulation of the PL occurs on the peaks associated with the dots, and not on features associated with the surrounding material. This measurement represents therefore, the first unequivocal assignment of an FIR transition to intersublevel absorption in quantum dots.

We have extended our earlier work on Optically Detected Cyclotron Resonance (ODCR) to a time-resolved study, again utilising the Ti:sapphire and FELIX systems. We have made measurements of time-resolved cyclotron resonance in InGaAs/GaAs quantum wells, to investigate the effect of electron-hole scattering on the lifetimes of these low dimensional quantum states. We note that, in addition, this technique may be used to directly determine lifetimes in situations where the band is parabolic and saturation cyclotron resonance is not possible.

## Femtosecond mid-infrared study of carrier dynamics in self-organized InAs/InAlAs quantum dots

E. Péronne, J. F. Lampin, and A. Alexandrou

*Laboratoire d'Optique Appliquée, ENSTA - Ecole Polytechnique - CNRS UMR 7639  
F-91761 Palaiseau, France*

O. Gauthier-Lafaye and F. H. Julien

*Institut d'Electronique Fondamentale, Université Paris-XI, CNRS URA 22  
F-91405 Orsay, France*

J. Brault and M. Gendry

*Laboratoire d'Electronique-LEOM, Ecole Centrale de Lyon, CNRS UMR 5512  
F-69131 Ecully, France*

The discrete nature of the energy levels in quantum dots leads to the so-called "phonon bottleneck effect". However, recent studies have shown evidence of fast carrier relaxation between quantum-dot levels in photoluminescence and interband absorption experiments and attributed it to Auger processes becoming important at high excitation densities [1].

In this work, we present femtosecond pump-probe experiments where the pump (800 nm, 150 fs, 200 kHz) excites electron-hole pairs in the barrier and the probe is tuned to the transition from the first to the second electron level,  $E1 \rightarrow E2$ , in the mid-infrared thus directly probing the difference in population between the two levels [2]. The experiments were performed on ten planes of 0.9-nm InAs / 50-nm  $\text{In}_{0.52}\text{Al}_{0.48}\text{As}$  self-organized quantum dots grown on InP(001) [3]. The high density of quantum dots ( $7 \times 10^{10} \text{ cm}^{-2}$ ) in these samples leads to strong normal-incidence infrared absorption of about 8% due to the transition  $E1 \rightarrow E2$  [4].

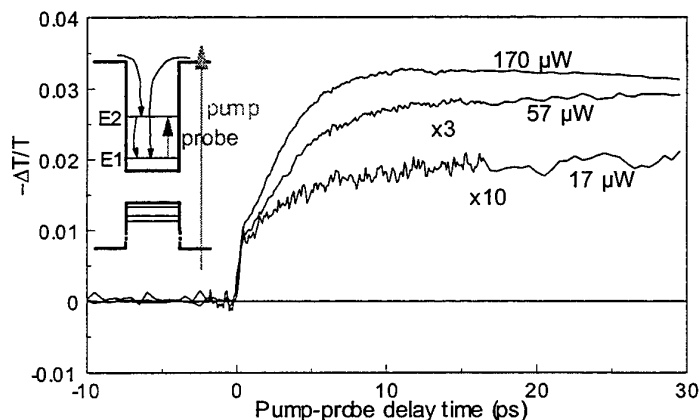


Fig. 1 Differential transmission as a function of pump-probe delay time for  $\lambda_{\text{probe}} = 10.6 \mu\text{m}$  and for three different pump intensities. The lowest pump intensity corresponds to the injection of approximately  $10^{11} \text{ cm}^{-2}$  electron-hole pairs. For better visibility, multiplication factors were used for the curves at lower pump intensity.

The initial fast rise time seen in Fig. 1 corresponds to free-carrier absorption due to the carriers injected in the barrier. The slower rise time of the signal reflects the capture and  $E2 \rightarrow E1$  relaxation process. The acceleration of this second rise time with increasing density shows the importance of Coulomb collisions for the relaxation. A rate equation model will be compared to the experimental results.

[1] B. Ohnesorge et al., Phys. Rev B **54**, 11532 (1996); V. I. Klimov and D. W. McBranch, Phys. Rev. Lett. **80**, 4028 (1998).

[2] M. K. Reed and M. K. Steiner Shepard, IEEE J. Quantum Electron. **32**, 1273 (1996).

[3] J. Brault et al., Appl. Phys. Lett. **73**, 2932 (1998).

[4] A. Weber et al., Appl. Phys. Lett. **74**, 413 (1999).

## Intersubband photocurrent spectroscopy on self assembled Ge quantum dots in Si

C. Miesner, O. Röthig, K. Brunner, and G. Abstreiter

*Walter Schottky Institut, TU München, Am Coulombwall, D-85748 Garching, Germany*

For midinfrared photodetector applications zero-dimensional semiconductor quantum dots may have some important advantages compared to two-dimensional quantum well structures due to the reduced intersubband relaxation rate, the delta-like density of states and modified polarisation selection rules. First intersubband absorption measurements on Ge dots in Si have been published recently by different groups. We investigated such Si/Ge dot structures by photocurrent spectroscopy accompanied by AFM, TEM, photoluminescence (PL) and absorption spectroscopy.

The samples under examination consist of ten stacks of Ge dots separated by i-Si spacer layers of 60nm thickness. They were grown at  $T_s=550^\circ\text{C}$  using solid-source MBE in a commercial chamber. Ge dots form by self assembling in the Stranski-Krastanov growth mode. Three samples with a nominal Ge coverage of 7.2ML, 8.0ML and 8.8ML were investigated. As a reference, a sample was grown in which the Ge dot layers were replaced by 2.5nm thick  $\text{Si}_{0.60}\text{Ge}_{0.40}$  quantum well layers. The dots were heavily boron doped in order to provide carriers for intersubband absorption. The entire structure is embedded in two boron doped Si layers which serve as the top and bottom contact for photocurrent measurements.

Structural characterization was performed by crosssectional HRTEM revealing a typical dot diameter of 75nm and a height of 6.5nm for the sample with 8.0ML Ge. The dot density of this sample is  $1 \times 10^9 \text{cm}^{-2}$ . No dislocations could be found by TEM. The effective band gap of the Ge dots was investigated by standard interband PL measurements. The PL spectrum consists of the typical Si related lines and a dot related line at an energy of about 0.80eV with a linewidth of about 100meV. With increasing amount of Ge deposited, the dot luminescence shifts slightly towards higher energies and broadens significantly. The broadening can be explained by an increasing inhomogeneity in dot size and an higher doping level for larger Ge coverage. The dot density decreases with increasing amount of Ge and thus the number of dopants per dot is higher in the samples containing more Ge. The blue shift of the luminescence may also be explained by state filling effects for an higher doping level.

For midinfrared photocurrent measurements,  $300\mu\text{m} \times 400\mu\text{m}$  mesas were etched using standard photolithography and wet chemical etching. Both, bottom (AlAu) and top contact (TiAu) metallization were made from the front side. Afterwards, samples were mounted into commercial IC sockets and wire bonded. The measurement system consists of a glowbar as light source, a chopper, a conventional grating monochromator and KRS5 lens optics. For the measurements, the sample is mounted in a He-gasflow cryostat. The photocurrent is measured in lock-in technique. Measurements were performed in waveguide geometry as well as in normal incidence geometry. A broad intersubband absorption ranging from 250meV to 550meV is observed in both geometries. We attribute it to intersubband transitions between hole levels within the dots. The position of the peak maximum depends on both the applied bias and the amount of Ge deposited. With increasing bias voltage, the peak position shifts towards lower energies for all three samples. The peak position decreases in energy with higher Ge content, in consistence with the PL results. The FWHM of the absorption line within the three samples is approximately 200meV and thus twice the FWHM value observed by PL. Midinfrared photocurrent in these samples was observed up to  $T=100\text{K}$ . The strong photoresponse observed in normal incidence together with the excellent dark currents, which are in the order of 10nA at an external bias of 2V and  $T=77\text{K}$ , demonstrate the huge potential for applying Ge quantum dots in midinfrared photodetector devices and arrays.

# Temperature dependence of Terahertz GaAs and InGaAs quantum cascade Light Emitting Diodes

*Michel Rochat<sup>1</sup>, Jérôme Faist, Mattias Beck,*  
University of Neuchâtel, CH-2000 Neuchâtel, Switzerland

*Ursula Oesterle, Marc Illegems*  
Swiss Institute of Technology, CH-1015 Lausanne, Switzerland

## ABSTRACT

We have shown<sup>2</sup> that narrow (0.7meV) line width terahertz emission from GaAs quantum cascade structures based on vertical transitions is possible at low temperature. Material and temperature dependence of GaAs and InGaAs quantum cascade light emitting diodes has been investigated. We demonstrate here for the first time, GaAs and InGaAs based devices, showing intersubband terahertz emission up to temperatures significantly above liquid nitrogen ( $T=100\text{K}$  and  $T=120\text{K}$  respectively). At low temperatures ( $T=10\text{K}$ ) and at low injection currents ( $30\text{ A/cm}^2$ ), the InGaAs based material structure show narrow electroluminescence peak (1.08 meV FWHM) at a photon energy of 15 meV. At high temperature ( $T=120\text{K}$ ), the FWHM do not exceed 1.42meV while keeping 15% of its initial intensity. We show that the decreasing intensity of the peaks with increasing temperature is well explained by hot electron depopulation of the excited state and from optical phonons emission.

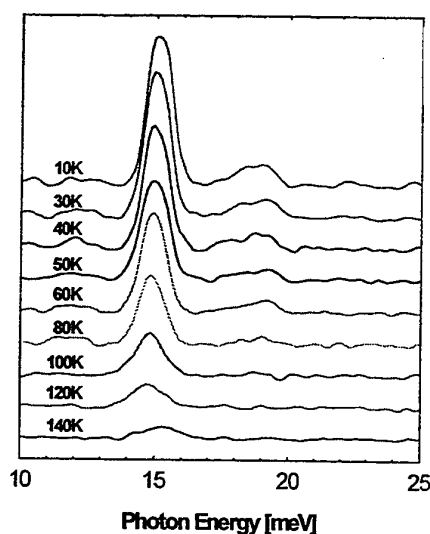


Fig1. Emission spectra of the InGaAs based structure at fixed drive current (50mA, corresponding to a current density of  $30\text{ A/cm}^2$ ) for increasing temperatures.

<sup>1</sup>E-mail : [Michel.Rochat@iph.unine.ch](mailto:Michel.Rochat@iph.unine.ch), phone: ++4132 7182948, fax: ++4132 718 2901

<sup>2</sup>Rochat *et al*, APL 73(25), 21 December 1998



## Narrow linewidth terahertz intersubband emission from three-level multiple quantum well structures

Benjamin S. Williams, Bin Xu, and Qing Hu

MIT, Dept. of EECS and Research Laboratory of Electronics, Cambridge, MA 02139

Michael R. Melloch

Purdue Univ., School of Electrical and Computer Engineering, West Lafayette, IN 47907

Intersubband transitions in cascaded semiconductor quantum wells are a promising source for generating coherent radiation in the terahertz (far-infrared) frequency range. A laser based on such transitions would be useful for high-resolution THz chemical and biological spectroscopy, and also as a local oscillator for astronomical THz heterodyne detection. Despite the great success of mid-infrared intersubband lasers, however, several obstacles remain for the development of intersubband THz lasers. The narrow subband separation corresponding to THz frequencies (4-40 meV) makes selective injection and removal of electrons difficult. The weak power level of spontaneous intersubband THz emission makes detection difficult, and is easily contaminated by thermal radiation. Finally, the long wavelength (30-300  $\mu\text{m}$ ) requires new methods for optical mode confinement. We have designed, simulated, and tested an electrically pumped unipolar three-level system based upon thirty cascaded triple-quantum-well modules. Electrons are injected into an excited state  $E_3$  via resonant tunneling, where they either emit a THz photon, or nonradiatively scatter into the lower state  $E_2$ . Electrons in  $E_2$  then quickly scatter via LO-phonons into the ground state  $E_1$  of the module, where they are injected into the next module. The radiative energy is smaller than the LO-phonon energy, which reduces fast LO-phonon scattering and favors a population inversion between the radiative levels  $E_3$  and  $E_2$ .

We report the observation of intersubband electroluminescence at 2.55 THz (10.5 meV), with a FWHM emission linewidth of 0.33 THz (1.36 meV). These measurements compare well with our calculated subband separation of 11 meV. The linewidth of the emission is dominated by the anticrossing separation (1.1 meV) between the injector level and excited level. Transport measurements verify electron injection through resonant tunneling. Intersubband emission was also observed at 80 K bath temperature, with only a slightly broader linewidth of 0.38 THz (1.58 meV). We also report our analysis of gain and losses and the feasibility to achieve lasing using this structure. Due to the long wavelength of the radiation compared with the thickness of the gain medium, and the increase in free-carrier optical scattering losses at longer wavelengths, conventional dielectric waveguides are not practical. Alternative waveguiding methods and their associated optical loss mechanisms are discussed.

This work was supported by NSF and ARO.

contact: Benjamin Williams

MIT 26-460

77 Massachusetts Ave

Cambridge, MA 02139

Ph:617-253-2431

FX:617-258-7864

bwilliam@mit.edu.

# Parabolic quantum wells and quantum cascade structures as electrically driven THz-sources

J. Ulrich<sup>a)</sup>, R. Zobl, K. Unterrainer, G. Strasser, and E. Gornik

*Institut für Festkörperelektronik, Technische Universität Wien, 1040 Wien, Austria*

We present measurements of THz-emission from two kinds of AlGaAs/GaAs heterostructures.

The THz-radiation from parabolic quantum wells [1] originates from the decay of intersubband plasmons. The latter are generated by application of a DC electric field in the plane of the layers. The collective character of the electron dynamics is supported by our results. In the temperature range of 20 – 240 K we observe single peak emission at a photon energy of 9.8 meV with a full-width at half-maximum of 1 - 2 meV (see Fig. 1). This energy corresponds to the harmonic oscillator frequency of an undoped parabolic well and not to the single electron energy levels. According to the generalized Kohn's theorem, the emission frequency is independent of electron-electron interaction and, as our experiments confirm, of the temperature dependent electron distribution on the well states. The optical output power decreases with rising temperature. We can interpret this behavior in terms of two thermally activated non-radiative channels. The high temperature ( $T > 100$  K) process has been identified as the plasmon decay via LO-phonon emission.

In quantum cascade structures [2], electrons are vertically transported through a cascade of minibands (see Fig 2 a). If the proper electric field is applied, the electrons are selectively injected into the second state of the transition wells and tunnel resonantly from its ground state into the adjacent miniband. We observe an emission peak at 17.3 meV that stems from the 2 – 1 transitions (see Fig 2 b). Comparing different sample geometries, we find a higher outcoupling efficiency from the edges of a long ridge ( $100 \times 3000 \mu\text{m}^2$ ) than from a mesa of comparable area with a grating coupler on top.

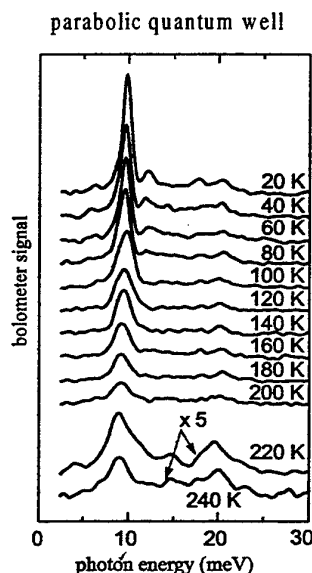


**Fig. 1:** Emission spectra of a parabolic quantum well of 140 nm width and 167 meV energetic depth in the temperature range 20 K - 240 K. The spectra were recorded using step scan Fourier-transform spectroscopy.

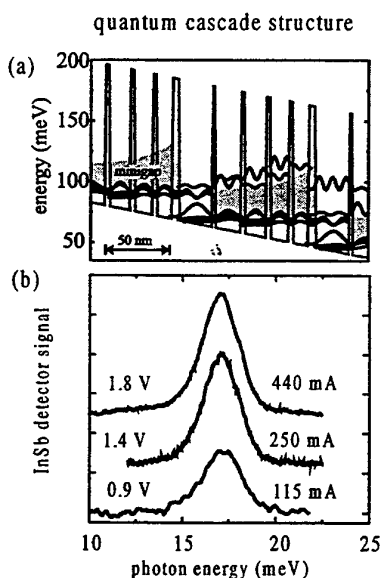


**Fig. 2:** a) Band structure of a quantum cascade structure. b) Emission spectra for three different biases at a temperature of 4.2 K. An InSb cyclotron resonance detector with a linewidth of 1.5 meV was employed.

## References:

- [1] J. Ulrich, R. Zobl, K. Unterrainer, G. Strasser, and E. Gornik, „Temperature dependence of far-infrared electroluminescence in parabolic quantum wells“, to be published in Appl. Phys. Lett. (scheduled for: May, 24<sup>th</sup> 1999).
- [2] M. Rochat, J. Faist, M. Beck, U. Oesterle, M. Illegems, Appl. Phys. Lett. 73, 3724 (1998).

<sup>a)</sup> E-mail: jochen.ulrich@tuwien.ac.at

# **RESONANT TUNNELING AND INTERSUBBAND POPULATION INVERSION EFFECTS IN ASYMMETRIC WIDE QUANTUM WELL STRUCTURES.**

V.N.Murzin, Yu.A.Mityagin, V.A.Chuenkov, A.L.Karuzskii, A.V.Perestoronin, L.Yu.Shchurova

P.N.Lebedev Physical Institute, Leninsky pr.,53,  
117924 Moscow, Russia.

The very prominent achievements of the last years are obviously the investigations of quantum cascade and quantum fountain lasers operating in the near and mid-infrared regions. In this paper we discuss the far infrared resonant tunneling laser version based on the intersubband transitions in wide quantum well structures with energy spacings of the order and below the LO phonon energy. The population inversion in the structures is achieved between the ground and the first excited subbands due to the difference in scattering relaxation processes with or without of the LO phonons emission and due to the selective wash out of carriers from the ground state by use of resonant tunneling to the neighbor quantum well.

On the base of vertical transport and optical investigation of the structures the relaxation life-time, resonant tunneling rate, intersubband optical absorption and amplification as well as the other characteristics are discussed revealing the possibility of intersubband population inversion and far-infrared stimulated emission in the systems. The analysis of the intersubband relaxation in quantum wells is based on the theoretical approach resulting in the analytical expressions for optical phonons, acoustic phonons and electrically charged impurities scattering rates. The vertical transport and photoluminescence investigations are carried out in superlattices [1] and asymmetric multiple quantum well structures [4] revealing the incoherent behavior of the resonant tunneling when it is combined with a relaxation process [2-4], resulting in the essential dependence of the tunneling time on the relaxation rate. The space charge effects are demonstrated resulting in disalignment of the resonant states and transformation of the whole resonant tunneling structure under electrical fields [1,5], which change dramatically the rate characteristics of resonant tunneling. The experimental evidence of the resonant tunneling as an effective way for selective redistribution of carriers resulting in population inversion throughout the lowest subbands in wide quantum well structure is shown.

The multiple quantum well structures on the base of GaAs/AlGaAs materials with laser transitions (near 160 cm<sup>-1</sup>) in wide quantum well (250Å) were designed and fabricated. The results of experimental transport and optical investigations of the structures under optical band-to-band pumping and current injection in electric fields are presented.

The work is supported by RFFI (99-02-17437) and FTNS Program (97-1048).

- [1] Yu.A.Mityagin, V.N.Murzin, JETP Lett., Vol.64, 155 (1996)
- [2] K.Leo, J.Shah, J.P.Gordon et al., Phys.Rev. B 42, 7065 (1990)
- [3] S.A.Gurvitz, I.Bar-Joseph, B.Deveaud, Phys.Rev.B 43, 14703 (1991)
- [4] V.N.Murzin, Yu.A.Mityagin, V.A.Chuenkov, Izvestiya RAN(phys.)(in print)
- [5] V.N.Murzin, Yu.A.Mityagin, Uspekhi Fizicheskikh Nauk (in print)

## Inter-subband relaxation due to electron-electron scattering in quantum well structures

*K. Kempa and P. Bakshi*

*Department of Physics, Boston College, Chestnut Hill, MA 02467, USA*

We present a full RPA formalism, and an efficient computational scheme for the inter-subband relaxation processes due to the electron-electron interactions in quantum well structures. Based on a full self-energy calculation, our formalism includes both single particle (Auger) and collective (plasmon) processes, and is applicable to strongly inhomogeneous, non-equilibrium steady state systems. Earlier approaches only dealt with the single particle (Auger) aspect of the electron-electron scattering, apart from a phenomenological static screening. Our approach includes the complete static and dynamic screening effects.

Electron-electron scattering dominates the physics of carrier relaxation in quantum nano-structures for which the inter-subband separation is less than the LO phonon energy. Thus a precise assessment of the inter-subband transport rates due to electron-electron processes is essential for designing structures used as active regions of devices for emission of radiation in the THz frequency range. This is *the* limiting mechanism in achieving population inversion, and reducing its deleterious effects (by appropriate structure design, or excitation scheme), could clear the way to a THz laser.

To show the efficacy of our formalism, we analyze two recent experiments<sup>1,2</sup>, which report (over an order of magnitude) different scattering rates for similar structures and similar carrier densities. We obtain quantitative agreement with both experiments, showing that the observed difference is due to different excitation levels of the electron population in these experiments. We have also shown, that the electron-plasmon scattering is responsible for the activated temperature dependence of the observed scattering rate in one of the experiments<sup>1</sup>. This effect cannot be explained by simplified (Auger-like) approaches, which ignore the collective effects.

1. N. Heyman, K. Unterrainer, K. Craig, B. Galdrikian, M.S. Sherwin, K. Campman, P.F. Hopkins, and A.C. Gossard, *Phys. Rev. Lett.* **74**, 2682 (1995).
2. M. Hartig, S. Haacke, P.E. Selbmann, B. Deveaud, R.A. Taylor, and L. Rota, *Phys. Rev. Lett.* **80**, 1940(1998); M. Hartig, J.D. Ganiere, P.E. Selbmann, S. Haacke, B. Deveaud, and L. Rota, results presented at the 24th ICPS Conference, Jerusalem, Israel, August 1998, paper TU3-A5.

# THE INTRA- AND INTER-SUBBAND RELAXATION OF NONEQUILIBRIUM ELECTRON POPULATIONS IN WIDE SEMICONDUCTOR QUANTUM WELLS

S.-C. Lee and I. Galbraith

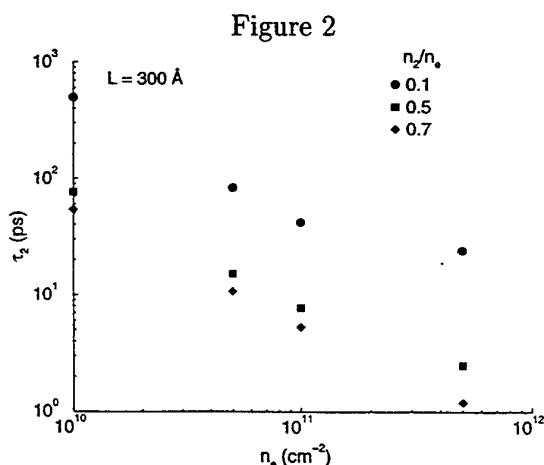
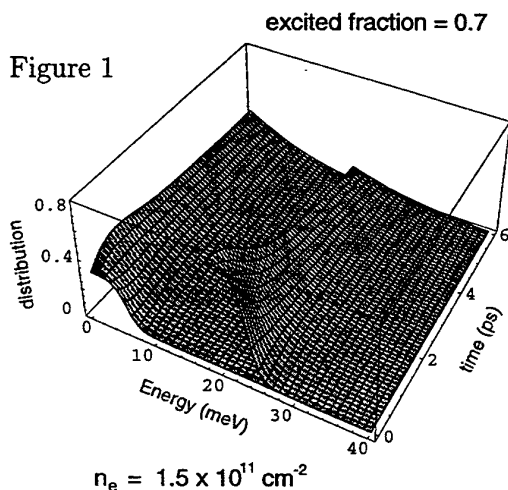
Department of Physics, Heriot-Watt University, Edinburgh EH14 4AS, U. K.

## Abstract

The operation of midinfrared intersubband quantum cascade lasers is influenced strongly by the electron - LO-phonon scattering process. In extending the operating wavelength of these devices to the far-infrared, the electron-electron scattering process also becomes significant because of the smaller intersubband energy separation. This additional competing non-radiative process also leads to population transfer between the subbands.

In this work, we focus on the electron-electron scattering process in GaAs/ $\text{Al}_x\text{Ga}_{1-x}\text{As}$  semiconductor quantum wells, looking in particular at the temporal evolution of nonequilibrium electron distributions and the intersubband population relaxation times resulting from these scattering processes. We calculate the evolution of the electron distributions through numerical integration of the Boltzmann collision integrals. The screening of the interaction between the electrons is modeled with the full dynamic, multisubband dielectric function derived in the random phase approximation (RPA). The RPA screening model describes the effect of both plasmons and pair excitations on the electron-electron scattering rates. We present results for the evolution of nonequilibrium distributions in two subbands with different fractions of carriers excited into the upper subband, including the highly nonequilibrium case of a population inversion between the subbands (Figure 1). We also present results for the intersubband population relaxation times due to electron-electron scattering processes for a given nonequilibrium distribution, again with different fractions of excited carriers, and as a function of carrier density (Figure 2). We find that the relaxation times decrease sharply with increasing carrier density, and with higher fractions of excited carriers in the upper subband.

Combining these calculations, with calculations of the electron - LO-phonon scattering rates, and with the inclusion of the radiative emission rate and current injection rate, we may determine self-consistently the electron distributions in the steady state. This gives us the capability to investigate the operating characteristics of intersubband quantum cascade light emitting devices.



## Monte Carlo modelling of far-infrared intersubband lasers

R W Kelsall, P Kinsler and P Harrison

Institute of Microwaves and Photonics  
School of Electronic and Electrical Engineering  
The University of Leeds  
Leeds  
LS2 9JT, UK  
e-mail: r.w.kelsall@leeds.ac.uk

Recent work has demonstrated that the intersubband laser concept can be extended to operation at far-infrared (FIR) wavelengths. The design of successful FIR intersubband lasers is critically dependent on optimisation of both radiative and non-radiative electronic transitions. This requires detailed modelling work to calculate transition rates, subband populations, energy distributions and lifetimes. In this paper, we demonstrate the use of a Monte Carlo algorithm to simulate the intersubband carrier dynamics in optically pumped GaAs/AlGaAs asymmetric quantum well (AQW) FIR laser designs. The simulation includes the energy-dependent electron-phonon and electron-electron scattering rates for all intra- and inter-subband processes, as calculated using Fermi's Golden Rule. The optical (CO<sub>2</sub> laser) pumping process is included via calculation of the exact intersubband absorption matrix element, with a Gaussian lineshape assumed for the incident beam. By tracking the *k*-space trajectories of a large ensemble of electrons, the simulation predicts time dependent subband populations and their respective energy distributions which represent an *exact* solution of the semi-classical Boltzmann equation. Pauli exclusion effects are self-consistently included by frequent sampling of these distributions.

Simulations of the optical pumping of 3- and 4-level AQW laser designs clearly show the influence of carrier heating effects on laser operation. In the 3-level systems, photoexcitation of hot carriers leads to strong non-radiative scattering of electrons into the lower of the two laser levels, thus inhibiting population inversion. On the other hand, in 4-level systems designed to operate via rapid phonon-mediated depopulation of the lower laser level, carrier heating enhances depopulation, with the result that population inversion is observed, and becomes stronger with increasing pump intensity. Comparison with estimates of subband populations based on lifetime calculations alone indicates the design value of such estimates and the greater accuracy provided by the Monte Carlo method.

# Coherent Dynamics of Photoexcited Semiconductor Superlattices with Applied Homogeneous Electric Fields

T. Meier, P. Thomas, and S.W. Koch

Department of Physics and Material Sciences Center, Philipps University,  
Renthof 5, D-35032 Marburg, Germany

corresponding autor: Torsten Meier

Phone: +49-6421-282025

Fax: +49-6421-287076

e-mail: torsten.meier@physik.uni-marburg.de

Calculations of linear and nonlinear optical properties of semiconductor superlattices in the presence of homogeneous electric fields applied in the growth direction are performed on the basis of a microscopic many-body theory. The theory includes the process of optical excitation, the Coulomb interaction among the carriers, carrier-LO-phonon coupling, and the acceleration induced by the electric field [1, 2, 3, 4, 5, 6, 7]. For dc-fields the Bloch-oscillation dynamics which can be measured in THz and FWM experiments is investigated. One focus of the treatment is the analysis of different mechanisms that induce a damping of the Bloch-oscillation-induced modulations of the THz-signal. In this context the signatures of intra- and intersubband carrier-LO-phonon scattering, carrier-carrier-scattering, and disorder are investigated [1, 2, 4, 5, 7, 8, 9]. For applied ac-fields the observability of dynamical localization, which may occur for appropriately chosen alternating applied fields, using optical spectroscopy is discussed. It is shown that dynamical localization modifies the effective dimension of the superlattice exciton and that it thus should be possible to observe dynamical localization directly due to its modifications of the linear optical absorption spectrum [1]. Besides the modifications of the linear optical properties also the nonlinear THz-spectroscopy is predicted to show distinct signatures of dynamical localization [7].

Furthermore, the combined action of ac- and dc- fields is investigated. Since the ac-field couples the dc-field-induced Wannier-Stark-resonances, there are strong modifications of the linear absorption spectrum, including the possibility of spectral regions with negative absorption. It is shown that the absorption depends on the amplitude, the frequency, and on the phase of the ac-field. The transport in this regime has been discussed in the picture of multi-photon-assisted tunneling. An analysis of the THz-signal shows that this type of spectroscopy is well suited to investigate this regime and that even in the presence of excitonic effects the picture of multi-photon-assisted tunneling basically survives [7].

## References

- [1] T. Meier, F. Rossi, P. Thomas, and S.W. Koch, *Phys. Rev. Lett.* **75**, 2558 (1995).
- [2] F. Rossi, T. Meier, P. Thomas, S.W. Koch, P.E. Selbmann, and E. Molinari, *Phys. Rev. B* **51**, 16943 (1995).
- [3] K.-C. Je, T. Meier, F. Rossi und S.W. Koch, *Appl. Phys. Lett.* **67**, 2978 (1995).
- [4] J. Hader, T. Meier, S.W. Koch, F. Rossi, and N. Linder, *Phys. Rev. B* **55**, 13799 (1997).
- [5] T. Meier, P. Thomas, and S.W. Koch, *Phys. Low-Dim. Struct.* **3/4**, 1 (1998).
- [6] A. Thränhardt, H.J. Kolbe, J. Hader, T. Meier, G. Weiser, and S.W. Koch, *Appl. Phys. Lett.* **73**, 2612 (1998).
- [7] T. Meier, P. Thomas, and S. W. Koch, to be published in "Ultrafast Phenomena in Semiconductors", K.T. Tsen, ed., Springer, New York.
- [8] F. Rossi, M. Gulia, P.E. Selbmann, E. Molinari, T. Meier, P. Thomas, and S.W. Koch, *Proceedings of the 23rd ICPS*, M. Scheffler und R. Zimmermann, eds., World Scientific, Singapore, 1775, 1996.
- [9] J. Hader, P. Thomas, and S.W. Koch, *Prog. Quant. Electronics* **22**, 123 (1998)

**Terahertz Conductance of Electrically Biased Bloch Oscillating Superlattices:  
Towards a Solid State Terahertz Oscillator.**

J.S. Scott, M.C. Wanke, S.J. Allen

Center for Terahertz Science and Technology  
University of California at Santa Barbara

K. Maranowski and A.C. Gossard

Materials Department  
University of California at Santa Barbara

D. H. Chow

HRL Laboratories

To further our goal of developing a solid state terahertz oscillator, we have explored terahertz dynamical conductance of electrically biased Bloch oscillating superlattices.

Superlattices with 8 nm quantum wells and 2 nm barriers, doped at  $\sim 10^{16}/\text{cm}^3$  were grown in the AlGaAs system. A degenerate quasi-optical array is used to effectively couple radiation into the superlattice. The array is a capacitive grid in which the superlattice is inserted in the slot and ohmic contact is made to the top and bottom of the superlattice. The electrically biased quasi-optical array exhibits a current-voltage characteristic similar to that of a single element but with increased current and voltage reflecting the effective series/parallel connection of many test devices.

The terahertz dynamical conductance is measured by loading a millimeter scale terahertz confocal resonator cavity with the quasi-optical array, measuring the transmission through the cavity and modulating the cavity transmission by electrically biasing the array. The UCSB free-electron lasers provide radiation from 120 GHz to 4.8 THz and drive the cavity system.

Magneto-transport, with the magnetic field in the plane of the array and normal to the superlattice direction, is used to determine that the momentum scattering time is .16 psec at room temperature. The electric field that saturates the superlattice current allows us to determine an energy relaxation time of 0.36 psec. The current-voltage characteristics are not multivalued. Rather, the current saturates, presumably due to electric field formation.

The modulated cavity transmission has been measured from 300 GHz to 3.4 THz. Large ( $\sim 100\%$ ) changes in cavity transmission are observed at low terahertz frequencies, diminishing to small ( $\sim 1\%$ ) changes at the highest frequencies. The terahertz conductance in the absence of a DC field is taken to be Drude and the conductance at strong DC field modeled following Ktitorov et al. (The later describes the appearance of terahertz gain and loss in Bloch oscillating superlattices under electrical bias.) Quantitative agreement with the Ktitorov model is obtained until the current density saturates due to the formation of electric field domains.

This work is supported by the Office of Naval Research through the Medical Free-electron Laser Program and the Army Research Office.



## Interminiband spectroscopy of biased superlattices

M. Helm<sup>1</sup>, W. Hilber<sup>1</sup>, G. Strasser<sup>2</sup>, R. DeMeester<sup>3</sup>, F. M. Peeters<sup>3</sup>, and A. Wacker<sup>4</sup>

<sup>1</sup> *Institut für Halbleiter- und Festkörperphysik, Universität Linz, A-4040 Linz, Austria*

<sup>2</sup> *Institut für Festkörperelektronik, Technische Universität Wien, A-1040 Wien, Austria*

<sup>3</sup> *Department of Physics, University of Antwerp (UIA), B-2610 Wilrijk, Belgium*

<sup>4</sup> *Institut für Theoretische Physik, Technische Universität Berlin, D-10623 Berlin, Germany*

Quantum-well intersubband transitions undergo a Stark-shift upon application of a vertical electric field. A strongly coupled superlattice, on the other hand, shows phenomena like negative differential resistance (NDR), Bloch oscillations, and the formation of a Wannier-Stark ladder (WSL). The evolution of the interminiband absorption spectrum under these conditions has, however, not been studied to date.

*We report here the first experiment which relates electronic transport and intersubband absorption in a biased superlattice [1]. This is made possible by using a gated step-scan technique with a Fourier transform spectrometer, which allows us to record infrared absorption spectra during a short (10  $\mu$ s) electric-field pulse [2].*

Our sample is a 300-period GaAs/Al<sub>0.29</sub>Ga<sub>0.71</sub>As superlattice with 50 Å wide quantum wells and 80 Å thick barriers, modulation doped to yield  $n = 2.25 \times 10^{11}$  cm<sup>-2</sup> per period and sandwiched between two heavily doped GaAs layers. The resulting widths of the first two minibands are  $\Delta_1 = 1.2$  meV and  $\Delta_2 = 30$  meV. The second miniband is located above the barriers at the onset of the quasi-continuum.

The current-voltage characteristic shows a linear rise followed by a sequence of many sharp NDRs due to domain formation. An analysis shows that in the high-field domain, tunneling does not occur to the adjacent SL period, but rather to the first excited state in the *next-nearest* quantum well.

The infrared absorption spectrum under application of the electric field does not show the regular WSL fan-like behavior, but a more complicated set of lines, whose strength grows with the applied voltage, but whose position remains voltage independent. This is, however, consistent with the domain formation observed in the transport experiment: Since the electric field in the low- and high-field domain is fixed, an increase of the voltage only increases the extension of the high-field domain.

On the basis of a numerical calculation which reproduces the measured spectra, the observed transitions can be identified as going from the ground state to Wannier-Stark ladders in the continuum, which are strongly coupled through Zener resonances. The present experiment, extended to the far-infrared region, may set the basis for measuring the spectral response of a Bloch oscillator.

### References:

- [1] M. Helm, W. Hilber, G. Strasser, R. De Meester, F. M. Peeters, and A. Wacker, *Phys. Rev. Lett.*, **82**, 3120 (1999).
- [2] W. Hilber, M. Helm, K. Alavi, and R. N. Pathak, *Appl. Phys. Lett.* **69**, 2528 (1996).

## Coherent Bloch oscillations in GaAs/AlGaAs superlattices

T. Dekorsy, M. Först, G. Segschneider, A. Bartels, and H. Kurz  
Institut für Halbleitertechnik II, RWTH Aachen, D-52056 Aachen, Germany

<sup>L. Jönsson</sup>  
A. Ghosh and J.W. Wilkins  
Ohio State University, Columbus, Ohio, USA

K. Köhler  
Fraunhofer-Institut für Angewandte Festkörperphysik,  
D-79108 Freiburg, Germany

R. Hey and K. Ploog  
Paul Drude Institut für Festkörperphysik,  
D-10117 Berlin, Germany

We report on the femtosecond time-resolved detection of coherent Bloch oscillations in GaAs/AlGaAs superlattices. By employing new experimental techniques, we are able to gain important insight into the Bloch oscillations dynamics concerning their spatial amplitude and their direct coupling to LO phonons.

An intriguing subject is the determination of the spatial amplitude of coherently oscillating wavepackets in a superlattice. Due to Wannier-Stark localization the amplitude decreases with increasing static electric field applied to the superlattice. This subject has been carefully studied in FWM experiments [1]. Here we present a new way to determine the spatial amplitude of Bloch oscillations by a two-color fs electro-optic detection scheme. Bloch oscillations are resonantly excited in a GaAs/AlGaAs superlattice with a fs laser pulse derived from a Ti:sapphire laser. The longitudinal field associated with the coherent displacement of the wavepacket is probed by a synchronously pumped optical-parametric oscillator operating at an energy well below the bandgap (0.83 eV). The electro-optic signal based on the Pockels effect can be calibrated by a modulation of the electric field applied to the superlattice. Thus the displacement of the wavepackets can be traced quantitatively with a time resolution of 150 fs. For a tuning range of 1 THz to 3 THz we derive a decrease of the spatial amplitude from 21 nm to about 6 nm. These values are in good agreement with a quantum-mechanical calculation of the wavepackets.

The direct coupling of Bloch oscillation to optical phonons is observed in a superlattice with a wide electronic miniband of 60 meV. By employing a Ti:sapphire laser with 20 fs pulse duration and 1 GHz repetition rate we achieve an 2 orders of magnitude increase in signal-to-noise ratio for time resolved electro-optic measurements [2]. This system allows us to observe for the first time Bloch oscillations with frequencies well above the LO phonon resonance at 8.8 THz. When the Bloch frequency is tuned in resonance with the optical phonon, LO phonons are resonantly excited by the direct coupling via the longitudinal polarization. The coherent phonon amplitude decreases again for higher Bloch frequencies. The resonant excitation of phonons by Bloch oscillations is accounted for by a theoretical model including plasmon, phonons and Bloch oscillations in the superlattice [3].

[1] V.G. Lyssenko et al., Phys. Rev. Lett. **79**, 301 (1997).

[2] T. Dekorsy et al., Phys. Rev. B **50**, 8106 (1994).

[3] A. Ghosh and J.W. Wilkins, unpublished.

<sup>L. Jönsson</sup>

# Generation and Manipulation of Bloch Wave Packets

F. Löser, M. Sudzius, C.P. Holfeld, V.G. Lyssenko, K. Leo  
*Institut für Angewandte Photophysik, Techn. Universität Dresden, 01062 Dresden, Germany*

Y. Kosevich  
*Max-Planck-Institut für Physik komplexer Systeme, 01187 Dresden, Germany*

M. M. Dignam  
*Physics Department, Lakehead University, Thunder Bay, Ontario, Canada P7B 5E1*

K. Köhler  
*Fraunhofer-Institut für Angewandte Festkörperphysik, 79108 Freiburg, Germany*

Bloch oscillations as predicted by Bloch and Zener were recently [1] observed in semiconductor superlattices (SL). By applying an external electric field to this system, optical excitation creates wave packets of Wannier-Stark states which correspond to Bloch-oscillating electrons in time domain. The center of mass of these wave packets performs real-space oscillations. Recently, we have presented a technique which allows to directly follow the spatial motion [2]: By investigating the change of the spectral peak position of the Wannier-Stark-ladder (WSL) transitions, we are able to directly trace the displacement of the wave packet and prove that Zener's predictions of a harmonic spatial motion were correct.

Here, we show that the spatial dynamics of the oscillation can be manipulated by means of optical techniques: The oscillation amplitude strongly depends on the initially created wave packet composition. For excitation below and above the Wannier-Stark-ladder center, the amplitude of the wave packet oscillation is much larger than for excitation at the center of the WSL [3]. Thus, we are able to intentionally create wave packets whose dynamics reaches from breathing-mode oscillations with nearly zero amplitude to a long-distance motion over many SL periods. We theoretically show that the spatial dynamics can only be fully described if excitonic correlations are taken into account and if the scattering of the wave packet is considered. The theoretical predictions are tested in experiments where parameters like scattering time and spectral shape of the laser are varied.

- [1] J. Feldmann *et al.*, Phys. Rev. B **46**, 7252 (1992); K. Leo *et al.*, Solid State Commun. **84**, 943 (1992).
- [2] V.G. Lyssenko *et al.*, Phys. Rev. Lett. **79**, 301 (1997).
- [3] M. Sudzius *et al.*, Phys. Rev. B **57**, R12693 (1998).

Corresponding author: Christian P. Holfeld

e-mail: holfeld @ iapp.de  
 Fax/Phone: +49 351 463 7065 / 4903

*Abstract submitted to the 5-th Int. Conf. on Intersubband Transitions in Quantum Wells (ITQW'99), September 7-11, 1999, Bad Ischl, Austria*

## **QWIP FPAs for high-performance thermal imaging**

H. Schneider, M. Walther, J. Fleißner, C. Schönbein, R. Rehm, W. Pletschen, E. Diwo, K. Schwarz, J. Braunstein, and P. Koidl

*Fraunhofer-Institut für Angewandte Festkörperphysik, Tullastraße 72, D-79108 Freiburg, Germany*

J. Ziegler and W. Cabanski

*AEG Infrarot-Module GmbH, Theresienstraße 2, 74072 Heilbronn, Germany*

We report on the development of GaAs/AlGaAs quantum well infrared photodetectors (QWIPs) for infrared sensors. We have realized several QWIP camera systems for thermal imaging in the 8-12  $\mu\text{m}$  atmospheric window. These cameras show noise-equivalent temperature differences better than 10 mK and 20 mK for 256x256 and 640x512 FPAs, respectively. The excellent temperature resolutions demonstrate the high potential of QWIPs for high-performance thermal imaging. In addition, we have achieved a pixel operability of more than 99.9% without any cluster defect. Large GaAs-based QWIP FPAs can thus be produced on a stable technological platform.

In order to achieve these high temperature resolutions, our QWIPs are operated at very small electric fields (about 3 kV/cm). This low-bias operation is possible without sacrificing detectivity since the detectors have been optimized to obtain a high emission probability already at small fields. The behavior of the detectivity is obtained experimentally from the measured noise current and the responsivity of test devices. We will present theoretical estimates how these parameters determine the performance of a QWIP camera.

We also address the possibility to improve the temperature resolution even further by using QWIP structures in which the photoexcited carrier mean free path is controlled by additional epitaxial layers. While maintaining a high emission probability, these devices also have a capture probability close to 100%. We thus obtain a high detectivity in combination with a small photoconductive gain, such that the photocurrent is matched to the small charge handling capacity of the readout circuit. This adaptation is useful in particular for large arrays. In addition, these detectors are shot-noise limited since the recombination noise is suppressed. The performance of FPA sensors based on these detectors will be discussed.

*Contact person:* H. Schneider

*email:* hschneider@iaf.fhg.de *phone:* (0049) 761-5159 359 *fax:* (0049) 761-5159 400

# Recent Developments and Applications of Quantum Well Infrared Photodetector Focal Plane Arrays

**S. D. Gunapala and S. V. Bandara**

M/S 302-306, Jet Propulsion Laboratory, 4800 Oak Grove drive, Pasadena,  
CA 91109, USA

(818) 354-1880 – Voice, (818) 393-4540 – Fax  
sarath.d.gunapala@jpl.nasa.gov

## ABSTRACT

There are many applications that require long wavelength, large, uniform, reproducible, low cost, stable, and radiation-hard infrared (IR) focal plane arrays (FPAs). For example, the absorption lines of many gas molecules, such as ozone, water, carbon monoxide, carbon dioxide, and nitrous oxide occur in the wavelength region from 3 to 18 micron. Thus, IR imaging systems that operate in the long wavelength IR (LWIR) region (6 - 18 micron) are required in many space borne applications such as monitoring the global atmospheric temperature profiles, relative humidity profiles, cloud characteristics, and the distribution of minor constituents in the atmosphere which are being planned for future NASA Earth and planetary remote sensing systems. Due to higher radiation hardness, lower 1/f noise, and larger array size the GaAs based Quantum Well Infrared Photodetector (QWIP) FPAs are very attractive for such space borne applications compared to intrinsic narrow band gap detector arrays. In this presentation we will discuss the optimization of the detector design, material growth and processing that has culminated in realization of large format long-wavelength QWIP FPAs, portable and miniature LWIR cameras, holding forth great promise for myriad applications in 6-18 micron wavelength range in science, medicine, defense and industry. In addition, we will present some system demonstrations using broadband, two-color, and high quantum efficiency long-wavelength QWIP FPAs.

## New designs and applications of corrugated QWIPs

K. K. Choi, A. C. Goldberg  
US Army Research Laboratory, Adelphi MD 20783

C. J. Chen, L. P. Rokhinson, D. C. Tsui  
Princeton University, NJ 08544

N. C. Das, A. La  
NASA Goddard Space Flight Center, Greenbelt MD 20771

### ABSTRACT

Corrugated QWIPs use total internal reflection to couple normal incident light into the detectors. The coupling efficiency is independent of the pixel size and the detection wavelength. The corrugated structure thus adds simplicity, versatility and sensitivity to the quantum well infrared technology. Besides practical applications, it can also be used for basic study.

We applied the corrugated coupling to a two-stack quantum well structure. We obtained equally effective coupling in both the MW and the LW bands, with which sensitive remote temperature sensing can be performed. Temperature sensing is one of the important applications of two-color C-QWIPs.

We have fabricated two C-QWIPs with their corrugations oriented in orthogonal directions for polarization-sensitive detection. We demonstrated that for partially polarized light, the photocurrent ratio from these two detectors depends only weakly on the intensity of the radiation but much more strongly on the degree of polarization and the polarization angle. This feature of detection can be very useful in scenes with extremely small or large intensity contrast. We have used this composite detector to identify objects of different materials based on the state of polarization of the reflected light.

There have been no direct measurements on the absorption coefficient  $\alpha$  of light traveling parallel to the QWIP material layers (as occurred in an efficient coupling scheme). By measuring the responsivity of C-QWIPs with different sidewall separations, we obtained the intensity decay function of light propagating away from each sidewall, with which  $\alpha$  of different QWIP materials can be directly measured.

$256 \times 256$  C-QWIP FPAs with different wavelengths were demonstrated. Infrared imageries with good aesthetic attributes were obtained. Besides the reduction of dark current, the measured internal QE of a C-QWIP is also high, usually above 20%. This value of QE is in agreement with rigorous electromagnetic field simulations.

We have also investigated new C-QWIP designs with different sidewall profiles. From the principle of parity symmetry, any symmetric sidewall profiles will give an optical interference minimum at the center of two opposing sidewalls. In order to further improving the C-QWIP sensitivity, additional vertical trenches are etched into the C-QWIP structure to remove those active materials that do not produce photocurrent. The result of this approach will be presented. We have also investigated several dielectrics for conformal contact isolation. We found that with a suitable dielectric, the entire corrugated structure can be covered with metal, which tends to further increase the detector sensitivity by about 40 %.

# Optical interference and nonlinearities in quantum well infrared photodetectors

M. Ershov, A. G. U. Perera, V. Letov, S. G. Matsik, W. Z. Shen  
Department of Physics and Astronomy, Georgia State University  
Atlanta, GA 30303, USA

H. C. Liu, M. Buchanan, and Z. R. Wasilewski  
Institute for Microstructural Sciences, National Research Council  
Ottawa, Ontario K1A 0R6, Canada

Photoconductivity of quantum well infrared photodetectors (QWIPs) is determined by the photogeneration rate from the QWs and the transport of the photoexcited carriers. Both of these processes are influenced by the spatial distribution of optical power across QWIP, which can be nonuniform due to the light reflection and interference. The effect of optical interference on QWIP performance has been demonstrated recently [1]. Conventional theories of QWIPs are incapable to explain this effect, since they assume the constant photogeneration rate. The purpose of the present work is investigation of the effect of optical interference on nonlinear properties of QWIPs.

We consider GaAs/AlGaAs QWIPs with multiple QWs illuminated by a monochromatic coherent radiation (from CO<sub>2</sub>-laser) in a 45-degree coupling geometry. The reflection of light from the top metal contact creates an interference pattern in the QWIP active region with a strong variation of optical power. Numerical simulation shows that when the photocurrent is less than the dark current, the total excitation rate is due to thermal excitation, and electric field is distributed uniformly. The photocurrent is proportional to the total optical power within QWIP [2], and is not sensitive to the details of optical power profile. This case corresponds to the linear regime of QWIP operation. However, when the photocurrent dominates over the dark current, the generation rate and the excited carrier concentration are not uniform, resulting in the redistribution of the electric field across QWIP. As a result, the electric field is strongly reduced in the illuminated regions, causing the decrease of escape probability and drift velocity. The field in the unilluminated regions is increased and enhances the thermo-emission [2]. These factors lead to the saturation of photocurrent with incident power, and, therefore, to the decrease of responsivity. Furthermore, the signal-to-noise ratio is also decreased, resulting in an increase of the noise equivalent power (NEP). Both the photocurrent gain  $g_p$  and the noise gain  $g_n$  are suppressed, and their ratio  $g_p/g_n$  becomes less than unity.

The effects of optical interference can be important in the case of non-monochromatic excitation for QWIPs with a narrow absorption linewidth. Optical interference can be detrimental for QWIP applications when the total current is dominated by the photocurrent, such as heterodyne detection and low-temperature operation. Several recently observed effects (increase of NEP in heterodyne detection, and responsivity decrease at low temperature) can be explained by the effects considered in this work. Our theoretical considerations will be supported by experimental investigations.

This work has been supported in part by NSF (grant #ECS 9809746).

- [1] H. Schneider et al., Appl. Phys. Lett. **74**, p. 16 (1999).
- [2] M. Ershov, Appl. Phys. Lett. **73**, p. 3432 (1998).

# MONTE CARLO PARTICLE MODELING OF ELECTRON TRANSPORT AND CAPTURE PROCESSES IN AlGaAs/GaAs MULTIPLE QUANTUM WELL INFRARED PHOTODETECTORS

M. Ryzhii and V. Ryzhii

Computer Solid State Physics Laboratory  
University of Aizu  
Aizu-Wakamatsu City, 965-8580, Japan

Electron transport and capture processes play important roles in the performance of quantum well infrared photodetectors (QWIPs). The dark current in QWIPs, their responsivity, and photoelectric current gain are directly determined by the probability of the electron capture into the QWs. The dependence of the capture probability on the electric field strongly affects the spatial distribution of the self-consistent electric field in QWIPs.

The dominant mechanism of the capture of electrons in QW structures is associated with the electron transitions from the continuum states into the bound states in the QWs due to the optical phonon emission. Thus, the capture rate depends not only on the microscopic probability of the electron continuum-to-bound transitions, but on the number of electrons having the energy  $\epsilon$  less than the optical phonon energy  $\hbar\omega_0$  as well. As a result, the capture rate essentially depends on the energy distribution of electrons in the continuum states. This distribution changes with varying electric field,

In this work, we present the results of the study of the vertical electron transport and the electron capture in multiple QWIPs using an ensemble Monte Carlo (MC) modeling. We calculated the dependences of the vertical electron drift velocity  $v_d$  and the commonly used capture parameter  $p_c$  (macroscopic capture probability) as functions of the electric field. The QW structures under consideration consist up to 100 GaAs QWs separated by relatively thick AlGaAs barriers. The MC model employed uses the band structure and scattering parameters of GaAs and AlGaAs taken from previous publications adjusted for liquid nitrogen temperatures. The electron transport in the continuum states is considered in the framework of the  $\Gamma$ -, L-, and X- valleys conduction band. The number of the particles used in the MC calculations is 50,000. The original part of the model includes the interaction of the incident electrons with the QWs. This interaction results in the capture, reflection, and transmission of electrons passing the QWs. The L- and X-electrons are assumed to be uncaptured. The reflection and transmission coefficients for the  $\Gamma$ -electrons as functions of their energy are calculated on the base of the Kane model. The reflection (transmission) of the L- and X-electrons from the QWs is considered classically due to relatively large effective masses of such electrons.

The calculated vertical mobility and saturation velocity of electrons in AlGaAs/GaAs QWIPs are markedly lower than those in bulk AlGaAs. It is shown that the main mechanism of the reduction of the vertical drift velocity in the QW structures is associated with the electron reflection from the QWs. The capture parameter exhibits dramatic roll-off with increasing electric field attributed to the redistribution of electrons over the energies with a substantial decrease of the fraction of the low-energy  $\Gamma$ -electrons. The presence of ionized donors in the inter-QW barriers can essentially influence the electron transport and capture in QWIPs with relatively thick barriers due to a significant corrugation of the conduction band edge.

The obtained field dependences of  $v_d$  and  $p_c$  match the available experimental data. These dependences can be incorporated in the QWIPs models using analytical and numerical drift-diffusion approaches.



## Quantum Interference Phenomena in Electron Intersubband Transitions

W. Pötz

Physics Department

845 W. Taylor Str.

University of Illinois at Chicago, U.S.A.

Fax: (312) 996-9016; e-mail: wap@uic.edu

In the quantum transport regime, transition rates between different energy levels depend on the relative phase of competing coupling mechanisms. It is reached when one probes a system on a timescale at or below its characteristic phase breaking time. In a semiconductor, this typically occurs on a pico- or subpicosecond timescale. This fundamental principle of quantum mechanics significantly alters material properties on short timescales and offers an additional "control knob" to control optical and transport properties in form of the relative phase between competing pathways.[1] For example in semiconductors, coherent control of photocurrent has been demonstrated in this fashion.[2, 3]

A non-phenomenological theoretical description and account of quantum interference and control phenomena calls for a microscopic treatment of the intricate dynamics brought forth by this many-body problem, including electron-electron and electron-phonon interactions. Based on a microscopic theory of nonequilibrium carrier dynamics in confined semiconductor structures we show feasibility of coherent control of electron inter(sub)band transitions via several control schemes.[?] Combined with structural design coherent control of a variety of physically relevant quantities, such as optical absorption, optical gain, THz emission, and final-state selection has been predicted.[5, 6, 7, 8] In addition, processes which are unique to solids, such as phonon emission in intersubband transitions, can be controlled coherently.[9] In this case, the transfer of electrons from a subband doublet to a lower-lying subband can be controlled by the phase of a coherent microwave field which resonantly couples the doublet. Here, quantum interference occurs between electron-phonon and electron-photon interaction. Variations of the net phonon emission rate by up to a factor of two has been predicted.

In addition, we explore theoretically to what extent absorption lineshapes can be manipulated by *structural design* of semiconductor heterostructures. We use GaAs/AlGaAs multiple quantum well structures to establish the presence of Fano resonances associated with electronic intersubband transitions. Guided by Young's double-slit experiment, we identify increasingly improved structures to display Fano resonances.

## References

- [1] See, for example, *Coherent Control in Atoms, Molecules, and Semiconductors*, edited by W. Pötz and W. A. Schroeder, (Kluwer, Dordrecht, 1999).
- [2] E. Dupont, P. B. Corkum, H. C. Liu, M. Buchanan, and Z. R. Wasilewsky, *Phys. Rev. Lett.* **74**, 3596 (1995).
- [3] A. Hachè, Y. Kostoulas, R. Atanasov, J. L. P. Hughes, J. E. Sipe, and H. M. van Driel, *Phys. Rev. Lett.* **78**, 306 (1997).
- [4] W. Pötz, *Phys. Rev. B* **54**, 5647-5664 (1996).
- [5] W. Pötz, *Phys. Rev. Lett.* **79**, 3262-3265 (1997).
- [6] X. Hu and W. Pötz, *Appl. Phys. Lett.* **73**, 876-878 (1998).
- [7] W. Pötz, *Appl. Phys. Lett.* **72**, 3002-3004 (1998).
- [8] W. Pötz, *Appl. Phys. Lett.* **71**, 395-397 (1997).
- [9] X. Hu and W. Pötz, *Phys. Rev. Lett.* **82**, 3116-3119 (1999).

This work has been supported in part by the U.S. Army Research Office.

# Observation of Electromagnetically induced transparency in a three-subband semiconductor quantum well.

C.C. Phillips<sup>a</sup>, E. Paspalakis<sup>a</sup>, G.B. Serapiglia<sup>a</sup>, C. Sirtori<sup>b</sup>, and K.L. Vodopyanov<sup>a</sup>,

<sup>a</sup> Physics Department, Imperial College, London SW7 2BZ, UK  
tel +44-171-594 7575 /fax 7580, e-mail chris.phillips@ic.ac.uk

<sup>b</sup> Laboratoire Central de Recherches, Thompson-CSF, Domaine de Corbeville,  
91404 Orsay CEDEX, France

Electromagnetically induced transparency (EIT), typically uses a strong "coupling" EM field in atomic systems to establish a quantum coherence between e.g. levels ( $|2\rangle$  and  $|3\rangle$ ) of a 3-level "cascade" system. This controls the linear optical properties at photon frequencies close to e.g. the

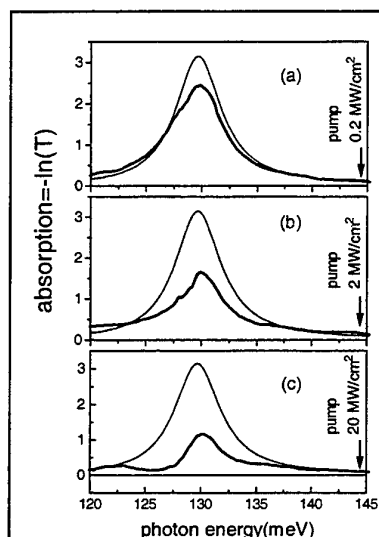


**Fig.1. Evolution, with coupling laser power, of the 1-2 intersubband absorption line with the coupling laser tuned to the 2-photon 1-3 subband resonance. Thin line linear 1-2 absorption without coupling laser**

$|1\rangle \rightarrow |2\rangle$  absorption resonance and can render an opaque medium transparent, and dramatically modify its refractive index<sup>1</sup>. By eliminating linear absorption at resonance, EIT allows  $\chi^{(2)}$  resonant optical non-linearities to be exploited and because optical gain can be available without linear absorption, EIT allows for true inversionless lasing.

We report for the first time, the observation of EIT in a QW system. ISB transitions are unattractively broad for EIT studies, but have the advantage that the dipole matrix elements and energies of the participating transitions can be engineered at will. We use a InGaAs/AlInAs MQW<sup>2</sup>, with subband spacings  $E_{12} = 130$  meV and  $E_{23} = 163$  meV. Driving these with  $\sim 90$  psec "Coupling" ( $\omega_c$ ) and "probe" ( $\omega_p$ ) laser pulses from a mid-IR optical parametric generator<sup>3</sup> at  $\sim 20$  MW/cm<sup>2</sup> gave a Rabi frequency  $\mu E/\hbar \sim 6$  meV/ $\hbar$  which compares with the  $\sim 13$  meV linewidth of the 1-2 transition. The absorption changes were measured by spectrally scanning the weak probe pulse.

With  $\hbar\omega_c \sim E_{12}$  the  $E_{12}$  absorption line saturates readily but only a weak EIT effect was seen. With  $\hbar\omega_c \sim E_{23}$  (i.e the classic Autler-Townes scheme), no EIT effect was seen but with  $2\hbar\omega_c \sim E_{13}$  the  $\sim E_{12}$  absorption line develops a pronounced EIT quantum interference feature, spectrally narrower than the bare  $E_{12}$  absorption linewidth, the depth of which increases with coupling laser intensity (Fig.1).

In the lattercase, because the QW states are, to within a transition linewidth, equally spaced in energy, all 3 states are *simultaneously* driven into quantum coherence by the coupling field and we believe that this is a crucial factor in observing EIT with these comparatively broad transitions. The data are accurately modelled with a numerical density-matrix EIT spectrum calculation, using only experimentally derived energies and dephasing parameters and which includes the 2-photon coupling mechanism for the first time. The potential impact of this effect on ISB lasers and other non-linear devices will be discussed.

We report also similar pump-probe spectroscopy studies on samples where non-parabolicity allows the  $k_{||}$  distribution of electrons in a 3 subband system to be inferred from their absorption energies. Distinct "phonon-bumps", arising from sequential LO phonon emission in inter- and intra-subband scattering events are clearly resolved. By coupled rate-equation modelling of the spectral strengths and broadening behaviours of these and the induced  $E_{23}$  absorption features, critical scattering rate and non-equilibrium phonon density data are extracted which have important implications for the design of ISB based devices.

<sup>1</sup> See e.g. S.E. Harris, Physics Today, June 1997, p.36

<sup>2</sup> J. Faist, F. Capasso, C. Sirtori, D.L. Sivco, A.L. Hutchinson, S.N.G. Chu, and A.Y. Cho, Appl. Phys. Lett. **63**, 1354 (1993)

<sup>3</sup> K.L. Vodopyanov, and V. Chazapis, Opt. Commun. **135**, 98 (1997)

## Quantum computation with quantum dots and Terahertz cavity quantum electrodynamics

Mark Sherwin (1,2) and Atac Imamoglu (1,2)

(1) Physics Department and Center for Spintronics and Quantum Computation,  
UCSB

(2) ECE Department, UCSB

The last couple of years have seen an explosion of interest in the field of quantum computation. The interest is driven by the possibility of making devices which process quantum information, and which could possibly perform tasks which are impossible for devices which process classical information (for example, the computer on which this abstract is being written). Examples of potential applications include provably secure encryption, factoring large numbers, and sorting large databases. A number of implementations have been proposed using trapped atoms and ions, liquid phase NMR, electrons on the surface of liquid helium, semiconductors, and superconductors.

I will present a proposal in which a bit quantum information (a qubit) is stored in the two lowest energy levels of a single electron confined in a quantum dot (QD). Many such QDs are placed in a microcavity which resonates at Terahertz frequencies. A pair of gates controls the energy levels in each QD. An arbitrary rotation of the state vector of a single qubit can be effected by applying a voltage pulse to a gate which tunes the energy-level difference between QD states into resonance with a laser at frequency  $\omega_L$ . A "controlled not" (CNOT) operation between an arbitrary pair of qubits in the quantum computer can be effected by a sequence of voltage pulses which tune the energy level difference between QD states into resonance with modes of the cavity at frequency  $\omega_c$  or the laser at  $\omega_L$ . Together, the one- and two qubit operations form a "universal" set of quantum logic gates, meaning that an arbitrary computation could be carried out by a sequence of these gates. The duration of a CNOT operation is estimated to be much shorter than the time for an electron to decohere by emitting an acoustic phonon.

As with all proposals for quantum computation, the obstacles to implementation of this one are formidable. A research program at UCSB is currently aimed at growing and characterizing QD structures which might become qubits in the quantum computer described above. The status of this research will be discussed.

This research is supported by the Army Research Office under grant ARO DAAG55-98-1-0366, and a David and Lucile Packard Foundation Fellowship (A. I.).

## SECOND-HARMONIC GENERATION IN InAs/GaAs SELF-ASSEMBLED QUANTUM DOTS

**T. Brunhes, P. Boucaud, and S. Sauvage**

Institut d'Électronique Fondamentale, UMR CNRS 8622, Bât. 220,  
Université Paris-Sud, 91405 Orsay, France.

**F. Glotin, R. Prazeres, and J.-M. Ortega**

CLIO/LURE, Bât. 209 D, Université Paris-Sud  
91405 Orsay, France.

**A. Lemaître, and J.-M. Gérard**

France Telecom, CNET Bagneux,  
196 Av. H. Ravera, 92225 Bagneux, France.

**V. Thierry-Mieg**

Laboratoire de Microstructures et Microélectronique, UPR CNRS 20,  
196 Av H. Ravera, 92225 Bagneux, France.

Optical transitions, referred to as intraband transitions, can take place between the confined levels in the conduction band or in the valence band of self-assembled quantum dots. Absorption measurements have shown that both z-polarized and in-plane polarized intraband transitions can be optically active in the mid-infrared spectral range.

Apart from the absorption spectroscopy, one may wonder if optical nonlinear susceptibilities associated with intraband transitions can be as large as those associated with intersubband transitions in quantum wells. Three factors support the existence of large nonlinearities : i. the dipole matrix elements of the intraband transitions are of the order of a fraction of nm ; ii. resonance conditions between intraband transitions and the optical exciting field can be eventually achieved ; iii. the homogeneous broadening of the intraband transitions is expected to be very small due to the predicted slowing of the intradot relaxation.

In this work, we have investigated second-harmonic generation in InAs/GaAs self-assembled quantum dots. The studied samples consist of n-doped, p-doped and undoped InAs/GaAs quantum dots grown by molecular beam epitaxy. The quantum dot layers are embedded in a mid-infrared waveguide. The nonlinear optical experiments have been carried out with the free-electron laser CLIO.

Mid-infrared second-harmonic generation associated with the quantum dots was observed in p-type samples. Frequency doubling is obtained for a pump beam polarized either in the layer plane or along the quantum dot growth axis. The most efficient conversion process occurs for an in-plane excitation at 168 meV (7.4  $\mu\text{m}$  wavelength). The second-order nonlinear susceptibility associated with this resonant process is experimentally deduced by comparison with the bulk GaAs nonlinear susceptibility. A susceptibility as large as  $2 \times 10^{-7}$  m/V is deduced for one quantum dot layer plane.

The experimental results are interpreted on the basis of a three-dimensional numerical calculation of the confined states in the lens-shaped quantum dots. We show that the nonlinear susceptibility is enhanced by the resonance with the in-plane polarized  $h_{000}-h_{101}$  and  $h_{101}-h_{29}$  intraband transitions. The theoretical nonlinear susceptibility is found in agreement with the experimental one.

The second-order susceptibility enhancement will be compared to the one observed for third-harmonic generation in p-type quantum dots. These measurements demonstrate the potentialities of self-assembled quantum dots for nonlinear optics in the mid-infrared.

## Intersubband electro absorption and retardation in coupled quantum wells: The role of interface scattering

R. Kapon\*, N. Cohen\* V. Thierry-Mieg\*\*, R. Planel\*\* and A. Sa'ar\*

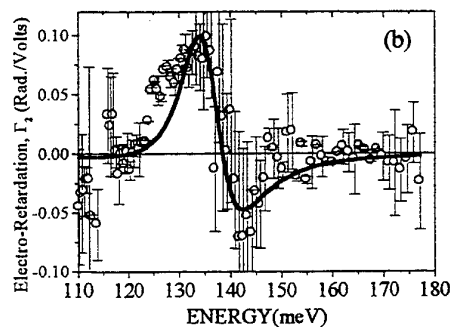
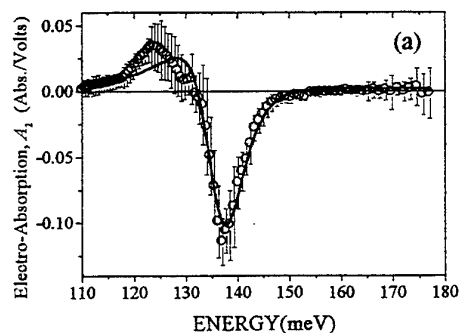
\* Department of Applied Physics, The Fredi and Nadine Hermann School of Applied Science, The Hebrew University of Jerusalem, Jerusalem 91904, Israel

\*\* Laboratoire de Microstructures et Microelectronique - CNRS, 196 Avenue H. Ravera, BP107, 92225 Bagneux, France

The large second order optical nonlinearities associated with intersubband transitions in quantum wells can give rise to efficient electro-optical modulation of infrared light in properly designed structures. However, there are several fundamental processes such as the Stark shift of the energy levels, charged carrier transfer, quantum interference and linewidth broadening that can contribute to the modulation process. In addition, due to the resonant nature and the inherent anisotropy of intersubband transitions, electro-optical modulation originates from either electro-absorption or electro-retardation or both.

In this work we present a systematic experimental study aimed at resolving the various contributions to electro-optical modulation in a multiple coupled quantum wells structure. Using a set of eight-cross/parallel polarizer-analyzer measurements we were able to resolve the spectral dependency of the dc electric field induced absorption and phase-retardation due to intersubband transitions. The measured values of these coefficients are shown in Fig. (a) and (b) below respectively (symbols).

Results of our experiment were fitted to a model that allows all quantum properties of the structure, i.e., energy levels, envelope states, carrier densities and linewidths, to vary with the external dc electric field. Each one of these effects gives rise to a different spectral behavior in the resulting electro-optical modulation thus allowing us to estimate the strength of its contribution to the overall modulation. The results of the fitting process, shown by the solid lines in Figs (a) and (b), suggest that apart from the Stark effect, a major contribution to the modulation process comes from the linewidth broadening effect. The estimated coefficient associated with this process is 0.76 meV/Volts. We propose a simple model that correlates this effect with alloy disorder and interface roughness scattering that give rise to electron dephasing. The larger degree of electron localization near the interfaces in the presence of a dc electric field is responsible for this effect.



## GaAs Quantum cascade lasers

C. Sirtori, P. Kruck, S. Barbieri, M. Beck, P. Collot, J. Faist, and J. Nagle  
Thomson-CSF, Laboratoire Central de Recherches, 91404 Orsay, France

The Quantum Cascade (QC) laser is an excellent example of how quantum engineering can be used to design and develop new laser materials in the mid-ir. By controlling the quantum well widths and the tunnelling barrier thickness it is possible to create artificial potentials where level separations, dipole matrix elements, lifetimes and scattering times are mainly dependent on the potential design. This allows to conceive new materials (*material by design*) where electronic and optical properties can be tailored not only for demonstrate new physical effects but also to optimise device performance.

The material system in which QC lasers have been first demonstrated and subsequently developed is InGaAs/InAlAs grown lattice matched on InP. However the nature of QC lasers is not bound to a specific material system and therefore it is possible to reproduce these devices in other material systems. Recently we demonstrated laser action in structures made of GaAs/Al<sub>x</sub>Ga<sub>1-x</sub>As. The use of this material gives an additional technological value to QC lasers since GaAs technology is the most widespread and low-cost of all III-V compound semiconductors and presently represents more than 90% of the world-wide market for semiconductor lasers in terms of produced units.

Device performance are anyhow affected by the material properties. Especially the high aluminium content cladding layers have important consequences on characteristics due to the presence of deep donor levels (DX centers). Electrons trapped in these defects can be released upon white light illumination, with strong consequences on threshold current densities and slope efficiencies. To avoid this instability has been removed using a new waveguide concept based entirely on plasmon enhanced confinement, where the optical confinement is achieved without AlGaAs cladding layers. In these devices peak output power in excess of 600mW has been observed at 77 K, with threshold current density of 5 kA/cm<sup>2</sup>. The maximum operating temperature is 200K.

## Intersubband and interminiband GaAs/AlGaAs quantum cascade lasers

G. Strasser, S. Gianordoli, L. Hvozda, W. Schrenk, K. Unterrainer,  
and E. Gornik

Institut für Festkörperelektronik, TU Wien, Wien, Austria

Email: Gottfried.Strasser@tuwien.ac.at

Since the development of unipolar semiconductor lasers based on intersubband transitions in quantum wells [1], continuous progress in device operation and performance of these so-called quantum cascade lasers has been achieved, reaching from the realization of superlattice lasers based on interminiband transitions [2] up to non-cascaded structures with only one single optical transition [3]. However, till 1998 lasing was restricted to a single material system, InGaAs/InAlAs lattice matched to InP. The realization of unipolar light emitter based on the model material system GaAs/AlGaAs showing electroluminescence [4], optically pumped [5] and finally electrically pumped [6] lasing in GaAs/AlGaAs structures was reported lately.

We intend to present here the design, growth and operation of unipolar semiconductor lasers based on the material system GaAs/AlGaAs. The intersubband structure essentially follows the design considerations given by the Bell Labs group [1,3] with the modifications necessary due to the different material system. The GaAs/AlGaAs intersubband laser working at a wavelength of 10 micrometer consist of a three quantum well active region comparable to the one given in [6]. The active cells are separated by miniband funnel injectors and the whole structure is embedded into conducting cladding layers to ensure proper electron injection and waveguiding. Subsequently grown intersubband laser with nominally identical active zones are used to compare different cladding structures.

Additionally to the intersubband lasers we intend to report on the first GaAs based interminiband laser. To have miniband formation under external electric field the active superlattice region is chirped as described in Ref. [2] for the InGaAs/InAlAs material system. As cladding layers highly doped GaAs layers are used to embed the active regions. These interminiband laser with undoped superlattice regions work at a wavelength of 13 microns, the longest wavelength of a GaAs laser so far.

All laser structures are characterized by measuring current-voltage characteristics as well as integral and spectral optical outputs. Spectral measurements are performed using a Fourier-transform step-scan spectrometer. Light is collected using  $f/0.7$  optics and focused on a LN<sub>2</sub> cooled HgCdTe detector. For all structures lasing is achieved below 10 kA/cm<sup>2</sup> current density and the collected output power values are well above 0.1 W per facet.

[1] J. Faist et al., Science **264**, 553 (1994)

[2] G. Scarmacio et al, Science **276**, 773 (1997), A. Tredicucci et al, Appl. Phys. Lett. **74**, 638, (1999)

[3] C. Gmachl, et al, Appl. Phys. Lett. **73**, 3830, (1998)

[4] G. Strasser, et al., Appl. Phys. Lett. **71**, 2892, (1997)

[5] O. Gauthier-Lafaye et al, Appl. Phys. Lett. **74**, (1999)

[6] C. Sirtori et al., Appl. Phys. Lett. **73**, 3486 (1998)

## Spectroscopic Studies of GaAs/AlGaAs Quantum Cascade Structures.

L.R.Wilson, P.T.Keightley, J.W.Cockburn, J.P.Duck, M.S.Skolnick

*Department of Physics and Astronomy, University of Sheffield, Sheffield S3 7RH, UK.*

J.C.Clark, G.Hill, M.Moran, R.Grey

*Department of Electronic and Electrical Engineering, University of Sheffield, Sheffield S1 3JD, UK.*

We have used complementary intersubband and interband optical measurements to study the bias dependence of the carrier distribution and energy level alignment within a GaAs-AlGaAs quantum cascade (QC) LED. Intersubband photocurrent (PC) measurements probe the active region up to the threshold for current flow. At higher bias, interband photoluminescence (PL) and intersubband electroluminescence (EL) measurements enable optical transitions involving states in the bridging region to be studied. The success of these measurements is enabled by the high quality of our GaAs/AlGaAs based structures which exhibit linewidths of  $\sim 5\text{meV}$  as compared to the  $10\text{-}15\text{meV}$  found in the commonly used InGaAs/AlInAs structures. The principal results of the work are:

- At low bias ( $V \sim 0\text{V}$ ), an almost complete transfer of electrons from the dopant atoms in the bridging region to the electron ground state in the active wells occurs.
- With increasing forward bias, the electrons are redistributed throughout the bridging region and upper states in the active wells.
- At turn-on in the current-voltage characteristics, electron levels in the bridging region and the active well become aligned.
- The measured bias dependence of transition energies is in good agreement with that calculated from self-consistent Poisson-Schrödinger simulations.

In addition to this work we have also fabricated and studied a number of QC lasers. GaAs-AlGaAs devices exhibit threshold current densities of  $\sim 6\text{kA/cm}^2$  at  $10\text{K}$ , and lase up to a temperature of  $200\text{K}$ . This improved laser performance coupled with higher light output power relative to published work indicates the high quality of both the growth and processing of our samples. A sudden increase in threshold current at  $\sim 180\text{K}$  is observed for these devices. This is contrary to the behaviour seen in our InGaAs-AlInAs QC lasers which show a gradual increase in threshold current up to room temperature. Further investigations are in progress to identify the reasons for the different temperature performance of lasers based on the two materials systems.



### Interband Cascade Lasers: Progress and Challenges

Rui Q. Yang, J. D. Bruno, J. L. Bradshaw, J. T. Pham, D. E. Wortman

*U.S. Army Research Laboratory, 2800 Powder Mill Rd, Adelphi, MD 20783-1197*

Interband cascade (IC) lasers, utilizing optical transitions between the conduction and valence bands in a staircase of Sb-based type-II quantum well (QW) structures, represent a new class of semiconductor mid-IR light source. IC lasers reuse each injected electron by making use of the broken band-gap alignment in type-II QWs to form cascade stages, leading to a quantum efficiency greater than the conventional limit of unity. Furthermore, they can circumvent the fast phonon scattering loss in intersubband lasers and suppress Auger recombination through band-structure engineering. Thus, mid-IR IC lasers are promising for obtaining high output power. Since their first demonstration in early 1997, IC lasers have been improved with encouraging results. However, their potential has been exploited to a much lesser degree compared to other semiconductor lasers.

In this presentation, we will describe the recent progress of IC lasers grown in a Varian Gen-II MBE system at ARL, which have exhibited significantly higher differential quantum efficiencies and peak powers than previous IC lasers. These mid-IR (3.8-3.9  $\mu\text{m}$ ) IC lasers based on type-II InAs/GaInSb QWs were able to operate at temperatures up to 217 K, which is higher than the previous record (182 K) for an IC laser at this wavelength. We observed from several devices at temperatures above 80 K, a slope greater than 750 mW/A per facet, corresponding to a differential external quantum efficiency exceeding 460%. A peak optical output power exceeding 4 W/facet was observed from a device at 80 K, which is the highest ever reported from any single mid-IR diode laser at emission wavelengths beyond 3 microns. Also, most devices were able to operate repeatedly without suffering from damage at high currents ( $>10 \text{ kA/cm}^2$ ) in contrast to previously reported IC lasers. However, threshold current densities from devices are still significantly larger than theoretical calculations and even higher than the lowest value observed from previously reported lasers. We will discuss challenging issues related to reducing threshold and power dissipation to achieve CW type-II IC lasers.

# Antimonide Interband and Intersubband Mid-IR and Terahertz Lasers

I. Vurgaftman, C. L. Felix, W. W. Bewley, E. H. Aifer, L. J. Olafsen,  
D. W. Stokes, J. R. Meyer, M. J. Yang, and H. Lee<sup>†</sup>

Naval Research Laboratory, Washington, DC 20375

<sup>†</sup>Sarnoff Corporation, Princeton, NJ 08543-5300

We report significant improvements in the performance of antimonide mid-IR lasers with "W" active regions. For optical pumping, cw operation is observed nearly to room temperature (290 K) at  $\lambda = 3.0 \mu\text{m}$  and to  $T_{\text{max}} = 130 \text{ K}$  at  $7.1 \mu\text{m}$ . At  $\lambda = 3.2 \mu\text{m}$  and  $T = 77 \text{ K}$ , cw output powers as high as 0.5 W are obtained. Cavity-length measurements confirm that the primary factor limiting the performance of these type-II interband lasers is a high internal loss ( $\geq 90 \text{ cm}^{-1}$  at  $T = 300 \text{ K}$ ) associated with valence intersubband transitions. We discuss the modeling of these processes, and propose modified structures that are predicted to suppress the intervalence resonances. An alternative approach, which completely eliminates the intervalence absorption, is to construct an antimonide quantum cascade laser. Detailed simulations indicate that the small mass and large conduction-band offset characteristic of InAs/AlAsSb quantum wells can be exploited to increase both the intersubband optical matrix element (gain) and the phonon non-radiative lifetime. The calculated threshold current density of  $1.2 \text{ kA/cm}^2$  for a  $\lambda = 8.8\text{-}\mu\text{m}$  emitter should allow cw operation up to ambient temperature.

While intersubband lasers are quite attractive for wavelengths in the 5-20  $\mu\text{m}$  range, our modeling predicts that interband lasers will eventually regain the advantage at even longer wavelengths in the THz regime. There the dominant QCL non-radiative relaxation process, in which two electrons in the upper subband each scatter to the lower subband with opposite momentum transfers, is non-activated and has a much shorter lifetime at low temperatures than that for the thermally-activated Auger process that dominates in interband devices. Type-II W THz lasers should therefore achieve much higher optical gain, and also superior confinement of the optical mode when a low-index substrate is used for the bottom cladding layer and diamond for the top cladding layer. Testing on mid-IR devices has already demonstrated that the diamond-pressure-bonding (DPB) technique not only provides an excellent thermal bond, but also allows topside optical pumping through the diamond heat sink.

Because THz quantum well lasers will tend to be somewhat gain-starved, loss minimization is even more critical than in the mid-IR. Fortunately, intervalence absorption is energetically forbidden for very small photon energies, hence the dominant mechanism should be free-carrier absorption assisted by interface roughness scattering. Detailed quantum calculations show that for TE polarization and sheet carrier densities of a few times  $10^{10} \text{ cm}^{-2}$  (required to reach threshold), the standard semiclassical expression overestimates the absorption coefficient by as much as a factor of 2. We predict that a  $\lambda = 27\text{-}\mu\text{m}$  W laser should operate pulsed up to 60 K, cw to 35 K, and emit powers exceeding 100 mW. Operation at 4.2 K is projected to wavelengths as long as 100  $\mu\text{m}$ .

## Mid-infrared intersubband electroluminescence in InAs/GaSb/AlSb type-II cascade structures

K. Ohtani\* and H. Ohno

*Laboratory for Electronic Intelligent Systems, Research Institute of Electrical Communication, Tohoku University, Katahira 2-1-1, Aoba-ku, Sendai 980-77, Japan*

We report *intersubband* electroluminescence in InAs/GaSb/AlSb type-II cascade structures. The light source based on intersubband transition in type-II InAs/GaSb/AlSb heterostructures offers a number of advantages over type-I GaInAs/AlInAs quantum cascade laser (QCL) [1], [2]. The InAs/GaSb type-II broken gap heterostructure blocks electrons injected into excited state in the quantum well reducing the current leakage path and extracts efficiently from the ground state by interband tunneling. Also the InAs/AlSb type-II staggered heterostructure has a wide tunability of intersubband transition energy due to the large conduction band offset ( $\sim 1.35\text{eV}$ ). A recent theoretical appraisal of type-II Sb-based intersubband lasers shows that the threshold current is almost a factor 4 lower than the theoretical prediction for the type-I QCL [3].

The samples were grown on undoped InAs(100) substrates by a solid source molecular beam epitaxy system. After growth of 700nm Si-doped ( $3 \times 10^{17}\text{cm}^{-3}$ ) n-type InAs as a bottom contact layer, 10 period of injector structure and active layers were grown. The injector structure consisted of digitally graded InAs/AlSb superlattices in which the InAs layers were Si doped to  $n=2 \times 10^{17}\text{cm}^{-3}$ . The active layer consisted of an InAs/GaSb coupled QW which was made of 10ML AlSb barrier, 30ML InAs quantum well, 25ML GaSb quantum well, and 5ML AlSb barrier. After growth of the injector/active layer structures, 200nm Si-doped ( $3 \times 10^{17}\text{cm}^{-3}$ ) InAs layer was grown as a top contact layer. The grown structures were processed into  $300\mu\text{m} \times 300\mu\text{m}$  mesa by wet etching and the photolithography. The sample edge was then polished  $45^\circ$  wedge for light emission measurements.

The electroluminescence measurement was performed with Fourier transform infrared (FT-IR) spectrometer using lock-in detection technique. Current pulse at 15kHz with duty cycle of 50% was used for electroluminescence measurements. An emission peak at 77K was observed at 233meV, corresponding to the wavelength of  $5.6\mu\text{m}$  with full-width at half-maximum (FWHM) being 14meV. The emission peak energy was in close agreement with the transition energy (218meV) between the ground state and the first excited state of InAs QW using multi-band  $k \cdot p$  theory. The position of the peak shows a small red shift with increasing injection current. The spectrum was polarized mostly perpendicular to the layer, which shows that the light emission is due to the intersubband optical transition. The spectrum shape of the intersubband cascade luminescence was found to be narrower and more symmetric compared to that of the interband cascade luminescence of the same wavelength range.

[1] H. Ohno, L. Esaki, and E. E. Mendez, Appl. Phys. Lett. 60, 3153 (1992)

[2] R. Q. Yang and J. M. Xu, Phys. Rev. B46, 6969 (1992)

[3] I. Vurgaftman, J. R. Meyer, F. H. Julien, and L. R. Ram-Mohan, Appl. Phys. Lett. 73, 711 (1998)

\*E-mail: keita@riec.tohoku.ac.jp, Fax: +81-22-217-5555

## Intersubband transitions for optical communication devices in novel InGaAs-AlAsSb quantum well structures

A. Neogi<sup>1,2</sup>, H. Yoshida<sup>1</sup>, T. Mozume<sup>1</sup>, N. Georgiev<sup>1,2</sup>, and O. Wada<sup>1</sup>

<sup>1</sup>Femtosecond Technology Research Association, 5-5 Tokodai, Tsukuba 300-2635, Japan

<sup>2</sup>New Energy and Industrial Research Development Organization, 1-1-3 Higashi Ikebukuro, Tokyo 170, Japan

Efficient intersubband transition (ISBT) related phenomena and devices in quantum wells are critically limited to the 2  $\mu\text{m}$  to 20  $\mu\text{m}$  spectral regime due to the band-offset between the well and the barrier material. However, ISBTs have potential application in the optical communication regime for the development of ultrafast all-optical switching devices, modulators, photodetectors, and near-infrared lasers [1-3]. Narrow InGaAs/AlAs (6-7 monolayer) QWs grown on GaAs substrates applied to reduce the ISBT wavelength from the mid-infrared regime to the communication wavelength regime ( $\sim 1.55 \mu\text{m}$ ) is inefficient due to the lattice mismatch between the well and the barrier material, and the carrier leakage from the QW [1]. We have therefore developed a novel system with a large conduction band offset (1.75 eV) using InGaAs/AlAsSb QWs lattice matched to InP substrate to achieve ISBT in the communication wavelength regime at 1.45 -1.55  $\mu\text{m}$  using 2-3 nm, MBE grown single InGaAs/AlAsSb QWs (Fig.1) [2].

Single QWs usually has a lower figure of merit at resonance and has a relatively slower response (2-3 ps). By utilizing the multilevel states  $c_n$ , ( $n = 1,2,3,4$ ) arising from the minibands of a coupled double quantum well (C-DQW) structure, a large nonlinearity with ultrafast recovery time (850 fs) can be achieved [3]. We have thereby grown a C-DQW based on our proposed model for designing an all-optical switch, and present the ISB absorption spectroscopy of the structure.

A pair of 3 nm Si doped ( $3 \times 10^{18} \text{ cm}^{-3}$ ) In<sub>0.53</sub>Ga<sub>0.47</sub>As QWs coupled together by a 2-nm AlAs<sub>0.56</sub>Sb<sub>0.44</sub> central barrier and bound by an outer barrier layer of 10 nm AlAs<sub>0.56</sub>Sb<sub>0.44</sub> was grown with the period  $N_{\text{dqw}}$  varying from 30-60. Near-infrared polarization resolved transmission spectra were measured at room temperature with a conventional optical absorption measurement setup. The polarization resolved transmission spectra for the designed C-DQW is shown in Fig.2, with the conduction band eigenstates deduced from the experimental results in the inset. The polarization angle dependence in Fig.2 clearly indicates that the 1-4 and 2-3 transitions are resonant at 1.3  $\mu\text{m}$  and 1.55  $\mu\text{m}$  respectively. A comparison of Fig.1 and 2 clearly reveals the splitting of the conduction eigenstates due to the coupling of the two adjacent wells separated by the 2nm narrow barrier. This is the first report on the observation of intersubband absorption at 1.3  $\mu\text{m}$ . The results also show that the designed C-DQW is promising for ultrafast all-optical switching and ultrashort pulse generation in the 1.55  $\mu\text{m}$  regime using ultrashort control light pulses at either 1.3  $\mu\text{m}$  or 1.55  $\mu\text{m}$ .

1. T. Asano, S. Noda, T. Abe, A. Sasaki, *Jpn. J. Appl. Phys.*, **35**, 1285 (1996).
2. T. Mozume, T., H. Yoshida, A. Neogi, and M.Kudo, *Jpn. J. Appl. Phys.*, **38**, 1286 (1999).
3. H. Yoshida, T. Mozume, T. Nishimura, and O. Wada, *Electron. Lett.*, **54**, 913, (1998).

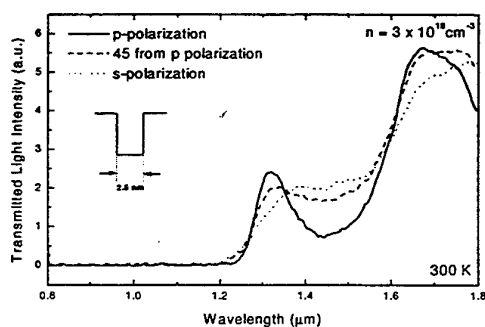


Fig.1. Polarization resolved spectra of a Single QW

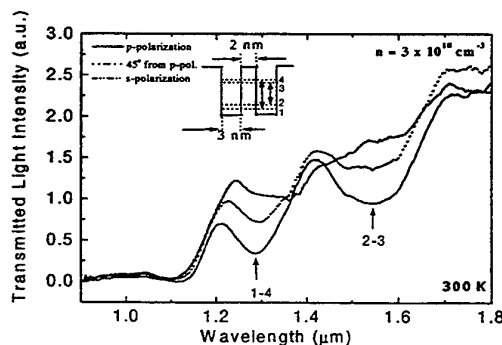


Fig.2. Polarization resolved spectra of a C-DQW

This work was performed under the management of the Femtosecond Technology Research Association (FESTA), which is supported by New Energy and Industrial Technology Development Organization (NEDO).

## Investigation of mid-infrared intersubband transitions in modulation doped CdS/ZnSe quantum wells

M. Göppert, R. Becker, A. Dinger, S. Petillon, C. Maier, M. Grün, C. F. Klingshirn

*Institut für Angewandte Physik, Universität Karlsruhe, Kaiserstr. 12,*

*D-76128 Karlsruhe, Germany*

Email: goeppert@ap-pc513a.physik.uni-karlsruhe.de

We report on the first investigations of intersubband transitions in modulation doped cubic type II CdS/ZnSe multiple quantum wells (MQWs). The samples were grown by molecular-beam-epitaxy on (001)-oriented GaAs substrates using compound sources. The structures are n-type doped with chlorine. The sheet carrier concentration in the CdS layers varies between  $5 \cdot 10^{10} \text{ cm}^{-2}$  and  $10^{13} \text{ cm}^{-2}$ . The infrared measurements were done in waveguide geometry using a BRUKER IFS 113v Fourier spectrometer. The different refraction indexes in the middle infrared of GaAs-substrate ( $n_{\text{GaAs}} = 3.3$ ) and CdS/ZnSe heterostructure ( $n_{\text{ZnSe}} = 2.4$ ,  $n_{\text{CdS}} = 2.3$ ) increase the electric field component in growth direction and cause a strong intersubband absorption. To the present, we have observed intersubband transition energies ( $e1 \rightarrow e2$ ) up to 450 meV depending on the well width. The intersubband absorption lines fit to a Lorentzian lineshape. The full width at half maximum depends on the doping concentration and varies between 16.5 meV and 37 meV. The measured oscillator strength of the intersubband transitions agrees with the theoretically expected values. The type II band alignment of CdS/ZnSe structures results in case of the MQWs in luminescence decay times of a few tens of nano seconds. This allows optical pumping with a  $\text{Ar}^+$ -laser of interband transitions to generate a substantial density of additional carriers. The increase of the optically generated additional intersubband absorption could be observed even without using Lock-In techniques.

## **Intersubband excitations in low dimensional semiconductor structures**

S. Das Sarma

*University of Maryland, College Park, USA*

I will discuss intersubband excitations in low dimensional semiconductor nanostructures from a theoretical perspective emphasizing the role played by many body effects in observable phenomena. Among the topics to be covered are the issues of intersubband transition broadening or linewidth, mode coupling phenomena, excitonic effects, exchange interaction, and possible quantum phase transitions. I will also attempt to provide a critical perspective on the experimental observability and relevance of various many body effects in low dimensional semiconductor structures.

This work has been supported by the US-ARO and the US-ONR.

## Collective effects in intersubband transitions

R. J. Warburton, C. Jabs, K. Weilhammer, and J. P. Kotthaus

*Sektion Physik der Ludwig-Maximilians-Universität and Center for NanoScience,  
Geschwister-Scholl-Platz 1, 80539 München, Germany*

M. Thomas and H. Kroemer

*Materials Department and QUEST, University of California, Santa Barbara,  
California 93106*

It is well known that collective effects shift the energy of an intersubband resonance away from the separation of the single-particle states. However, compared to the separation between the single-particle states, the shifts tend to be small. The purpose of this paper is to present results from experiments on InAs quantum wells which show that although the collective effects may have only a slight effect on the energy they alter dramatically the nature of the transition.

Experimental results are presented on InAs/AlSb quantum wells for temperatures between 4 K and 600 K. Remarkably, the linewidth of the intersubband resonance changes by only about 50% in this huge temperature range. At all temperatures, the linewidth increases rapidly with decreasing well width. Insight into these phenomena comes from experiments on samples with two occupied subbands where two intersubband resonances can be seen. The lower resonance broadens rapidly above 200 K but the higher resonance does not. The explanation is that the lower mode is scattered by thermally excited single particle transitions between the second and third subbands. Calculations in the Ando model give excellent agreement with the experiments. We argue that this process, Landau damping, is the dominant scattering mechanism of the intersubband resonance.

We have explored these ideas further by studying a related resonance in these samples, namely the intrasubband plasmon. It too exhibits damping when it is energetically close to single-particle transitions, in this case inter-Landau level transitions in a magnetic field.

# DIRECT OBSERVATION OF DYNAMICAL SCREENING OF THE INTERSUBBAND RESONANCE

Phone: +41-56-310 4566, Fax: +41-56-310 4551, Email: stephan.graf@psi.ch

S. Graf<sup>1</sup>, H. Sigg<sup>1</sup>, K. Köhler<sup>2</sup>, W. Bächtold<sup>3</sup>

<sup>1</sup> Paul Scherrer Institute, CH-5232 Villigen-PSI, Switzerland

<sup>2</sup> Fraunhofer Institut für angewandte Festkörperforschung, Tullastrasse 72,  
D-79108 Freiburg i.Br., Germany

<sup>3</sup> Laboratory for Electromagnetic Fields and Microwave Electronics, ETHZ,  
CH-8092 Zürich, Switzerland

Over the last decade, many papers have been published related to the dynamical screening of the intersubband resonance (ISR) in quantum well (QW) systems. It is commonly accepted by now, that in simple systems like GaAs with parabolic and parallel subbands, the screening leads to a blue shift of the resonance, the so called depolarization shifted or dressed ISR. In principle, neither absorption measurement nor photoconduction of a QWIP detector give access to the undressed excitation. Therefore, experimental data to sustain existing models are limited to the dependence of the ISR on temperature [1], light intensity [2], and carrier density [3].

Our approach, to be presented, is to compare the line profile of the ISR absorption with the simultaneously measured spectral response of the photon drag current. The absorption has been obtained from pulsed photoconduction measurements at room temperature (RT) under positive and negative bias. The photon drag signal has been obtained from the same measurements by adding the signals from either polarity. The experiments are performed at the free electron laser facility FELIX.

Since the photon drag effect crucially depends on the  $k$ -dependence of the IS transition via the Doppler effect, which is essentially a single particle effect, its spectrum contains the information of the undressed excitation. As an example, we find on a 30 period, modulation doped multi QW system made of 82 Å wide GaAs wells and 260 Å wide  $\text{Al}_{0.35}\text{Ga}_{0.65}\text{As}$  barriers, with  $0.87 \cdot 10^{12} \text{ cm}^{-2}$  electrons per well, the center position of the photon drag at  $832 \text{ cm}^{-1}$ . The peak position of the absorption, however, is at  $870 \text{ cm}^{-1}$ .

Surprisingly, this large blue shift of approximately  $40 \text{ cm}^{-1}$  as well as the spectral dependence, is very close to the shift and spectra predicted by Załuźny in his recent paper on the dynamical screened photon drag effect, although it is a  $T=0\text{K}$  calculation [4]. We also discuss the dependence of the depolarization shift on the radiation intensity, which is evidence for the importance of screening effects not only for applications at RT but also at high intensities close to saturation.

## References:

- [1] Huang, Gumbs, Manasreh, Phys. Rev. B. **52**, 14126 (1995)
- [2] Craig et al., Phys. Rev. Lett. **76**, 2382 (1996)
- [3] Ramsteiner et al., J. Appl. Phys. **67**, 3900 (1990)
- [4] Załuźny, Solid State Comm. **103**, 435 (1997)



## Many-body effects in the intersubband resonance of in-plane localized electron systems

C. Metzner and G.H. Döhler

*Institut für Technische Physik, Universität Erlangen, Germany*

It is now well established that, at usual carrier densities, the experimentally observed intersubband resonance is a collective, plasmon-like response of the interacting electron gas. The manybody effects cause a density-dependent blueshift of the resonance peak, relative to the intersubband separation. At the same time, the electron-electron interactions can distort the absorption line shape, which in a single particle model would be determined by nonparabolicity effects (inhomogeneous broadening) and various homogeneous broadening mechanisms.

The effects mentioned above have been successfully described by a dynamic depolarization theory with exchange-correlation corrections, assuming free motion of the electrons parallel to the layers. However, in real systems there is an unavoidable lateral potential modulation due to charged impurities or interface fluctuations, which may lead to in-plane localization of the carriers. In this situation, the system can be viewed as a random array of „natural quantum dots“, which are dynamically coupled by the long range Coulomb interaction.

We have developed a linear response theory of dynamic screening (direct Coulomb interaction), which starts directly from in-plane localized single particle states. Since the lateral potential modulation is included exactly, we can properly describe the limit of strong disorder (for example, center doped quantum wells), or layers of self-assembled quantum dots. Due to the break-down of the  $\mathbf{k}$ -conservation rule, intra- conduction-band absorption is possible for arbitrary polarization directions of the excitation light.

We apply our theory to a simple model system and calculate the z-polarized intersubband-absorption spectrum as a function of electron density. In the low density limit, the spectrum reflects the single particle level distribution, which is determined by the interplay of the disorder induced random potential and intersubband correlation effects [1]. For intermediate densities, the spectrum is strongly deformed by the manyparticle interactions. At higher densities, the absorption line assumes an approximately Lorentzian shape and is increasingly blue shifted (depolarization effect). The emergence of this collective line can be traced back to a mutual phase adaption of the localized single electron oscillators [2].

In the case of in-plane polarized light and intermediate densities, we obtain a narrowing and a red shift of the absorption line. This can be understood in a model of local oscillators with pure dipole-dipole interactions, a situation which is directly applicable to dense arrays of self-assembled quantum dots.

[1] C. Metzner, M. Hofmann and G.H. Döhler, *Phys. Rev. B* **58**, 7188 (1998).

[2] C. Metzner and G.H. Döhler, accepted for publication in *Phys. Rev. B* (1999).

## High-power tunable quantum fountain unipolar lasers

O. Gauthier-Lafaye<sup>(1)</sup>, B. Seguin-Roa<sup>(1)</sup>, F. H. Julien<sup>(1)</sup>,  
P. Collot<sup>(1)</sup>, C. Sirtori<sup>(2)</sup>, J. Y. Duboz<sup>(2)</sup>, G. Strasser<sup>(3)</sup>.

<sup>(1)</sup> Institut d'Electronique Fondamentale, UMR 8622 CNRS,  
Bat. 220, Université Paris-Sud, 91405 Orsay, France

<sup>(2)</sup> Thomson-CSF, Laboratoire Central de Recherches  
Domaine de Corbeville, 91404 Orsay, France.

<sup>(3)</sup> Institut für Festkörperelektronik, Technische Universität Wien  
Floragasse 7/1, 1040 Wien, Austria

The recent demonstration of quantum well unipolar lasers such as the current injection quantum cascade (QC) laser<sup>1</sup> or the optically pumped quantum fountain (QF) laser<sup>2</sup> opens new prospects for the development of high-power long-wavelength lasers operating above liquid nitrogen temperature. In QC lasers, tunneling of electrons from injector regions provides population inversion. In QF lasers, selective optical pumping from the ground subband is used to efficiently promote electrons in the upper subband. The active region of a QF laser consists of quantum wells exhibiting three bound electron states. Electrons excited in the upper state radiate to the intermediate state, giving rise to the infrared emission. Population inversion as well as fast recycling of electrons into the ground state is provided by insuring a short lifetime of electrons in the intermediate state through an enhanced scattering with LO-phonons<sup>3</sup>. Although operation of QF lasers imposes the use of an external pumping source, these lasers offer the advantages of a simplified design and have less stringent material requirements as compared to QC lasers. With no current flow, doping of the cladding layers and metal contacts are not necessary, which results in low free-carrier absorption internal losses at long-wavelengths. In addition, the laser can be operated far above threshold with much less thermal penalty than in a current injection device. QF lasers are then expected to exhibit superior performances in terms of output power at long-wavelengths above 10  $\mu\text{m}$ . Powerful QF lasers are of interest for applications such as remote trace gas sensing units or LIDAR systems.

During the talk we will review recent developments on QF lasers emitting in the 14-15  $\mu\text{m}$  wavelength range under optical pumping by a pulsed CO<sub>2</sub> laser. We will show that record-high output powers (>6W per facet) can be achieved by optimizing the QF laser design. We also demonstrate that the lasing wavelength can be tuned by as much as  $\Delta\lambda/\lambda \approx 2.5\%$  by tuning the pump wavelength<sup>4</sup>. Very recent results obtained on broad-area QF unipolar lasers fabricated with a top grating in order to efficiently couple the pump radiation will also be reported. We will show that outstanding performances can be achieved in terms of optical power, beam quality and pump threshold.

<sup>1</sup> J.Faist, F. Capasso, D. Sivco, C. Sirtori, A.L. Hutchinson, S. N. G. Chu and A.Y. Cho, "Quantum cascade laser", *Science* **264**, 553 (1994).

<sup>2</sup> O. Gauthier-Lafaye, P. Boucaud, F.H. Julien, S. Sauvage, S. Cabaret, J.-M. Lourtioz, V. Thierry-Mieg, R. Planel, "Long wavelength ( $\approx 15.5$  micrometer) unipolar semiconductor laser in GaAs quantum wells", *Appl. Phys. Lett.*, **71**, 3619 (1997); O. Gauthier-Lafaye, F. H. Julien, P. Boucaud, S. Sauvage, J.-M. Lourtioz, V. Thierry-Mieg, R. Planel, "Long-wavelength (15.5  $\mu\text{m}$ ) quantum fountain intersubband laser in GaAs/AlGaAs quantum wells", *Proc. SPIE*, **3284**, 224 (1998).

<sup>3</sup> F.H. Julien, A. Sa'ar, J. Wang and J.-P. Leburton, "Optically pumped intersubband emission in quantum wells", *Electron. Lett.* **31**, 838 (1995).

<sup>4</sup> O. Gauthier-Lafaye, F. H. Julien, S. Cabaret, J.M. Lourtioz, G. Strasser, E. Gornik, M. Helm, P. Bois, "High-power GaAs/AlGaAs Quantum Fountain Unipolar Laser emitting at 14.5  $\mu\text{m}$  with 2.5% tunability." *Applied Physics Letters* **74**, 1537 (1999).

## Emission of mid-infrared radiation and intersubband population inversion in near-infrared laser QW structures

L.E.Vorobjev, D.A.Firsov, V.A.Shalygin, Zh.I.Alferov \*, N.N. Ledentsov\*, V.M.Ustinov\*, Yu.M.Shernyakov\*, and V.N.Tulupenko\*\*

*St.Petersburg State Technical University, St.Petersburg 195251, Russia*

*\*A.F.Ioffe Institute, St.Petersburg 194021, Russia*

*\*\*Donbass State Engineering Academy, Kramatorsk 343913, Ukraine*

The new possibility to obtain the intersubband population inversion under current injection of the electrons into the structure with InGaAs/AlGaAs quantum wells (QWs) is discussed. The QWs are embedded into  $i$ -layer of  $p^+ - i - n^+$  heterostructure. We consider the QWs of funnel shape with three electron levels and find the conditions to realize the mid-infrared (MIR) stimulated emission due to intersubband electron transitions under simultaneous stimulated emission of the near-infrared (NIR) radiation due to interband transitions ( $h\nu \approx E_g$ ).

The electron population at the energy levels in QWs under current injection is determined by the fast intersubband and intrasubband relaxation processes. It is possible to create the metastable exited level and to get the population inversion of electrons due to small wavefunction overlapping for 3-2 and 3-1 subbands and because of the peculiarities of polar optical phonon scattering. Interband NIR stimulated emission limits the ground subband concentration rise under increasing injection current above the threshold of NIR lasing.

The intersubband transition probability and population inversion rate are calculated for InGaAs/GaAlAs QWs with three electron levels. We have also calculated the optical gain under direct optical transitions between subbands 3 and 2. Finally, we have designed the heterostructure with 10 QW layers and composite waveguide that confines both MIR and NIR radiation. For MIR radiation it has the factor of optical confinement  $\Gamma \approx 0.1$ . In this structure the MIR lasing is possible when injection current exceeds the threshold of NIR lasing by 6 times. Similar simulation was performed for the case of interband ( $h\nu > E_g$ ) optical pumping of the laser.

The experimental data on spontaneous MIR emission from InGaAs/AlGaAs QWs under simultaneous NIR lasing are presented and discussed. So, the first step in the development of MIR laser of new type with current or optical pumping has been done.

## Modulated resonant Raman and photoluminescence spectroscopy of Bragg confined asymmetric coupled quantum wells.

M. Levy<sup>(a)</sup>, R. Kapon<sup>(b)</sup>, A. Sa'ar<sup>(b)</sup>, R. Beserman<sup>(a)</sup>, V. Thierry-Mieg<sup>(c)</sup>, R. Planel<sup>(c)</sup>

(a) Solid State Institute and Physics Department, Technion, Israel Institute of Technology, Haifa 32000, Israel

(b) Department of Applied Physics, The Fredi and Nadine Hermann School of Applied Science, The Hebrew University of Jerusalem, Jerusalem 91904, Israel

(c) Laboratoire de Microstructures et Microelectronique - CNRS, 196 Avenue H. Ravera, BP107, 92225 Bagneux, France.

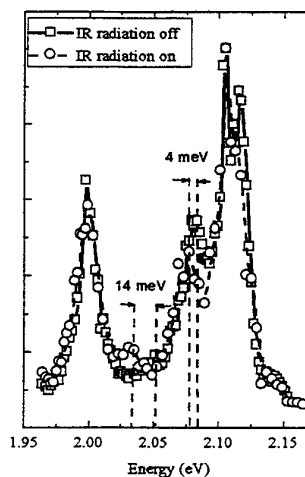
The presence of Bragg reflectors on each side of a quantum well causes the above the barrier quasi-continuum energy levels to separate into two classes of states. The first group, called Bragg states, are highly localized in the quantum well (QW) region due to the Fabri-Perot effect of the reflectors while the second group form mini-bands in the continuum that mainly extend over the reflectors. Despite several reports on above the barrier states in Bragg confined structures none of these works provide a direct evidence to the existence of two different classes of above the barrier states.

In this work we provide experimental evidence for the existence of the two classes of states discussed above. Using the newly developed method of locally modulated resonant Raman spectroscopy (RRS) we were able to resolve each group of states from the other.

The local modulation in our structure was achieved by charged carrier transfer between a wide QW (WQW) and a narrow QW (NQW) induced by intersubband optical excitation. This process gives rise to a local space charge field across the coupled QW region but not across the Bragg reflectors. Hence, local modulation of the RRS signal from the highly localized Bragg states is observed whereas mini-band states are not affected by this process.

We measured the RRS spectra for GaAs and AlAs modes in all layers that constitute the QW structure. We observed 3 continuum levels at 2.01 eV, 2.07 eV and 2.08 eV. The first state can only be observed in the RRS originating in the QW layers. This indicates that this level is localized above the QW region. On the other hand the resonances at 2.07 eV and 2.08 eV appear in all phonon spectra which demonstrating the extended nature of these levels.

In the photo-induced RRS spectra we observe a red shift of 14 meV for the Bragg confined level, 4 meV for the 2.08 eV level while no shift was observed for the 2.07 eV level. These results are in agreement with our model of a higher localization of the Bragg state in the QW.



## Ultrafast dynamics of intersubband excitations

T. Elsaesser, R.A. Kaindl, S. Lutgen, and M. Woerner

*Max-Born-Institut für Nichtlineare Optik und Kurzzeitspektroskopie,*

*D-12489 Berlin, Germany*

Intersubband excitations play an important role for ultrafast carrier dynamics in quasi-two-dimensional semiconductors and for device applications, e.g., in quantum cascade lasers. We present a study of the coherent and incoherent dynamics of intersubband excitations in a pure electron plasma on ultrafast time scales. Femtosecond spectroscopy in the mid-infrared allows for real-time monitoring the different relaxation processes following intersubband excitation of electrons in GaInAs/AlInAs quantum wells. Such measurements give direct insight into the relevant microscopic scattering mechanisms. We observe a decay of coherent intersubband polarizations on a time scale of several hundreds of femtoseconds which is governed by electron-electron scattering [1]. From such data, the homogeneous broadening of the intersubband absorption line is derived. Electrons excited to the  $n=2$  conduction subband undergo intersubband scattering to the  $n=1$  subband by emission of longitudinal optical phonons with characteristic time constants of 1 ps. This is followed by thermalization of the backscattered electrons on a similar time scale, involving both electron-electron and electron-phonon scattering [2]. Eventually, the hot electron distribution cools down to lattice temperature within about 50 ps [3].

- [1] R.A. Kaindl, S. Lutgen, M. Woerner, T. Elsaesser, B. Nottelmann, V.M. Axt, T. Kuhn, A. Hase, and H. Künzel, *Phys. Rev. Lett.* 80, 3575 (1998)
- [2] S. Lutgen, R.A. Kaindl, M. Woerner, T. Elsaesser, A. Hase, H. Künzel, M. Gulia, D. Meglio, and P. Lugli, *Phys. Rev. Lett.* 77, 3657 (1996)
- [3] S. Lutgen, R.A. Kaindl, M. Woerner, A. Hase, and H. Künzel, *Solid State Commun.* 106, 425 (1998)

# HOLE-BURNING IN INHOMOGENEOUSLY BROADENED INTERSUBBAND ABSORPTION BANDS OF QUANTUM-WELL-STRUCTURES

A. Seilmeier, S. R. Schmidt, J. Kaiser

Physikalisches Institut, Universität Bayreuth, D-95440 Bayreuth, Germany

☎+49 921 553162, FAX+49 921 553172, email Alois. Seilmeier@uni-bayreuth.de

Hole burning is a powerful tool to investigate the inhomogeneous broadening of absorption lines. It is used in this paper to investigate the broad intersubband absorption bands of quantum well structures. In such experiments only transient holes on an ultrafast time scale can be observed due to the electronic nature of the absorption.

We report on the observation of transient population holes in intersubband absorption profiles on a picosecond time scale. A first infrared pulse of 2ps duration and a spectral width of 1.2 meV excites electrons to the first excited subband. The subsequent change of the intersubband absorption is measured time and frequency resolved by a second independently tunable infrared pulse. The data are taken on n-modulation doped multiple GaAs/Al<sub>0.35</sub>Ga<sub>0.65</sub>As quantum well structures with 5.9 nm wide GaAs quantum wells embedded in between 36 nm thick Al<sub>0.35</sub>Ga<sub>0.65</sub>As layers of various doping concentrations. At 300K the samples show a broad absorption band in the order of  $\Delta v \sim 10$  meV at  $v \sim 150$  meV ( see broken line in Fig.1a ).

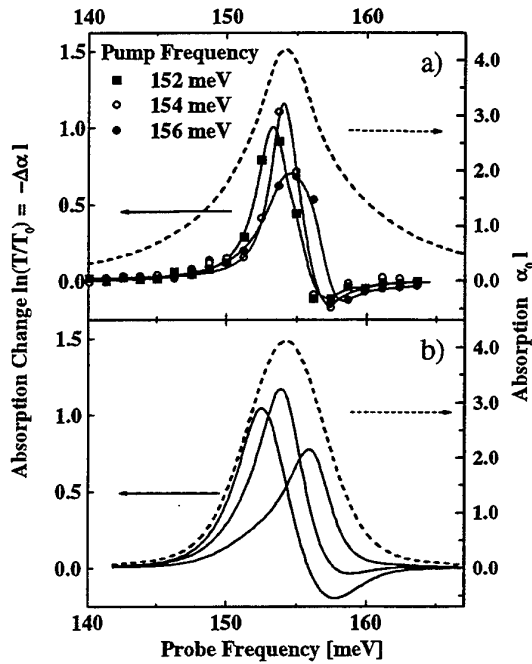


Fig. 1: Intersubband absorption (broken line) of a sample doped with  $n^{2D} = 3 \times 10^{11} \text{ cm}^{-2}$  Si atoms per layer and spectra of transient holes (solid lines) after excitation at three different pump frequencies. a) experimental data b) results of numerical calculations.

Around delay time  $t_D = 0$  population holes in the intersubband absorption band are found. At a relatively low excitation intensity of  $400 \text{ kW/cm}^2$ , which is close to the saturation intensity, bleaching of the absorption is observed at frequencies close to the pump frequency. In Fig. 1a the change in absorption  $\Delta\alpha l$  due to intersubband excitation is shown which directly reflects the population hole. The holes grow - as expected - with rising intensity, but also with increasing delay times from  $t_D = -1$  to 1ps. Simultaneously a small shift of the intersubband transition frequency is found which also increases as a function of time. The observed hole spectra are compared with detailed model calculations as shown in Fig. 1b. At room temperature a homogeneous linewidth of approximately 2 meV and an inhomogeneous broadening of 6 meV is deduced for this sample. At lower temperatures a decrease of the homogeneous linewidth and, surprisingly, an increase of the inhomogeneous broadening up to 10 meV is found. The dependence of the spectral holes on the delay time and on the excitation intensity is discussed in the paper. Fluctuations in the sample parameters and the nonparabolicity of the energy dispersion are considered as relevant broadening mechanisms.

# Time Resolved Intersubband Optical Transitions in Resonantly Optically Pumped Semiconductor Lasers - Gain from Correlated Electron and Hole Plasmas

I. Shtrichman, U. Mizrahi, D. Gershoni and E. Ehrenfreund

*Physics Department and Solid State Institute, Technion-Israel Institute of Technology, Haifa 32000, Israel*

K.D. Maranowski and A.C. Gossard

*Materials Department, University of California, Santa Barbara, California 93106*

We use visible - infrared dual beam time resolved spectroscopy for experimental studies of laser heterostructures containing quantum structures within their active layers. By tuning the probe energy through the intersubband absorption spectrum and measuring its relative strength, a direct measurement of the population of carriers in various momentum states within the first lasing subband is obtained.

GaAs/AlGaAs semiconductor heterostructure laser structures were optically excited with various excitation densities, below or above their lasing threshold. The excitation, by an above bandgap, spectrally tunable, picosecond optical laser pump pulse, is followed by a mid infrared picosecond probe pulse, spectrally tuned to the quantum structure intersubband optical transition resonances. By changing the delay time between the pump and the probe pulses we study the temporal evolution of the photoexcited carriers after the excitation pulse, before and after the lasing action starts. We have measured and temporally resolved the intersubband absorption spectrum of these optically pumped heterostructure lasers.

In Fig. 1 we display the time resolved photoinduced absorption transients of an optically pumped laser, above and below its interband lasing threshold, at 10 K. The absorption was monitored at the maximum of the e1-e2 transition resonance (172 meV), while the laser was pumped directly into its heavy-hole excitonic resonance. The figure clearly demonstrates that the lifetime of the photogenerated population is drastically reduced above the lasing threshold.

We follow the dynamics of the spectrally integrated intersubband absorption intensity (not shown) and conclude that the quasi-Fermi level is pinned as the laser reaches threshold and that the depletion of the lasing state takes place within few tens of picoseconds. Using our time resolved photoinduced intersubband absorption technique, we are able to monitor the temporal evolution of the carrier momentum distribution in the first subband, immediately after excitation [1].

The implications of our experimental studies and the new light that they shed on the gain nature and the lasing mechanism in semiconductor lasers can now be compared with the predictions of theoretical studies. We will discuss the possible observations of various carrier phases depending on their densities and temperatures:

(1) Gas of weakly interacting electrons and holes. (2) Excitons and excitonic molecules. (3) Degenerate Bose gas of excitons. (4) Electron hole Fermi liquid. (5) Bose-Einstein excitonic condensate, or excitonic-insulator [2].

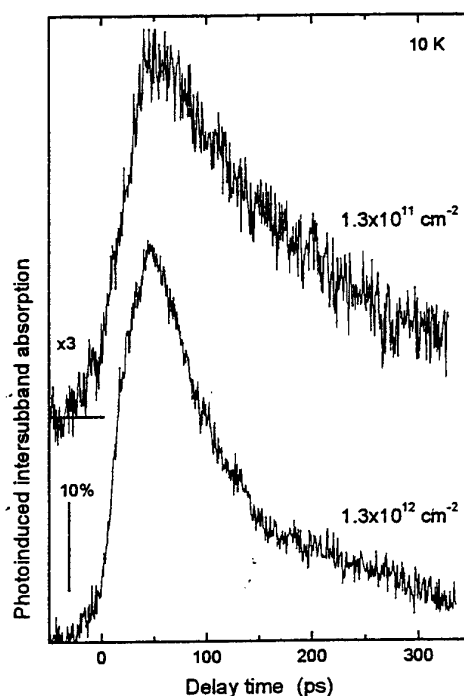


Fig.1: Photoinduced intersubband absorption transients for excitation density below and above threshold

- [1] R. Duer, I. Shtrichman, D. Gershoni and E. Ehrenfreund, "Momentum Redistribution Times of Resonantly Photogenerated 2D Excitons", *Phys. Rev. Lett.* **78**, 3919, (1997).
- [2] L.V. Keldysh "Macroscopic Coherent States of Excitons in Semiconductors", in "Bose-Einstein Condensation", Eds: A. Griffin, D.W. Snoke and S. Stringari, University Press, Cambridge, 1995.

## Time-resolved intersubband spectroscopy of semiconductor nanostructures

R. Bratschitsch, R. Kersting, T. Müller, G. Strasser, and K. Unterrainer  
Institut für Festkörperelektronik, TU-Wien, Austria  
Rudolf.Bratschitsch@tuwien.ac.at

W. Fischler  
Institut für Experimentalphysik, Universität Innsbruck, Austria

J. N. Heyman  
Macalester College, St. Paul, MN, USA

Time-resolved studies of intersubband transitions using mid- and far-infrared radiation have been carried out to analyze the different relaxation mechanisms in doped quantum wells [1, 2]. We present experiments that reveal the time evolution of intersubband transitions in undoped GaAs/AlGaAs quantum wells.

A femtosecond near infrared laser pulse generates a coherent superposition of two quantum well energy levels if its spectral width is larger than the intersubband spacing  $\Delta E$ . As a result, coherent THz radiation with a frequency corresponding to the interlevel spacing is emitted. The spectrum of the THz emission is recorded by a THz autocorrelation measurement: two temporarily delayed femtosecond pulses hit the sample and the resultant THz radiation is measured with a bolometer (Fig. 1). A Fourier transformation of this autocorrelation trace then gives the spectrum of the coherent emission.

The beating between the two quantum well levels can also be observed in degenerate near infrared pump-probe experiments. We observe several oscillations in the reflectivity signal with the same frequency as in the THz autocorrelation measurements (Fig. 2). The frequency doesn't change with pump intensity but the damping time increases with decreasing pump intensity which allows an investigation of the density dependent scattering mechanisms inside the quantum well.

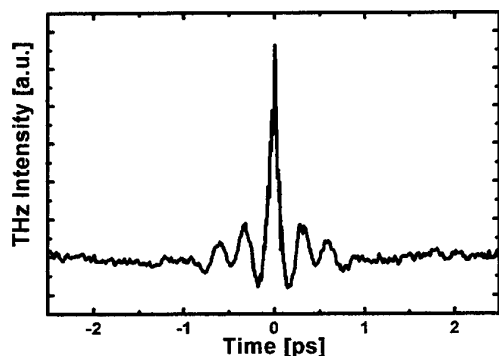


Fig. 1: THz-autocorrelation (AC) signal of an undoped double quantum well recorded at  $T= 4.5$  K

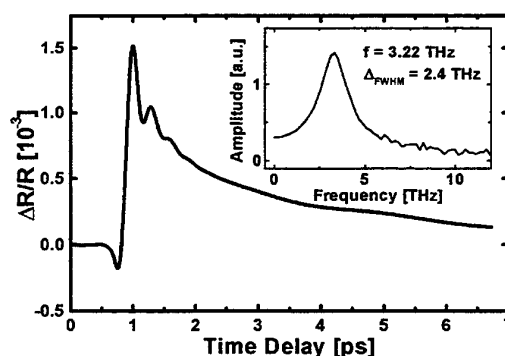


Fig. 2: Relative change in reflectivity as a function of time delay between pump and probe beam; inset: Fourier transform of the extracted oscillations

The time evolution of the population of the different quantum well levels is investigated in a visible pump/THz probe experiment. The optically excited carriers in the quantum well (visible pump) are probed by a transmitted THz pulse that is tuned to the energy spacing of the intersubband transition.

- [1] R. A. Kaindl, S. Lutgen, M. Wörner, T. Elsässer, B. Nottelmann, V. M. Axt, T. Kuhn, A. Hase, H. Künzel, Phys. Rev. Lett. **80**, 3575 (1998).
- [2] J.N. Heyman, R. Kersting, K. Unterrainer, Appl. Phys. Lett. **72**, 644 (1998).

This work has been supported by the Austrian Science Foundation (FWF START Y47).



Abstract submitted to the 5-th Int. Conf. on Intersubband Transitions in Quantum Wells (ITQW'99), September 7-11, 1999, Bad Ischl, Austria

## Noise current investigations of g-r-noise limited and shot-noise limited QWIPs

R. Rehm, H. Schneider, C. Schönbein, and M. Walther

*Fraunhofer-Institut für Angewandte Festkörperphysik, Tullastraße 72, 79108 Freiburg, Germany*

GaAs/AlGaAs-based QWIPs are increasingly used for high performance IR camera systems operating in the 8-12  $\mu\text{m}$  regime. Noise measurements provide an important method to obtain the detectivity which critically determines the temperature resolution of such a camera system. Furthermore, noise measurements also give important experimental clues for the understanding of the underlying transport mechanism.

We describe the experimental setup used for highly sensitive noise measurements and the assessment of two classes of QWIPs. In the context of conventional bound-to-continuum QWIPs, we have performed a detailed study of the photoconductive gain  $g_{ph}$  as obtained from the g-r-noise. At low applied voltages  $g_{ph}$  is proportional to the electric field. Subsequently  $g_{ph}$  reaches a maximum and decreases again with increasing field (see Fig. 1). We associate this negative differential behavior with intervalley scattering processes.

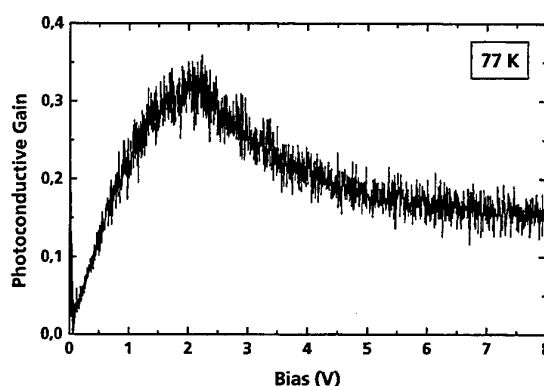


Fig. 1: Photoconductive gain of a conventional QWIP

The second class of QWIPs [1] is characterized by a potential distribution which is shown schematically in Fig. 2. As indicated by the arrows, the carriers are emitted from a wide, doped GaAs quantum well. Subsequently they drift across an AlGaAs barrier. A narrow AlAs barrier blocks further carrier transport in the continuum. The carriers are thus captured into the narrow, undoped quantum well. The captured electrons tunnel through the AlAs barrier and reach the subsequent period. In this way, the photoexcited carrier mean free path corresponds to one period. Due to the deterministic nature of the carrier capture, this type of QWIP is limited by shot-noise. This reduction from g-r-noise to shot-noise has been theoretically predicted by a model of W.A. Beck [2]. Our experimental results nicely confirm his predictions.

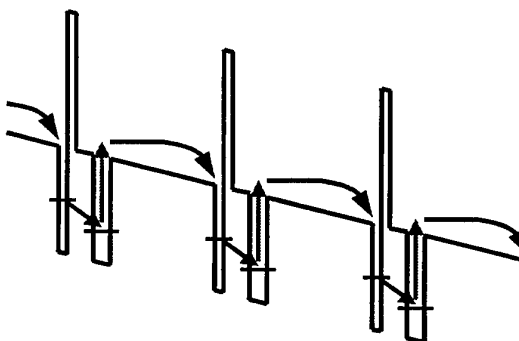


Fig. 2: Three periods of the conduction band edge of a Four-Zone-QWIP [1]

[1] H. Schneider, C. Schönbein, M. Walther, K. Schwarz, J. Fleissner, and P. Koidl, *Appl. Phys. Lett.* **71**, 246 (1997)

[2] W. A. Beck, *Appl. Phys. Lett.* **63**, 3589 (1993).

Contact person: R. Rehm

email: [rehm@iaf.fhg.de](mailto:rehm@iaf.fhg.de) phone: (0049) 761-5159 353 fax: (0049) 761-5159 400

# **Trap Effects on Dark Current Transients in GaAs/AlGaAs Quantum Well Infrared Photodetectors**

A. G. U. Perera, S. G. Matsik, Y. W. Yi, M. Ershov  
Georgia State University  
H. C. Liu, M. Buchanan, Z. R. Wasilewski  
NRC-Canada

Variations in the dark current in quantum well IR detectors can have significant effects on the performance. Long time scale transients can require long settling times before the start of illumination. In this work, experimental results showing very slow ( $\sim 30$  minutes for  $T = 120$  K) dark current transients in n-type GaAs/Al<sub>0.27</sub>Ga<sub>0.73</sub>As quantum well photodetectors (QWIPs) are reported. The transients with typical amplitudes of 0.1 to 1% of the steady state current have been observed at temperatures from 77 K up to 170 K. Lattice heating is an unlikely explanation since the 77 K data is measured with the QWIP immersed in liquid N<sub>2</sub>. Similar to the case of persistent photoconductivity,[1] these effects are believed to be associated with deep levels. Here the initially ionized levels act as traps reducing the positive charge in the structure as opposed to the persistent photocurrent case where the initially neutral traps are photoionized decreasing the positive charge. The time constant of the dark current decreases with increasing temperature with an experimentally determined activation energy of 75 meV. A fitting of the capture cross section to  $s(T) = s_0 \exp(E_c/k_B T)$  gave an estimate of the capture activation energy of  $E_c \sim 40$  meV. The reported activation energies range from 70[2] to 350[3] meV for MBE grown AlGaAs with values as low as 20 meV[4] being reported for LPE growth. As the temperature decreases the time constant becomes very large ( $t \sim 10^7$ - $10^8$  s at 77 K) causing the expectation of dark current variations on long time scales for operating detectors. A model explaining the influence of trap recharging on dark current is being considered.

Work supported in part by NSF grant #ECS 9809746.

[1] V. N. Ovsyuk, M. A. Dem'yanenko, V. V. Shashkin, and A. I. Toropov, *Semiconductors* **32**, 1082 (1998).

[2] P. K. Bhattacharya, A. Majerfeld and A. K. Saxena, *Gallium Arsenide and Related Compounds* 1978, p. 199, C. M. Wolfe, ed. The Institute of Physics, 1979.

[3] S. Ghosh and V. Kumar, *J. Appl. Phys.* **75**, 8243 (1994).

[4] H. Watanabe and A. Usui, *Proc Int. Symp. GaAs and Related Compounds*, Las Vegas 1986. *Inst. Phys Conf. Ser. No. 83*, p. 1, (1987).

# EFFECTS OF ELECTRON AND PHOTON TRANSPORT IN INTEGRATED QWIP-LED PIXELLESS IMAGERS

V. Ryzhii, I. Khmyrova, and Ph. Bois,<sup>†</sup>

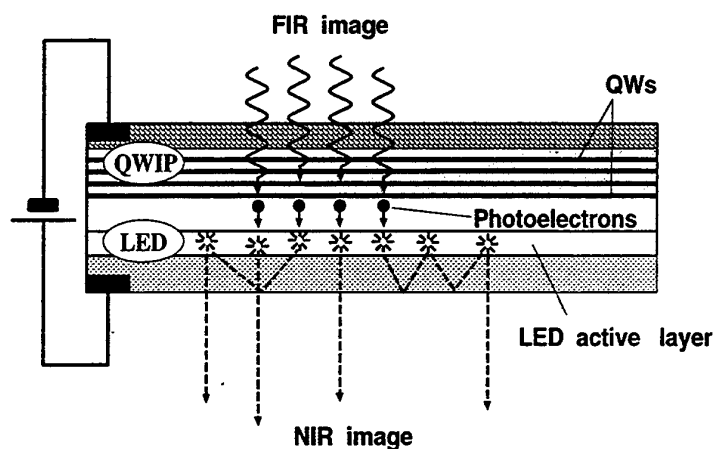
University of Aizu, Aizu-Wakamatsu City, 965-8580, Japan

<sup>†</sup> Laboratoire Central de Recherches, Thomson - CSF, 91404 Orsay, France

An integrated quantum well infrared photodetector (QWIP) and light-emitting diode (LED) pixelless imaging device was recently proposed, realized, and studied theoretically [1,2]. In the QWIP part of the device a far-infrared (FIR) radiation image is converted into nonuniformly distributed current of the electrons (holes) photoexcited from the QWs due to their transitions from the bound states into the continuum states. The nonuniform photocurrent is injected into the LED part of the imager. It leads to nonuniform near-infrared (NIR) radiation (NIR image). The QWIP-LED performance is limited by uniform injection of electrons from the QWIP emitter and lateral spreading of the photoelectrons in both the QWIP and LED parts [2]. The lateral uniformity of the injected current is due to equipotentiality of the QWs. The injected current reduces the image contrast. However, as shown previously [2], in QWIP-LED devices with large enough number of the QWs this effect can be weak. The lateral diffusion of the photoelectrons results in some smearing of the output NIR image in comparison with the incident FIR image.

In this work we show that the main mechanism of the image smearing limiting the QWIP-LED pixelless imager performance can be associated with the lateral transport of the emitted NIR photons, their reabsorption in the LED active region with the generation of the electro-hole pairs, and reemission from this region caused by the recombination of such pairs. Due to low efficiency of the photon escape from the LED active region the reabsorption and reemission of NIR photons can take place far enough from the site where the injected electrons recombine.

A schematic view of the QWIP-LED pixelless imaging device, principle of its operation, and mechanisms responsible for the image smearing are shown in figure.



The device model employed for the calculation of the QWIP-LED characteristics includes the diffusion equation which takes into account both the photoelectrons recombination and their generation by the reabsorbed radiation. This equation is supplemented by an equation describing the propagation of NIR radiation along the LED active region. The developed model yields the contrast transfer characteristic of the imager as a function of the scale of nonuniformity of the incident image as well as electrical and optical parameters of the device structure. Strong dependences of the characteristics on the structural parameters give a flexibility for the device optimization.

[1] L. B. Allard, H. C. Liu, M. Buchanan, and Z. R. Wasilewski, *Appl. Phys. Lett.*, **70**, 2784 (1997).

[2] V. Ryzhii, H. C. Liu, I. Khmyrova, and M. Ryzhii, *IEEE J. Quantum Electron.*, **33**, 1527 (1997).

# **Circuit Model for Quantum Well Infrared Photodetectors and its Comparison with Experiments**

Y.H Chee and G. Karunasiri<sup>(a)</sup>

Department of Electrical Engineering

Centre for Optoelectronics

National University of Singapore

Singapore 119260

## **Abstract**

This paper presents a PSPICE model for quantum well infrared photodetectors (QWIP). Bias dependence of the dark current and photocurrent is accurately described by the model with the aid of analogue behaviour modelling (ABM) technique in PSPICE. The model can be easily integrated with the readout electronics for circuit optimisation. In addition, we have also incorporated the temperature dependence of dark current into the model for analysing the effects of operating temperature on the performance. The various design parameters of the QWIP can be fed into the model as user defined inputs to simulate the detector performance. Experimental data of different QWIP structures were compared with the simulated results and their good agreement verifies the accuracy of the PSPICE model.

---

<sup>(a)</sup> E-mail : [elekg@nus.edu.sg](mailto:elekg@nus.edu.sg)

Submitted to ITQW'99, Bad Ischl, Austria

## Quantum Grid Infrared Photodetectors

L. P. Rokhinson\*, C. J. Chen\*, D. C. Tsui\*, G. A. Vawter<sup>†</sup>, and K. K. Choi<sup>‡</sup>

*\*Department of Electrical Engineering, Princeton University*

*<sup>†</sup>Sandia National Laboratories, USA*

*<sup>‡</sup>U. S. Army Research Laboratory*

(April 28, 1999)

Performance of quantum well infrared photodetectors (QWIP) is determined by both the properties of the multiple quantum wells (MQW) and the light coupling scheme. While intrinsic parameters of the MQW region can be readily optimized, the optical coupling become the key issue for the improvement of QWIP due to the dipole selection rule. We proposed quantum grid infrared photodetector (QGIP) in which the additional lateral confinement in a QWIP structure is achieved by patterning the active material into either a lamellar or crossed grid gratings. In addition to the expected intrinsic normal incident absorption from the lateral quantization, the grid also serves as a diffraction grating to direct part of the incident light into parallel propagation.

We have fabricated and analyzed QGIPs with line patterns of lithographical line widths  $w_l$  ranging from 0.1 to 5  $\mu\text{m}$ . Low-damage reactive ion beam etching was employed to produce vertical sidewalls. For large  $w_l > 0.5 \mu\text{m}$  the coupling efficiency of a QGIP is determined by the diffraction and can be reproduced by numerical simulation of the field distribution within the grid<sup>1</sup>. We found that etching the QGIP at a 30° blaze angle improves coupling efficiency 1.8 times, compared with the vertical sidewall profile and 2.2 times compared with the reference edge-coupled device. Although the best detector performance occurs at  $w_l \approx 1.5 - 2.5 \mu\text{m}$ , the detector starts to improve when  $w_l < 0.5 \mu\text{m}$ , indicating a possible quantum confinement effect.

---

<sup>1</sup>Numerical calculations were done by T. Tamir *et. al*, Politechnical University, Brooklyn, NY

**GaAs/AlGaAs microresonator quantum cascade lasers**

*S. Gianordoli<sup>a</sup>, L. Hvozdar, G. Strasser, T. Maier, N. Finger, K. Unterrainer, and  
E. Gornik*

*Institut für Festkörperelektronik, Technische Universität Wien, Floragasse 7,  
A-1040 Wien*

We intend to report the realization of the first electrical pumped GaAs/AlGaAs microcylinder lasers. Design and fabrication of the special resonator shapes (circular and stadium like cross section) are presented. Threshold characteristic and optical output at cryogenic temperatures of these quantum cascade lasers emitting at 10  $\mu\text{m}$  are investigated depending on the size and deformation of the resonators. Far field characteristics are compared and directionality of the emission is investigated depending on the deformation. The larger the deformation of an ideal circular cross section to a stadium like one the more the emission should be directed. We try to resolve a so-called bow-tie-mode for strongly deformed resonators. A decrease of the threshold current density is expected for this special mode. The lowest threshold current of 318 mA is obtained till now for a microcylinder resonator with circular cross section. This value is the smallest reported for a GaAs/AlGaAs quantum cascade lasers. For achieving lower threshold currents the size of the resonators is reduced step by step. The emission of the microlasers was analyzed spectrally using Fourier transform spectroscopy. Single mode emission was detected using step scan mode for 100  $\mu\text{m}$  diameter circular microlasers with a side mode suppression better than 20 dB. The maximum working temperature of the microcylinder lasers is 165 K.

---

<sup>a)</sup> Electronic mail: stefan.gianordoli@tuwien.ac.at

## GaAs/AlGaAs quantum cascade laser - a source for gas absorption spectroscopy

L. Hvozdar, S. Gianordoli, G. Strasser, W. Schrenk, K. Unterrainer and E. Gornik  
*Solid State Electronics, TU Wien, Austria*

V. Pustogow, Ch.S.S.S. Murthy, M. Kraft, B. Mizaikoff  
*Institute of Analytical Chemistry, TU-Wien, Austria*

We report on the first application of the recently developed GaAs/AlGaAs electrically pumped quantum cascade lasers (QCL) [1], in spectrophotometry and spectroscopy in the mid infrared band. Ridge lasers emitting in the 10  $\mu\text{m}$  range with peak power of 100mW are used for absorption measurements in the gas phase. The laser radiation is transmitted through a gas cell and detected by a  $\text{LN}_2$  cooled MCT detector. A well defined mixture of an analyte and a carrier gas, flows through the gas cell at standard ambient conditions. The dependence of the absorption on the concentration is recorded. Spectral analysis of the light transmitted through the cell with the analyte is performed using a fourier transform spectrometer. Strongly absorbed modes as well as modes with small absorption (fig.1) can be resolved in the spectrum and are compared with the Hitran database spectra.

An on-chip mid-infrared absorption sensor is a possible way to realize a small compact "sniffer" tuned to a particular chemical species or pollutant. Well known mid-infrared photovoltaic properties [2] of the intersubband QCL devices are employed. An optical coupling between two sections of a QCL separated by an air gap is observed. A longer section acts as a laser source and the opposite standing, shorter section as a photovoltaic detector. The response of the QCL "photodiode" is recorded as a function of the drive current of the laser (output intensity). The MCT detector response is recorded simultaneously. A prove of a feasibility of an on-chip absorption sensor based on a QCL laser and the same QCL structure in the photovoltaic regime is given.

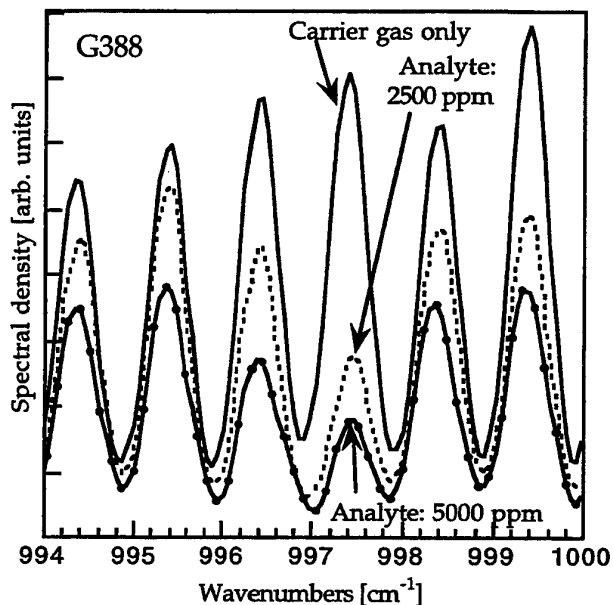


**Figure 1** Part of the spectrum of a QCL transmitted through the gas cell for pure carrier gas (solid line), 2500ppm of analyte (dashed) line and 5000ppm of analyte (solid line with dots) in the mixture.

- [1] C. Sirtori, P. Kruck, S. Barbieri, P. Collot, J. Nagle, M. Beck, J. Faist, U. Oesterle, *Appl. Phys. Lett.* **73**, 3486 (1998).
- [2] G. Strasser, P. Kruck, M. Helm, J.N. Heyman, L. Hvozdar, E. Gornik, *Appl. Phys. Lett.* **71**, 2892 (1997).

# Long wavelength ( $\lambda = 10.5\mu\text{m}$ ) quantum cascade lasers based on photon-assisted tunneling transitions in strong magnetic field

*Stéphane Blaser<sup>1</sup>, Laurent Diehl, Jérôme Faist, and Mattias Beck*  
 Institut de physique, Université de Neuchâtel

## ABSTRACT

The studies on quantum cascade laser based on a photon-assisted tunneling ('diagonal') transition at  $10.5\mu\text{m}$  in strong magnetic field will be presented<sup>2</sup>. The performances of these lasers are a small threshold current at low temperature ( $1.4 \text{ kA/cm}^2$ ), an optical power up to  $45 \text{ mW}$  at  $80\text{K}$  and a lasing operation obtained up to  $200\text{K}$ . The insert of the figure 1 shows the band diagram of two periods of the structure.

A strong magnetic field ( $B$ ) was applied parallel to the layers on this structure. The effect of such a field on diagonal transitions is to shift the dispersion curves of the electronic states by  $k = \frac{eB\langle z \rangle}{\hbar}$  (see insert of fig.1). All the transition parameters are then modified by the applied magnetic field. Our luminescence spectra taken on non-lasing structures show at a constant bias, a strong decrease, a broadening and a blue-shift of the luminescence peak (see fig. 1). In contrast, besides the broadening, a one-particle model predicts a red shift of the emission.

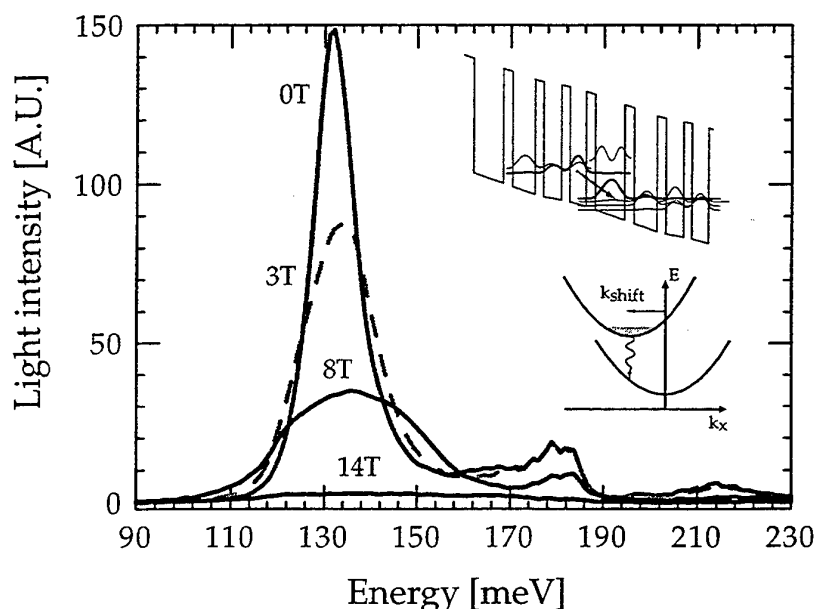


Fig. 1: Luminescence spectra versus applied magnetic field. The two inserts show respectively two periods of the band diagram structure and a scheme of the  $k$ -shift of the dispersion curve due to the field.

Studies in perpendicular magnetic field will also be discussed.

<sup>1</sup> E-mail: [Stephane.Blaser@iph.unine.ch](mailto:Stephane.Blaser@iph.unine.ch), phone: ++41 32 7182949, fax: ++41 32 7182901

<sup>2</sup> Faist *et al.*, Nature **387**, 777 (1997)

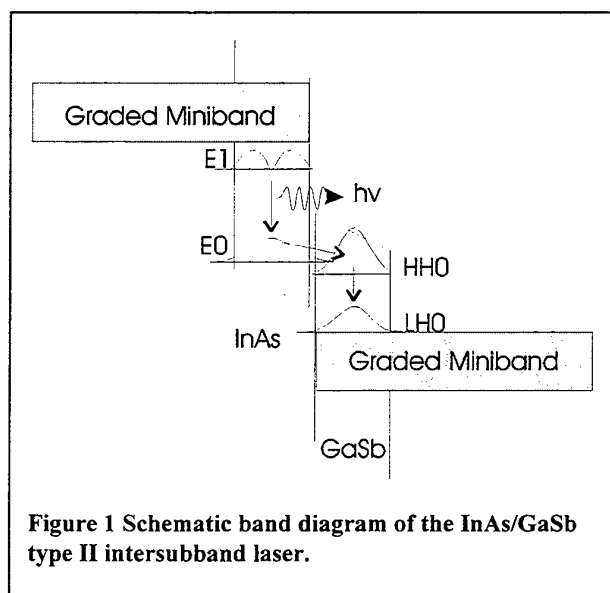


## Designs for a Quantum Cascade Laser using interband carrier extraction.

V.J.Hales, A.J.L. Poulter and R.J.Nicholas

*Department of Physics, Clarendon Laboratory, Oxford University, Parks Road, Oxford, OX1 3PU, U.K.*

We describe the use of interband coupling in the design of Quantum Cascade laser structures in order to achieve efficient carrier extraction and enhanced tunability. Using the crossed gap alignment in the InAs/GaSb system should make it possible to achieve shorter lifetimes for the lowest level while having a large barrier to tunnelling from the upper state thus generating a longer upper state lifetime. Lasing occurs via a normal intersubband transition within a single InAs layer but the device utilizes interband coupling to quickly remove electrons from the QW ground state by annihilation with holes in the adjacent GaSb layer. We predict that the use of interband coupling and graded miniband transport will produce a device which could operate with relatively few layers per period. The detailed band structure is modelled under high electric field biasing by using eight-band  $k.p$  calculations and the momentum matrix modeling technique.



A typical device might be based on a 10-layer InAs/GaSb superlattice. Charge accumulation occurs due to the thick GaSb barrier layer causing build up in the population of the E1 level illustrated in figure 1. The carriers then relax via intersubband transitions and photon emission into the InAs well ground state. A population inversion is maintained between the two well states by the rapid removal of electrons from  $E_0$ , via interband transitions to  $HH_0$ . The transition is tailored to match LO phonon emission and further shorten the lifetime of carriers in state  $E_0$ . The heavy hole state then rapidly empties as electrons relax into the light hole barrier state,  $LH_0$  which is strongly coupled to the tailored electron miniband. The miniband then functions as both collector and injector regions of the laser.

This structure has two potential advantages over more conventional structures which use either intersubband emission and intraband extraction<sup>1</sup> or interband emission<sup>2</sup>. Firstly the broken gap system allows extraction from the lower well level directly into the adjacent layer without the need for conventional tunnelling, whilst maintaining a larger barrier to inhibit tunnelling from the upper state. Secondly, the energy levels in the active well can be tailored over a wide range of emission wavelengths without substantial leakage of carriers into the adjacent well.

<sup>1</sup> F.Cappasso, Science **246** 553(1994)

<sup>2</sup> R.Q. Yang, Superlatt. and Microstruct. **17** 77 (1995)

## The nature of the electron distribution functions in quantum cascade lasers

P. Harrison

*Institute of Microwaves and Photonics,  
University of Leeds, LS2 9JT,  
United Kingdom*

tel: +44-113 233 2043 fax: +44-113 244 9451

e-mail: p.harrison@ee.leeds.ac.uk

There has been much speculation about the nature of the electron distribution functions in quantum cascade lasers, in particular, '*are they non-equilibrium and if so, to what extent?*'. In order to address this, detailed calculations of the *inter*-subband and *intra*-subband electron-longitudinal phonon and electron-electron scattering rates in the real GaAs/Al<sub>x</sub>Ga<sub>1-x</sub>As device design of Sirtori's [1] are presented. The results suggest that two important conclusions relating to the electron distribution functions in the quantum well subbands can be drawn:

- The electron distributions in both the active region and the injector subbands *are* thermalised, i.e., they *can* be described by Fermi-Dirac distribution functions
- All the electron distributions have the *same* electron temperature

## References

- [1] C. Sirtori, P. Kruck, S. Barbieri, P. Collot, J. Nagle, M. Beck, J. Faist, and U. Oesterle. Gaas/al<sub>x</sub>ga<sub>1-x</sub>as quantum cascade lasers. *Appl. Phys. Lett.*, 73:3486, 1998.

# High-confinement waveguides for mid-IR devices

Petter Holmström

Laboratory of Photonics and Microwave Engineering, Department of Electronics,  
Royal Institute of technology (KTH), S-164 40 Kista, Sweden. E-mail: petterh@ele.kth.se.

It is well established in the literature that the ps relaxation time of carriers in a quantum well should allow very high speeds for intersubband electroabsorptive modulators. However in order to exploit the intrinsic high speed capability, the modulator size need to be compact so that the  $RC$  time constant of the device is minimized. To this end a tight confinement of the optical field is needed for a large overlap with the absorbing wells. Calculations on intersubband electroabsorptive modulators will be pursued further [1].

Here we analyze the use of heavily doped layers as a means to confine light. An efficient confinement can be achieved as a result of the large reduction of refractive index that is present just above the plasma frequency. The waveguide, which we here refer to as a plasma effect waveguide, is formed in the ordinary manner by cladding a relatively high index material with lower index material.

The plasma effect has been used frequently in longer wavelength,  $\lambda \approx 8\text{--}11\text{ }\mu\text{m}$ , quantum cascade lasers, e.g. ref. [2]. In that case a heavily doped layer is placed in the outer parts of a regular slab waveguide to reduce cladding layer thickness but without substantially affecting the confinement. Here we want to investigate possibilities to achieve a tight confinement when low losses are not crucial.

In Fig. 1 the real and imaginary parts,  $n$  and  $k$ , of the refractive index [3] of heavily doped InP is shown. Interestingly, for a given desired index step, the absorption due to plasmon excitation is virtually independent of the wavelength of the light. In fact it is decreasing slightly when the wavelength is decreased. The lower wavelength limit of the plasma effect waveguides (PEWG:s) is thus given by the maximum achievable free carrier concentration. In Sn-doped InP a free carrier concentration of  $3 \times 10^{19}\text{ cm}^{-3}$  using MOCVD has been achieved [4]. This limits the use of PEWG:s to wavelengths above  $4.5\text{ }\mu\text{m}$  in InP. Similar values apply to GaAs.

Another way to achieve a high confinement of the optical field is to use electromagnetic surface waves (surface plasmons) guided by a metal/semiconductor interface. Recently quantum cascade lasers emitting at  $8.0\text{ }\mu\text{m}$  and  $11.4\text{ }\mu\text{m}$  that relies on surface plasmons have been demonstrated [5]. In contrast to the doping waveguide the mode absorption of surface plasmons increases very markedly with reduced wavelength.

The transfer matrix method has been employed to solve for TM polarized modes, relevant for intersubband transitions. The mode overlap with the active layer that can be obtained in a PEWG at a certain waveguide absorption has been compared to surface plasmons at a gold semiconductor interface. The calculations indicate that the PEWG should be favourable for the shorter wavelengths, i.e.  $\lambda \approx 5\text{--}7\text{ }\mu\text{m}$ .

The PEWG and waveguides based on surface plasmons have the common advantage that the refractive index of the active layer becomes relatively unimportant for the optical mode confinement. Thus a higher bandgap material may be used in the active region with the potential benefit of e.g. lower nonparabolicity.

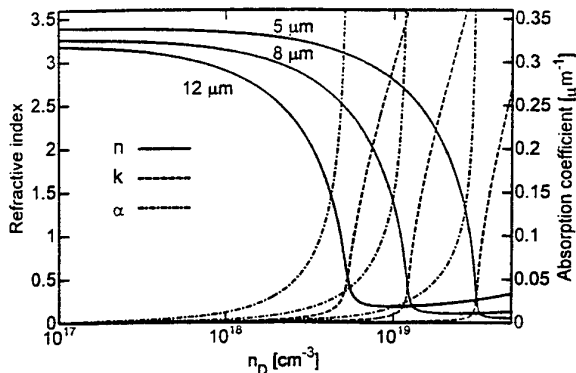


Fig. 1: Calculated real and imaginary part of the refractive index, as well as absorption coefficient of InP as a function of doping density. Results are given for three different wavelengths.

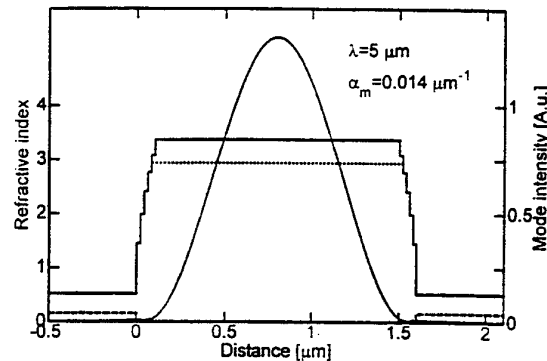


Fig. 2: Mode intensity profile and profile of the refractive indices in an InP plasma effect waveguide.  $\alpha_m$  is the waveguide absorption. Doping levels in the core and cladding layers are  $5 \times 10^{17}\text{ cm}^{-3}$  and  $3 \times 10^{19}\text{ cm}^{-3}$  respectively.

- [1] P. Holmström et al., to be submitted.
- [2] C. Sirtori et al., Appl. Phys. Lett. **66**, 3242 (1995).
- [3] B. Jensen, in *Handbook of optical constants of solids*, edited by E. D. Palik (Academic Press, San Diego, 1985), pp. 169–188.
- [4] C. J. Pinzone et al., J. Appl. Phys. **67**, 6823 (1990).
- [5] C. Sirtori et al., Opt. Lett. **23**, 1366 (1998).

## Waveguide Design Optimization for a Quantum Cascade Laser Emitting at 77 $\mu\text{m}$

**Vinod M. Menon, William D. Goodhue, Aram S. Karakashian**

*Photonics Center & Dept. of Physics and Applied Physics*

*University of Massachusetts Lowell, Lowell, Massachusetts 01854*

**L. R. Ram-Mohan**

*Dept. of Physics and Dept. of Electrical & Computer Engineering*

*Worcester Polytechnic Institute, Worcester, Massachusetts 01609*

We theoretically evaluate the dependence of waveguide design parameters on the performance of a quantum cascade laser (QCL) emitting at 77  $\mu\text{m}$ . A double plasmon enhanced waveguide is used in our GaAs/AlGaAs QCL system. The plasmon enhanced waveguide takes advantage of the decrease in the real part of the index by doping the cladding layers. This decrease in the real part of the index improves the confinement, but doping also increases the imaginary part of the index, which becomes important at these long wavelengths. The effects of the variation of material composition, layer thickness, doping concentration in the layers and the refractive index profile (e.g. graded) on the optical confinement and losses have been studied. These parameters have been optimized so as to obtain maximum optical confinement and minimum loss. Finally, we present an optimized design of the entire QCL structure along with the expected performance characteristics.

## Inter-subband plasmon emission based THz Lasers.

*P. Bakshi and K. Kempa*

*Department of Physics, Boston College, Chestnut Hill, MA 02467, USA*

We have proposed stimulated generation of plasmons (plasma instabilities) as a novel way to generate THz radiation from low dimensional semiconductor systems [1]. The micro-charge oscillations of such plasmons become the source of electromagnetic radiation in the THz range. This plasma instability based concept differs from the conventional lasers, since it is based on a collective phenomenon, in contrast to the single particle nature of the lasers. It is thus less susceptible to disruption due to higher temperatures, and various scattering effects. Also, since the plasmons are created internally and form a (coherent) collective mode of the electron gas itself, there is no need for an external feedback mechanism.

Having explored a variety of systems [1,2], we find that quantum well structures (QWS) operating under bias in a non-equilibrium steady state, with appropriate carrier injection and extraction [3,4], are the best candidates for a realization of this idea. At least three subbands are necessary to generate the plasma instability [2], with the first and third subband well populated and the second nearly empty (or vice-versa). The essential instability mechanism is the resonance of the two, up and down depolarization shifted intersubband plasmons, in such a structure [2].

We have developed a fully self-consistent computational scheme for designing such structures. The eigenstates are determined by the Schroedinger-Poisson scheme, the subband populations by rate balance equations, inter-subband transfer rates through a RPA self-energy calculation, and the injection-extraction rates by the transfer matrix for complex energies. The feasibility of plasma instability for the resulting non-equilibrium steady state is examined for each bias. The I-V curves, and the domains of instability (as a function of bias) are obtained for any structure. Full spectral response is also calculated. Experimental results on first generation structures confirm our predictions of the dynamic conductance vs bias, and (spontaneous) emission frequencies. Population inversion was insufficient to generate plasma instability in these bulk-doped structures. Preliminary experimental results on the newly designed (second-generation) structures show quantitative agreement with our calculation of the current vs bias. Calculations show that sufficient population inversion can be achieved in such structures to obtain plasma instability, and ensuing THz radiation.

1 P. Bakshi and K. Kempa, *Superlattices and Microstructures*, **17**, 363 (1995).

2. P. Bakshi and K. Kempa, *Condensed Matter Theories*, Eds. J. Clark and P. Panat, Nova Science Publishers, New York. vol. **12**, 399 (1997).

3. K. Kempa, P. Bakshi, and E. Gornik, *Phys. Rev. B* **54**, 8231 (1996).

4. K. Kempa, P. Bakshi, C.G. Du, G. Feng, A. Scorupsky, G. Strasser, C. Rauch, K. Unterrainer, and E. Gornik, *J. Appl. Phys.* **85**, 3708 (1999).

## Investigation of electric-field dependent population properties in a GaAs/(Al,Ga)As multiple, asymmetric double quantum well structure by photoluminescence spectroscopy

L. Schrottke, R. Hey, and H.T. Grahn

*Paul-Drude-Institut für Festkörperelektronik, Hausvogteiplatz 5-7, D-10117 Berlin, Germany*

*e-mail: lutz@pdi-berlin.de, phone: +49-30-20 377 339, fax: +49-30-20 377 515*

A multiple, asymmetric GaAs/(Al,Ga)As double quantum well representing a simplified version of the active region of a quantum cascade laser (QCL) is studied by photoluminescence (PL) spectroscopy. In this contribution, we discuss how PL spectra measured as a function of the applied electric field can be used to investigate the electronic transport properties as well as to measure the population of subband states in a QCL-related structure by means of a simple and reliable experimental technique. Since the creation of electrons *and* holes by photoexcitation is not compatible with the unipolar character of the QCL, the investigation focuses on the anti-Stokes PL signal of the narrower well, which is observed for excitation between the excitonic states of the two quantum wells and for sufficiently high electric fields. Furthermore, the complicated interplay of electron *and* hole distributions has to be analysed for an interpretation of the electric-field dependence of the PL signals, since the anti-Stokes signal gives direct evidence for transport of both, electrons and holes, through the (Al,Ga)As barriers.

The samples consist of a superlattice structure with a unit cell containing two wells and two barriers, which all have different thicknesses. While the differently thick barriers result in different transfer rates, which are expected to lead to an occupation inhomogeneity or even a possible population inversion between the electronic ground states of adjacent wells, the difference in the well widths leads to different transition energies for the two wells so that the wells following the thick barrier (with respect to the direction of the electric field) can be distinguished from the ones following the thin barrier through their respective PL energy. Due to the asymmetry of the unit cell, forward and reverse bias refer to different injection conditions.

An experimental quantity related to the occupation of the quantum well states, which we determined from the PL spectra, is the ratio  $\rho = I_n / I_w$  of the integrated intensity of the narrower  $I_n$  and wider well  $I_w$ . Within the framework of a simple model, which contains a rate equation system as well as the calculated electron and hole states derived from the solution of the Schrödinger equation in the one-band envelope function approximation, the electric-field dependence of  $\rho$  is discussed. Although this qualitative analysis reveals limits of our simple model, e.g. discrepancies in particular at higher injection currents, it demonstrates that population inversion is possible to achieve even in such a simplified cascade structure.

Pico- and Femto-Second Non-Linear Transmission/Reflectance  
of an Asymmetric Triple Quantum Well Structure

N. Sawaki, H.S. Ahn, K. Mizutani and M. Yamaguchi

Nagoya University, Dept. of Electronics, Chikusa-ku, Nagoya 464-8603, Japan

The electron transfer between GaAs quantum wells through a thin AlGaAs potential barrier is due either to resonant tunneling or phonon assisted tunneling process. In an application of a coupled quantum well structure to electronic or photonic devices, the build up of internal field due to the transfer of electrons between quantum wells will modify the performance/characteristics of the particular device/structure[1,2]. In this paper, we will demonstrate ultra fast optical response of an asymmetric coupled triple-quantum-well (ATQW) by the switching of the subband lineup from off-resonant to resonant state due to the build up of internal field.

An ATQW was prepared by MBE, and has three nominally undoped GaAs quantum wells of different widths ( 7.6, 8.8, and 10.8 nm) which are separated by nominally undoped 2 nm thick  $\text{Al}_{0.3}\text{Ga}_{0.7}\text{As}$  barrier layers. The transmission and reflectance of a laser light from a Ti-sapphire laser (pulse width 50 fs or 2 ps, wavelength 760-830 nm) was measured and analyzed with the pump-probe method at 77K and room temperature.

If the input (pump) pulse excites resonantly the narrowest well, high density electrons and holes are achieved in the narrowest well. The partial tunneling transfer of electrons from the narrowest well to the wider wells, while leaving holes in the original well (which is a slow process due to large effective mass), induces an internal field and the subband lineup in the conduction band is changed from off-resonance to resonance. At the triple resonance, the three ground levels in the conduction band of the ATQW exhibits strong Stark effect, which results in the strong optical non-linearity for the probe laser pulse. The time evolution of the transmission and reflectance were measured at various wavelengths. It was found that the nonlinear behavior is achieved within a few picosecond, which is determined by the tunneling transfer time of electrons between the GaAs quantum wells. The time dependent non-linear behavior suggests that the tunneling transfer is varied from slow (off-resonance) to fast (resonance) process. We will demonstrate that the ATQW can be an optically driven ultra-fast modulator which can be an alternative to the SEED's.

[1] H.S. Ahn, M. Yamaguchi, T. Kidokoro, N. Sawaki; *Semicond. Sci. & Tech.* 12(1997) 722.

[2] H.S. Ahn, M. Yamaguchi, N. Sawaki; *Jpn. J. Appl. Phys.* 37(1998) 45.

## Population inversion and amplification under intersubband transitions of 2D-holes in GaAs/AlGaAs heterostructures

N.A.Bekin, V.N.Shastin

*Institute for Physics of Microstructures of RAS, Russia, 603600, Nizhny Novgorod, GSP-105. E-mail: [shastin@ipm.sci-nnov.ru](mailto:shastin@ipm.sci-nnov.ru), tel: +7 8312 675037, fax: +7 8312 675553*

New sources of stimulated radiation in the mid-infrared spectral region have been already designed [1-2]. They utilize diagonal optical transitions between 2D-electron states in coupled or tripled quantum wells (QWs) in GaAs/AlGaAs and InGaAs/AlGaAs heterostructures. A population inversion in the active regions is achieved due to the nonelastic intersubband relaxation by spontaneously emitted polar optical phonons in the case of strongly nonequidistant electron spectra. The required structure of active levels is formed using two or three QWs separated by thin barriers. Depending on the excitation way there are two types of lasers based on unipolar transitions of 2D-electrons. They are cascade [1] (under current excitation) and fountain [2] (under optical excitation) lasers.

We analyze a possibility to create a unipolar laser based on intersubband transitions between 2D-hole states under optical pumping. Due to the light-hole and heavy-hole mixing the probability of these transitions, as follows from the calculations, are high enough even for normal incident radiation. This fact allows to increase essentially the excitation and the active region efficiency. Moreover, the specific 2D-hole spectra allow to avoid coupled QW structures. The structure simplicity is also a significant advantage and allows a fairly easy control of the heterostructure parameters to adjust stimulated emission to a desired spectral region stretching from the far-infrared to the mid-infrared wavelengths.

The calculation of the hole spectra and matrix elements has been performed for a 6 nm GaAs QW of  $\text{Al}_{0.31}\text{Ga}_{0.69}\text{As} / \text{GaAs}$  heterostructure. The frequencies of transitions (about 10 meV) between the active forth and fifth subbands lay in the long-wave-length region of weak lattice absorption. Under the pumping power of  $20\text{ kBT}/\text{cm}^2$  and the hole concentration of  $10^{11}\text{ cm}^{-2}$  the amplification coefficient is of the order of  $60\text{ cm}^{-1}$ . The estimation of a possible amplification coefficient and high efficiency compared to [2] leads us to a conclusion that p-type heterostructures are promising for the unipolar semiconductor laser design. Note that using Si-based heterostructures instead of the GaAs-based ones can extend sufficiently the frequency range of stimulated emission effects because of weaker lattice absorption.

The work was supported by the INTAS (#97-0856), RFBR (#99-02-17958) and The 1997 Basic and Applied Research Contest for the Young Scientists of RAS (Project #1).

[1] J.Faist, F.Capasso, D.Sivko, C.Sirtori, A.L.Hutchinson, S.N.G.Chu, A.Y.Cho. *Science* **264**, 553 (1994).

[2] O.Gauthier-Lafsy, P.Boucaud, F.H.Julien, S.Sauvage, S.Cabaret, J.-M. Lourtioz, V.Thiery-Mieg, R.Panel. *Appl. Phys.Lett.* **71**, 3619 (1997).



## Intersubband lasing under lateral electron transport in GaAs/AlAs multi-quantum-well heterostructures

V.Ya.Aleshkin, A.A.Andronov, E.V.Demidov

*Institute for Physics of Microstructures RAS, Nizhny Novgorod GSP-105, 603600, Russia,  
e-mail:aleshkin@ipm.sci-nnov.ru*

A new simple universal intersubband laser scheme based on hot electron intervalley transfer in GaAs/AlAs multi-quantum-well (MQW) heterostructure under lateral transport is discussed. The scheme provides IR lasing in a planar Gunn-like diode made of MQW heterostructure. The MQW structure is such that the lowest electron subband of the system is the  $\Gamma$  subband in a GaAs layer, while the lowest subband in the AlAs layer is the  $X_Z$ -valley subband. The  $X_Z$ -valley is situated in the Brillouin zone along the [001] growth direction, and its states interact (admix) with the  $\Gamma$ -valley states at heterointerface [1].

Under a strong lateral electric field the  $\Gamma$ -valley electrons are heated and perform  $\Gamma$ -L, L-X and  $\Gamma$ -X intervalley transfer and finally accumulate at the lowest  $X_Z$ -subband in AlAs layers with a low electron temperature. The accumulation is high due to a low  $X_Z$ - $\Gamma$  return rate through the heterointerface [2], due to small overlapping of wave functions of the  $X_Z$  and  $\Gamma$  subbands. This accumulation produces population inversion in the system. Two population inversions are possible here: the inversion between the lowest  $X_Z$  and  $\Gamma$  subbands and the inversion between the  $\Gamma$ -subbands. The latter can arise due to a preferable transfer from the X subbands in AlAs to the high  $\Gamma$ -subband because of increased overlapping the wave functions for high  $\Gamma$ -subbands. Both inversions can be used for lasing: the optical transition between  $\Gamma$ -subbands has a high oscillator strength, while the optical  $X_Z$  -  $\Gamma$  transition is allowed due to the X- $\Gamma$  wave functions admixture at the interface. The latter is appreciable in a resonant situation when the one from the upper  $\Gamma$  subband is a little bit lower than the  $X_{Z1}$  subband, so that there is an intersection point of these subbands at some momentum [3].

We have carried out a Monte-Carlo simulation of lateral electron transport for two different GaAs/AlAs MQW structures with an electron concentration of  $3 \cdot 10^{11} \text{ cm}^{-2}$  per period. In the first structure consisting of 85 Å GaAs and 17 Å AlAs layers an amplification is possible on  $X_{Z1}$ - $\Gamma_1$  and  $\Gamma_2$  -  $\Gamma_1$  transitions at a wavelength around  $\lambda \approx 9 \text{ }\mu\text{m}$ . For this structure the threshold fields for lasing are 8.5 kV/cm (80 K) and 14 kV/cm (300 K) and the amplification coefficients are  $\sim 200 \text{ cm}^{-1}$  (80 K) and  $\sim 50 \text{ cm}^{-1}$  (300 K). In the second structure consisting of 147 Å GaAs and 23 Å AlAs population inversions arise between the  $\Gamma_3$  -  $\Gamma_2$  and  $X_{Z1}$  -  $\Gamma_2$  subbands with optical transitions at about 15  $\mu\text{m}$  wavelength. In this structure the threshold fields are 5.5 kV/cm (80 K) and 9.5 kV/cm (300 K). The amplification coefficients are  $\sim 200 \text{ cm}^{-1}$  (80 K) and  $100 \text{ cm}^{-1}$  (300 K).

The work was supported by the RFBR (grant 99-17873) and by the Russian Scientific Program "Physics of Solid State Nanostructures (grant 98-02-1098), INTAS-RFBR (grant 95-0615).

1. H.C.Liu Appl.Phys.Lett. **51**, 1019 (1987).
2. V.Ya.Aleshkin, A.A.Adronov JETP Lett. **68**, 78 (1998)
3. V.Ya.Aleshkin, A.A.Andronov, E.V.Demidov Material Science Forum **297-298**, 221 (1999)

# INTRABAND POPULATION INVERSION OF HOT HOLES IN MQW InGaAs/GaAs HETEROSTRUCTURES EXCITED AT LATERAL CHARGE TRANSPORT

V.Aleshkin, A.Andronov, A.Antonov, N.Bekin, A.Gavrilenko, V.Gavrilenko, A.Korotkov, D.Revin  
*Institute for Physics of Microstructures of Russian Academy of Sciences, Nizhny Novgorod, Russia*

E.Uskova, B.Zvonkov, N.Zvonkov

*Physical-Technical Institute of Nizhny Novgorod State University, Russia*

Recently there has been considerable interest to the hot hole effects in strained multi-quantum-well (MQW)  $\text{In}_x\text{Ga}_{1-x}\text{As}/\text{GaAs}$  heterostructures in high lateral electric fields [1-3]. Highly nonequilibrium phenomena were revealed under real space transfer (RST) [4] conditions and the new mechanism of the intraband population inversion and FIR lasing at intersubband transitions was proposed [5,6]. In this paper hot hole distributions were probed by various experimental techniques and the simple experimental criterion for the population inversion was put forward.

$\text{In}_x\text{Ga}_{1-x}\text{As}/\text{GaAs}(001)$  MQW heterostructures under study were  $\delta$ -doped with C or Zn at 50 Å apart from the boundaries of each InGaAs QW. Current-voltage ( $I$ - $V$ ) characteristics exhibit a pronounced saturation at  $T < 150$  K and  $E \geq 1$  kV/cm. In the samples with "shallow" (with respect to the optical phonon energy) QWs the saturation current proved to increase (!) with the rise of the temperature in between 50-150 K thus testifying that the saturation results from RST from QWs to the barrier layers (where the mobility drops drastically due to the increase of the effective mass and to the strong ionized impurity scattering) rather than from the optical phonon scattering. From these data one can estimate the "barrier" hole temperature as low as  $T_b < 50$  K. Moreover from the degree of the saturation it is possible to estimate the ratio of the hole concentrations in barriers and in the QWs  $N_b/N_w \geq 1$  at  $E \approx 2.5$  kV/cm.

The shallow QWs seems to be most suitable for the realization of the population inversion between barrier and well states [5,6]. The key point of the inversion mechanism is the high effective carrier temperature in QWs and the low one in the barriers. The criterion for the inversion can be expressed in the simplest form for the case when not only the well but also barrier states are of 2D nature (that for example can take place if the barrier holes are confined in the selfconsistent Coulomb potential at the  $\delta$ -layers):

$$p = n_b/n_w = (N_b/N_w)(T_w/T_b)(m_w/m_b) > 1 \quad (1)$$

Here  $p$  is case the occupation number ratio of the lowest barrier and well states.

Direct information on the hot hole temperature in QWs was obtained from the measurements of cyclotron resonance (CR) emission at  $\omega = 4.2$  meV (peak sensitivity of n-GaAs detector) and the band gap absorption modulation in high lateral fields. The observed shift of the CR emission line with the hole heating in electric field corresponds to the increase of cyclotron mass  $m_w$  from  $0.12m_0$  up to  $0.19m_0$  [7] due to the strong nonparabolicity of the energy-momentum law. At the same time the investigation of transmittance modulation spectra under applied fields allows to monitor the evolution of hot hole distribution. Both techniques give the high values of hole effective temperature  $T_w$  in between 150-300 K. Substituting in (1) the experimentally obtained figures and the well known hole effective mass in GaAs  $m_b \approx 0.5 m_0$  one readily gets  $p > 1$  that means the realization of the population inversion in real MQW heterostructures. The estimations of the amplification coefficient at transitions between the upper (resonant with hole barrier states) and the lowest hole subbands in QWs (taking into account the Drude absorption by free carriers) give the figure  $\alpha \approx 20 \text{ cm}^{-1}$  at  $\lambda \approx 60 \mu\text{m}$ .

This research was made possible in part by Grants 97-02-16311 from RFBR and from Russian Scientific Programs "Physics of Solid State Nanostructures" (99-1128), "Physics of Microwaves" (3-17), "Fundamental Spectroscopy" (8/02.08), "Leading Scientific Schools" (96-15-96719) and "Integration" (540, 541).

1. V.Ya.Aleshkin, A.A.Andronov, A.V.Antonov *et al.*, *JETP Lett.* **64**, 520 (1996).
2. D.G.Revin, V.Ya.Aleshkin, A.A.Andronov *et al.*, *phys. stat. sol.(b)* **204**, 184 (1997).
3. V.N.Shastin, S.G.Pavlov, A.V.Muravjov *et al.*, *ibid.* **204**, 174 (1997).
4. Z.S.Gribnikov, K.Hess, G.A.Kosinovsky. *J.Appl.Phys.* **77**, 1337 (1995).
5. V.Ya.Aleshkin, A.A.Andronov, A.V.Antonov *et al.*, *ibid.* **204**, 563 (1997).
6. V.Aleshkin, A.Andronov, A.Antonov *et al.*, *Proc. 1997 International Semiconductor Device Research Symposium*, December 10-13, 1997 Charlottesville, USA, p.263.
7. V.Ya.Aleshkin, A.A.Andronov, A.V.Antonov *et al.*, In: *Ultrafast Phenomena in Semiconductors* ed. by S.Asmontas and A.Dargys. "Material Science Forum" (Solid State Physics & Engineering), Trans Tech Publications Ltd, Switzerland, 1999, v.297-298, p.261.

# Nonlinear intersubband optical response of multiple quantum well structures

M. Załuźny and C. Nalewajko

*Institute of Physics, M. Curie-Skłodowska University, 20-031,  
Lublin, pl. M. Curie-Skłodowskiej 1, Poland*

It has been proved, both theoretically and experimentally, that the intersubband optical absorption in single quantum wells and multiple quantum well (MQW) structures decreases as the intensity of incident light is increased [1-4]. In this paper we report the electromagnetic description of the intensity dependent intersubband optical response behavior of MQW structures in the range, where a commonly used slowly varying envelope approximation [3] does not apply. Such a situation is possible at a large angle of incidence of infrared radiation [5]. In our approach a quasi-two-dimensional electron gas in a quantum well is approximated by a 2D conducting sheet having intensity dependent 2D conductivity [4,5,6]. This conductivity describes optical response to the external field i.e., in principle, it can take into account the electron-electron interaction [6]. The electromagnetic field distribution in the structure and appropriate optical coefficients are calculated numerically by iteration method employing the  $2 \times 2$  transfer matrix formalism [5]. The results obtained (using a simple saturation model for the 2D conductivity) demonstrate the possibility of a bistable output of MQW structures.

A great advantage of our approach is that it automatically takes into account the electromagnetic coupling between QWs in the structure and a standing wave effect connected with background phase-matched interferences. Due to this it might be useful for the design of future optical devices based on nonlinear phenomena in MQW structures.

## References

- [1] F.H. Julien *et al.* Appl. Phys. Lett. **53** (1988) 116.
- [2] K. Craig. *et al.* Phys. Rev. Lett. **76** (1996) 2382.
- [3] C. Almoğy and A. Yariv, J. Nonlin. Opt. Phys. Mat. **4** (1995) 401.
- [4] M. Załuźny, Phys. Rev. B **47** (1993) 3995.
- [5] M. Załuźny and C. Nalewajko, Phys. Rev. B **59** (1999) 15 May.
- [6] T. Ando, Z. Phys. B **24** (1976) 219.

# Second-harmonic generation in asymmetric quantum wells:

## The role of many-body effect

V. Bondarenko

*Department of Theoretical Physics,*

*Institute of Physics, National Academy of Sciences of Ukraine,*

*pr. Nauky 46, Kiev, 252650, Ukraine, E-mail:victor@kelifos.physics.auth.gr*

M. Załuźny

*Institute of Physics, M. Curie-Skłodowska University,*

*pl. M. Curie-Skłodowskiej 1,*

*20-031, Lublin, Poland, E-mail:*

*zaluzny@tytan.umcs.lublin.pl*

### ABSTRACT

Recently Heyman *et al.* [1] have shown experimentally that the electron-electron interaction considerably modifies the second harmonic generation (SHG) spectrum (connected with intersubband transitions) in two-level asymmetric QWs. Authors present also an analytical expression for  $\chi^{(2)}(2\omega)$  (unfortunately, without any details).

In this paper we present a detailed derivation of  $\chi^{(2)}(2\omega)$  connected with the SHG in two-level asymmetric QWs. Our approach is based on the time dependent density matrix approximation (TDLDA) (in the nonretarded electric dipole approach) developed in our previous paper [2]. Calculating the effects induced by indirect Coulomb interaction we take into account (in contrast with Heyman *et al.*) a nonlinear dependence of the exchange-correlation potential on the electron density.

Numerical calculations demonstrate that the many-body effect changes not only the position of the peaks but also the value of the peaks. It is established that the nonlinearity of the exchange-correlation potential can strongly impact the peak values of the SHG spectrum. The role of the many-body effect is found to be outstanding when the depolarization and exciton-like shift of the intersubband resonance energy is comparable with the value of the intersubband energy gap. It is realized for the systems whose resonance frequency of pump radiation belongs just to terahertz region.

### References

- [1] J. N. Heyman *et al.*, Phys. Rev. Lett. **72** (1994) 2183.
- [2] M. Załuźny, Phys. Rev. B **51** (1995) 9757.

keywords: intersubband transitions, second harmonic generation

## Subband selective disorder in a quasi-2D system and its effect on the intersubband spectrum

M. Hackenberg, C. Metzner, M. Hofmann and G.H. Döhler

*Institut für Technische Physik, University of Erlangen, Germany*

In a modulation doped quantum well, even if the spacer layer is so thin to cause disorder localization of the carriers, the intersubband line is only weakly affected by the doping induced random potential. As demonstrated in Ref. [1], this insensitivity arises, because electrons in different subbands experience in-plane potential fluctuations with a strong spatial correlation („parallel fluctuations of the subband edges“) and transitions in the localization regime are „vertical in real space“. This intersubband correlation effect can be partly suppressed in systems with spatially indirect intersubband transitions, e.g. in a coupled double-well system (Ref. [2]), where one of the subbands is localized closer to the charged impurities. For a fundamental study of localization effects by intersubband absorption experiments it would be desirable, however, to observe transitions between the „disordered subband“ and an ideal, undisturbed „reference subband“.

Such a situation with „subband selective disorder“ can be realized by inserting a submonolayer of an approximately lattice-matched material (of higher or lower band gap) into the center of a quantum well (at  $z_c$ ). The in-plane atomic clusters formed within this inserted layer act as a random potential with finite lateral correlation length, but can in growth direction  $z$  be modelled by a delta-function at  $z_c$  (contact potential). They thus exert a strong influence on the ground subband ( $i=0$ ). Since the first excited subband ( $i=1$ ) in an un-biased (symmetric) quantum well has a node at the well center, electrons in this subband are not affected by the disorder. For the same reason there is no 0-1-intersubband scattering.

We have analyzed the above situation in a detailed numerical study, considering the case of a repulsive AlAs-submonolayer inserted into an remotely doped GaAs-AlGaAs quantum well. The well was assumed to be embedded into the intrinsic part of a p-i-n-structure, so that an electric field can be applied in growth direction. The cluster distribution within the inserted layer has been generated by a Monte-Carlo simulation and the resulting localized quantum states of the ground subband were calculated by direct diagonalization of the single-particle hamiltonian. Optical transitions between the disordered  $i=0$  states and the (plane wave like)  $i=1$  states have then been calculated by Fermi's Golden Rule. „Far-field“ intersubband spectra were finally obtained by averaging over many cluster distributions.

We find a very broad 0-1 absorption line, due to the complete break-down of the intersubband correlations. For a given statistics of the cluster distribution, the spectrum depends in a characteristic way on the electron density in the well, because the first electrons localize in the „void“ areas of the inserted AlAs layer as long as possible and only later occupy the repulsive AlAs clusters. Drastic changes of the spectrum occur with the application of an electric field, which shifts the node of the 1-subband away from the well center. Now, both subbands experience the disorder to a relative degree which can be controlled by the field strength. Our results demonstrate that the above system would be a very promising tool for experiments on electron localization by interface roughness.

Ref1: C. Metzner, M. Hofmann and G.H. Döhler, Phys. Rev. B **58**, 7188 (1998).

Ref2: C. Metzner, C. Steen, M. Hackenberg, M. Hofmann and G.H. Döhler, Paper #42,  
9<sup>th</sup> International Conference on Modulated Semiconductor Structures (MSS9, 1999)

## Absorption of in-plane polarized light in quasi-2D systems enabled by strong potential fluctuations

C. Steen, C. Metzner, M. Hofmann and G.H. Döhler

*Institut für Technische Physik, University of Erlangen, Germany*

Electrons in a 2D system become in-plane localized if the potential fluctuations, created for example by charged impurities, are sufficiently strong. In this regime, where subband index  $i$  and lateral wavevector  $\mathbf{k}$  are no longer good quantum numbers, the physics of optically induced electron transitions changes fundamentally compared to the case of ideal multi-subband systems. While the effect of disorder on the absorption of light polarized in the growth direction ( $\mathbf{z}$ ) is mainly a broadening of the intersubband line, dramatic changes occur for in-plane polarization. In the latter case, optical transitions are forbidden in the ideal system, because simultaneous conservation of energy and in-plane momentum is impossible. With disorder, however, both intra- and inter-subband optical transitions become allowed due to localization and subband mixing.

We have theoretically investigated absorption of far-infrared light in a modulation delta-doped quantum well for both polarization directions in the limit of strong doping disorder (thin spacer layer). The localized quantum states of the multi-subband system have been calculated by direct diagonalization of the hamiltonian, starting from a microscopic random distribution of the impurities in the n-doping layer. On the basis of this realistic single particle states, optical absorption spectra have then been calculated (using Fermi's Golden Rule) as a function of electron density. The spectra have then been averaged over an ensemble of impurity configurations. Static screening effects have been included by the non-linear Thomas-Fermi method (comp. Ref.[1]).

For the z-polarization we find an asymmetrically broadened intersubband line, which is however considerably narrower than the energy width of the potential fluctuations in the electron layer. This can be traced back to the intersubband correlation effect, first published in Ref. [2].

In the case of in-plane localization, a weaker and very broad absorption spectrum is found, which is due to non- $\mathbf{k}$ -conserving intra-subband transitions between electron states localized parallel to the layers. The peak width is here comparable to the broadening of the density of states due to the potential fluctuations. With increasing electron density, when the Fermi level scans through the energy spectrum of the electrons, the intra-subband peak becomes more and more pronounced and its maximum shifts to lower photon energies. This behaviour can be understood by analyzing the  $\mathbf{k}$ -spectrum of the localized electrons at different energies.

Our results demonstrate that valuable information can be obtained about electronic localization in strongly disordered two-dimensional systems with tunable electron density, by a simple measurement of light absorption for both polarization directions.

Ref1: C. Metzner, M. Hofmann and G.H. Döhler, *Superl. and Microstructures* **25**, 239 (1999).

Ref2: C. Metzner, M. Hofmann and G.H. Döhler, *Phys. Rev. B* **58**, 7188 (1998).

# Linewidth and dephasing of Terahertz-frequency collective intersubband excitations in a GaAs/AlGaAs square quantum well

J. B. Williams, M. S. Sherwin

*Physics Dept. and Center for Terahertz Science and Technology, U. C. Santa Barbara*

K. Maranowski, A. C. Gossard

*Materials Dept., U. C. Santa Barbara*

## Abstract:

Terahertz-frequency intersubband (ISB) transitions in semiconductor quantum wells are of interest due to the importance of many body interactions on the ISB relaxation dynamics, and the potential for making devices which operate at THz frequencies. The ISB absorption linewidth is proportional to the dephasing rate of the collective intersubband excitation. In order to examine the dephasing dynamics, we have carried out a detailed measurement of the ISB absorption versus charge density.

We present measurements of the linewidth of ISB transitions in a single 400 Å delta-doped GaAs/AlGaAs square quantum well, with a transition energy of ~10 meV. Separate back- and front-gates allow independent control of charge density ( $0.1$  to  $1e11$  cm<sup>-2</sup>) and DC bias ( $-0.25$  to  $0.05$  mV/Å).

The absorption peak positions are plotted against applied DC field, for several charge densities, in Figure 1. The linewidths (HWHM) are plotted against applied DC field, for the same set of charge densities, in Figure 2. The linewidth exhibits a sharp minimum at zero bias. The linewidth data are asymmetric about zero field, saturating at  $5 - 6$  cm<sup>-1</sup> for negative fields (charge density pushed away from the surface) but rising higher than that for positive fields (charge density pushed toward the surface).

The linewidth will be compared to scattering rates obtained from transport measurements. We will discuss a simple model of the damping of the collective ISB mode due to disorder scattering.

Supported by NSF-DMR, AFOSR, and ONR.

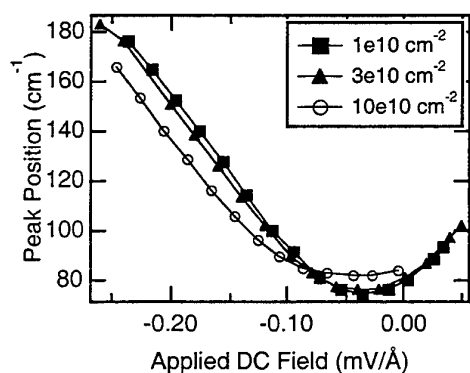


Figure 1. Peak position vs. DC field

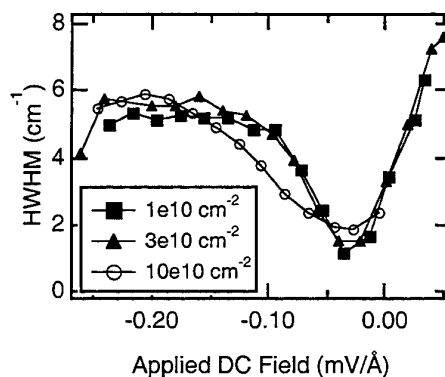


Figure 2. Linewidth (HWHM) vs. DC field

# First-Order Coherent THz Optical Sideband Generation From Asymmetric QW Intersubband Transitions.

C. Phillips<sup>a</sup>, M. Y. Su<sup>b</sup>, J. Ko<sup>c</sup>, L. Coldren<sup>c</sup> and M. S. Sherwin<sup>b</sup>

<sup>a</sup> Physics Department, Imperial College of Science and Technology, London, SW7 2AZ, UK tel +44-171-594 7575/fax 7580, e-mail chris.phillips@ic.ac.uk

<sup>b</sup> Physics department and Center for Terahertz Science and Technology, University of California, Santa Barbara, California 93106

<sup>c</sup> Materials Department, University of California, Santa Barbara, California 93106

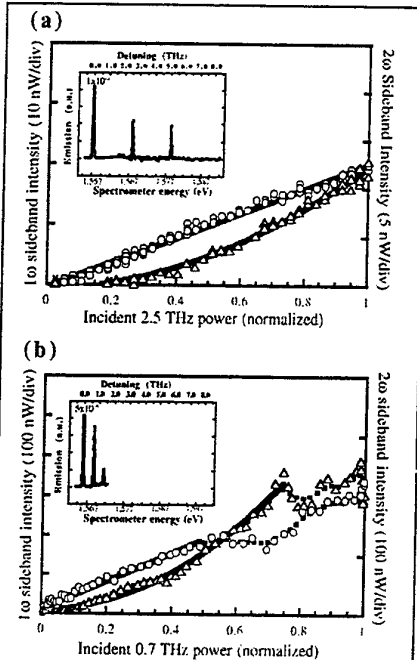


**Fig. 1:** THz power dependence, up to  $\approx 2$  kW, of the  $1\omega$  (circles) and  $2\omega$  (triangles) sideband intensities at 2.5 THz (a) and 0.7 THz (b) frequencies. Solid lines are linear and quadratic fits, characteristic of  $\chi^{(2)}$  and  $\chi^{(3)}$  perturbative processes, which break down at high intensities in the strong-field 0.7 THz case. Dotted lines are a guide to the eye. Insets: Typical sideband spectra.

normally propagating NIR beam, both frequencies chosen close to intersubband and interband QW resonances respectively.

Analysis of the experimental polarization selection rules confirms that the mixing is coherent and involves only virtual excitonic QW transitions.

With  $\omega_{\text{THz}}$  close to the intersubband resonance the NIR spectral and THz power dependence of the sideband generation efficiencies are characteristic of a perturbative process and can be quantitatively modeled with a  $\chi^{(2)}$  excitonic nonlinear susceptibility tensor (Figs. 1a, 2a,b). At low  $\omega_{\text{THz}}$  we find a complex strong-field regime involving a complicated interplay between non-perturbative modification of the QW states and a strong-field THz modulation of the NIR beam (Figs. 1b, 2c).

Experiments mixing THz and near-infrared (NIR) beams, resonant with intra- and interband QW transitions respectively, have recently generated strong optical "sidebands" [1,2] at frequencies  $\omega_{\text{sideband}} = \omega_{\text{NIR}} \pm 2n\omega_{\text{THz}}$ . Both beams propagated normal to the undoped symmetrical QW's. The mixing process was second-order resonant with dipole-allowed QW transitions, yielding a powerful QW spectroscopy tool when the laser frequencies were scanned.

Generating sidebands of all orders however (particularly the potentially efficient first order process) is important for potential applications in ultrafast THz AM and FM optical modulation schemes and would significantly extend the utility of the effect for QW spectroscopy.

Here we achieve this for the first time. We break the dipole-inversion symmetry by using a THz beam propagating in the plane of an asymmetric coupled QW. This mixes with a

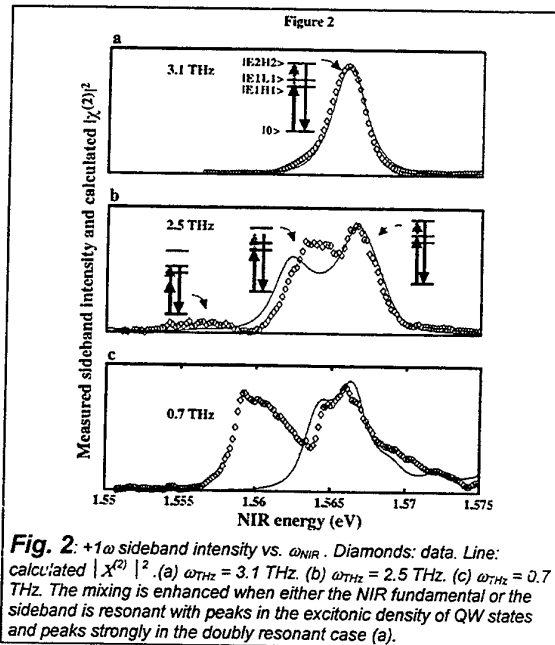


**Fig. 2:**  $+1\omega$  sideband intensity vs.  $\omega_{\text{NIR}}$ . Diamonds: data. Line: calculated  $|\chi^{(2)}|^2$ . (a)  $\omega_{\text{THz}} = 3.1$  THz. (b)  $\omega_{\text{THz}} = 2.5$  THz. (c)  $\omega_{\text{THz}} = 0.7$  THz. The mixing is enhanced when either the NIR fundamental or the sideband is resonant with peaks in the excitonic density of QW states and peaks strongly in the doubly resonant case (a).

[1] J. Kono, M.Y. Su, T. Inoshita, M.S. Sherwin, S.J. Allen, H. Sakaki, Phys. Rev. Lett. **79**, 1758 (1997).

[2] J. Cerne, J. Kono, T. Inoshita, M.S. Sherwin, M. Sundaram, A.C. Gossard, Appl. Phys. Lett., **70**, 3543 (1997).



# THEORETICAL STUDY OF INTERSUBBAND TRANSITIONS IN InAs/GaSb SEMIMETALLIC SUPERLATTICES IN A PARALLEL MAGNETIC FIELD

R. De Meester<sup>°</sup>, F. M. Peeters<sup>°</sup>, A. J. L. Poulter<sup>†</sup>, M. Lakrimi<sup>†</sup>, R. J. Nicholas<sup>†</sup>, N. J. Mason<sup>†</sup> and P. J. Walker<sup>†</sup>

<sup>°</sup>University of Antwerp (UA), Department of Physics, B-2610 Antwerpen.

<sup>†</sup> University of Oxford, Department of Physics, OX1 3PU Oxford, UK.

We have performed theoretical calculations in order to explain the different features visible in the absorption spectra of *InAs/GaSb* semimetallic superlattices. The analysis of the optical absorption of a single quantum well in the single electron approximation was performed and provides a qualitative explanation of the experimental results of A. Poulter *et al*<sup>1</sup> on the parallel magnetic field activated intersubband absorption. The theoretical results are extended to multiple quantum wells, which does not have any effect on the position of the transition peaks, and are generalized to include many electron effects like the dynamic screening of the electrons which leads to a depolarization shift, i.e. up-shift, of the transition energy. Furthermore, band-nonparabolicity has been included in our calculations using a simple two band model as originally derived by Kane<sup>2</sup> and resulting in a down-shift of the transition energy. With these extensions we were able to attain quantitative agreement with experimental results of Ref. 1 for the 30 nm wide sample and a qualitative agreement with the measurements on other samples.

We find, in agreement with the experiment, that there is a different behaviour for the Cyclotron Resonances (CR) in superlattices with wider wells as compared to CR in superlattices with smaller wells. In narrow well superlattices the absorption strength and the transition energy increases slowly with increasing magnetic field and absorption is due to the intersubband transition (IST) from ground state to first excited state. For wider wells there are more levels filled and the transitions at low magnetic fields can still be attributed to an IST. At higher field, this IST is masked by a stronger transition due to the three dimensional behaviour of these wide samples.

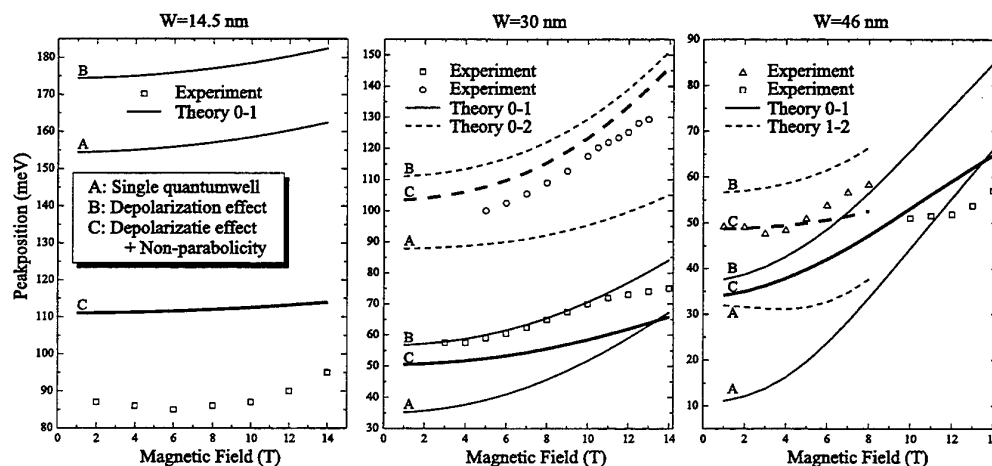


Figure: Theoretical calculated (lines) and experimentally measured (symbols) peak positions for three samples with a different well width ( $W$ ) and for increasing parallel magnetic field. We have plotted three different calculations for each transition. First the results for the single electron calculation (A), next the depolarization effect was added (B) and finally also non-parabolicity was included (C). We show the results from the lowest subband (0) to the first (1) (solid curve) and to the second (2) (dashed curve) subband.

<sup>1</sup>A. J. L. Poulter, M. Lakrimi, R. J. Nicholas, N. J. Mason and P. J. Walker, Phys. Rev B **59**, 10785 (1999)

<sup>2</sup>E. O. Kane, Journ. Chem. Solids **1**, 249 (1957)

# INTERSUBBAND TRANSITIONS IN InGaAs/AlGaAs MULTIPLE QUANTUM WELLS AND THEIR BEHAVIOR UNDER PROTON AND ELECTRON IRRADIATION.

M. O. Manasreh<sup>1</sup>, P. Ballet<sup>2</sup>, J. B Smathers<sup>2</sup>, G. J. Salamo<sup>2</sup>, Chennupati Jagadish<sup>3</sup>, and H. J. von Bardeleben<sup>4</sup>,

<sup>1</sup>Air Force Research Lab (AFRL/VSSS), 3550 Aberdeen Ave, SE, Bldg 426, Kirtland AFB, NM 87117-5776,

<sup>2</sup>Department of Physics, University of Arkansas, Fayetteville, AR 72701,

<sup>3</sup>Department of Electronic Materials Engineering, Research School of Physical Sciences and Engineering, Australian National University, Canberra, ACT 0200, Australia.

<sup>4</sup>Groupe de Physique des Solides, Universites Paris 6 & 7, CNRS, 2, Place Jussieu F-75251 Paris Cedex 05, France.

Intersubband transitions in molecular beam epitaxially grown n-type InGaAs/AlGaAs multiple quantum wells (MQWs) were studied using an optical absorption technique. The measurements were made in the temperature range of 77 – 300 K. The MQWs were designed and grown with either bulk barrier or short period superlattice (SPS) barriers. The wafers were cut into small samples and irradiated with 2 MeV electron and 1 MeV proton beams. The integrated areas of the intersubband transitions were studied as a function of temperature and irradiation doses. It is observed that the integrated areas were degraded faster in samples with SPS barriers as compared to samples with bulk barriers. In heavily proton irradiated samples (dose  $\sim 5.0 \times 10^{14} \text{ cm}^{-2}$ ), the intersubband transition was completely washed out. On the other hand, the intersubband transition was remained observable in electron irradiated samples up to a dose of  $1.0 \times 10^{17} \text{ cm}^{-2}$ . The degradation of the intersubband transition was partially explained in terms of irradiation induced defects. A negative persistent temperature effect (NPTE) was observed for intersubband transitions in heavily irradiated samples. This effect is explained in terms of electrons as being released from traps as the temperature is raised. The recovery of the NPTE occurred at two temperature stages around 150K and 250 K, which indicates that at least two irradiation induced electron traps are present in the samples.

## Thermal relaxation processes in $\text{Si}_{1-x}\text{Ge}_x/\text{Si}$ quantum wells studied by intersubband and inter-valence band optical spectroscopy

B. Adoram<sup>(a)</sup>, D. Krapf<sup>(a)</sup>, M. Levy<sup>(b)</sup>, R. Beserman<sup>(b)</sup>, S. Thomas<sup>(c)</sup>, K. L. Wang<sup>(c)</sup>, J. Shappir<sup>(a)</sup> and A. Sa'ar<sup>(a)</sup>

<sup>(a)</sup> Department of Applied Physics, The Hebrew University of Jerusalem, Jerusalem 91904, Israel

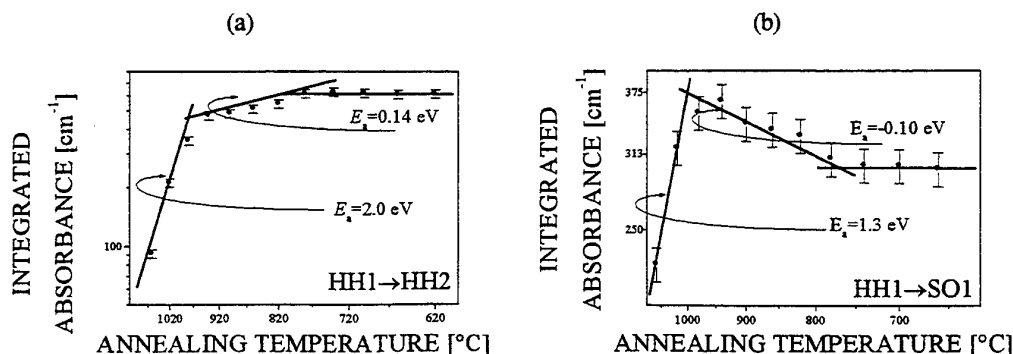
<sup>(b)</sup> Solid State Institute and physics department, The Technion, Haifa 32000, Israel

<sup>(c)</sup> Department of Electrical Engineering, University of California at Los Angeles, CA 90024 USA.

Pseudomorphic p-type silicon-germanium multiple quantum wells, grown on silicon substrates, exhibit optical intersubband and inter-valence band transitions at the mid-infrared wavelengths. These transitions are used to develop quantum well infrared photodetectors (QWIPs) that can monolithically be integrated with the readout circuit using a standard Si based VLSI technology. However, the integration approach requires the use of high-temperature thermal processes for oxidation, diffusion and mobility improvement during the detector fabrication stages.

In this work we present a systematic experimental study of the optical properties associated with intersubband and inter-valence band transitions in  $\text{Si}_{1-x}\text{Ge}_x/\text{Si}$  multiple quantum wells structure under high-temperature thermal treatments. The as grown structure exhibit two type of optical absorption lines: the first obeys the intersubband selection rules and is associated with the  $\text{HH1} \rightarrow \text{HH2}$  heavy hole transition while the second absorption line obeys the inter-valence band selection rules and is associated with the  $\text{HH1} \rightarrow \text{SO1}$  optical transition. After high-temperature furnace annealing in the range 600-1100 °C the infrared absorption spectra were measured and the variation of the optical transitions were recorded.

We observed the presence of two activation processes during the annealing (see Figs (a) and (b) below) that are assigned with strain relaxation and germanium diffusion. The first process, in the temperature range of 750-950 °C, is characterized by an activation energy of 0.1 - 0.14 eV and is positive for the intersubband transition, (i.e., decreasing of the absorption with the increasing temperature) and negative for the inter-valence band transition. The second process, in the temperature range of 950-1100 °C, is characterized by a larger activation energy of about 1.3 - 2.0 eV for both transitions. Raman and PL spectroscopy provide additional support for our interpretation of the activation processes. We propose a qualitative model, based on the Bir-Pikus deformation potential, to explain the above results.



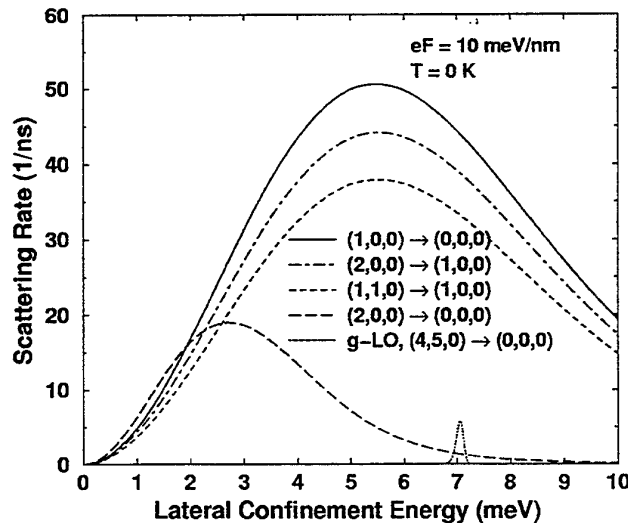
# Electron Relaxation in Silicon Quantum Dots by Acoustic and Optical Phonon Scattering

Manfred Dür and Stephen M. Goodnick

Department of Electrical Engineering, Arizona State University  
Tempe, AZ 85287-5706, USA

The relaxation of electrons in quantum dots (QDs) by means of acoustic and optical phonon scattering has been studied extensively over the past few years. Phonon scattering in zero-dimensional systems controls the decay of carriers to their band minima, which is of critical importance for potential applications in opto-electronic devices. However, most of the theoretical work so far has been devoted to QDs in GaAs. Relatively little has been reported concerning QDs in Si. The recent increased interest in QD structures based on the Si metal-oxide-semiconductor (MOS) technologies requires more thorough understanding of low-dimensional transport mechanisms.

In Si, electron-phonon scattering is more complicated than in GaAs because of its multivalley band structure and ellipsoidal energy surfaces. In the present work, we have generalized the theoretical framework for the description of electron-phonon scattering in Si-based QDs to account for these special features not present in GaAs-based structures. The device, which was fabricated recently [1] and is considered here, consists of an MOS capacitor with  $n$ -type inversion layer on a (100) surface of  $p$ -type Si. The confining potential normal to the Si/SiO<sub>2</sub> interface is modeled by a triangular quantum well. Other than in AlGaAs/GaAs heterojunctions, the quantization of the electronic motion can be controlled by varying the voltage applied to the top electrode. For the confinement in the lateral directions due to depletion gates in close proximity to the interface, we assume parabolic potentials. The interaction of electrons in the dot with bulk-like acoustic and optical phonons is treated within the deformation potential theory. For intravalley transitions, the angular dependence of the deformation potentials is included in the calculation, whereas for intervalley transitions we assume constant deformation potentials. The phonon frequencies are calculated from an adiabatic bond charge model. Results for intravalley and intervalley ( $g$ -process) electron transition rates within the two lowest lying valleys are shown in the figure. The electronic levels are labeled by a triple of integers  $(n_x, n_y, n_z)$ , where  $n_x$  and  $n_y$  denote harmonic oscillator states and  $n_z$  refers to the electric subband.  $F$  is the effective electric field in the inversion layer. These scattering rates have then be implemented in a simple transport model using Monte Carlo techniques to simulate the relaxation of electrons injected into the dot back to the ground state. We find that the relaxation time strongly depends on the confinement both in the normal and lateral directions.



[1] M. Khoury, D. P. Pivin, M. J. Rack, A. D. Gunther, and D. K. Ferry, Nanotechnology, in press.

# Fano Profile in Intersubband Transitions in Self-assembled InAs Quantum Dots

Ph. Lelong, S. -W. Lee, K. Hirakawa, and H. Sakaki

*Institute of Industrial Science, University of Tokyo,  
7-22-1 Roppongi, Minato-ku, Tokyo 106, Japan  
Fax: +81-3-3466-8308, Tel: +81-3-5452-5132  
Email: lelong@quanta.rcast.u-tokyo.ac.jp*

The recent advances in nano-fabrication have allowed us to realize the formation of InAs quantum dots (QDs) by molecular beam epitaxy (MBE) in the Stranski-Krastanov growth mode. By using a large energy separation between the discrete states in the QDs we have recently fabricated an infrared photodetector where the electrons are photoexcited from a bound state in the QDs to the continuum in GaAs quantum well and subsequently drained by modulation-doped lateral two-dimensional channels. An interesting result is obtained in the photocurrent spectrum measured in a normal incidence geometry (figure), which displays a Fano profile: a large peak (centered around 200 meV) accompanied by a well resolved quasi-loss of signal (indicated by the arrows) on both sides. This behavior has been observed for several experimental conditions, which indicates the intrinsic origin of the phenomena. The supposed explanation is based on the fact that the photon promotes one electron from the bound state in the InAs QD up to the GaAs continuum. It is well known in the atoms that the states in the continuum keep the memory of the discrete states, so called „resonance“. A similar behavior should take place in the case of the InAs/GaAs QDs.

To understand the interplay between the discrete state and the continuum we have developed a qualitative approach based on the initial model by Fano. The resonances are considered as a bound states connected with a continuum by an arbitrary coupling term. As for the bound states they interact with both the resonances and the continuum by a second coupling term (electron-photon). By fitting the strength of the couplings we are able to reproduce the shape of the photocurrent spectrum: the loss of signal as well as the peak - the latter corresponding to an enhancement of the intersubband transition probability when both the bound electron + one photon have an energy close to a resonance.

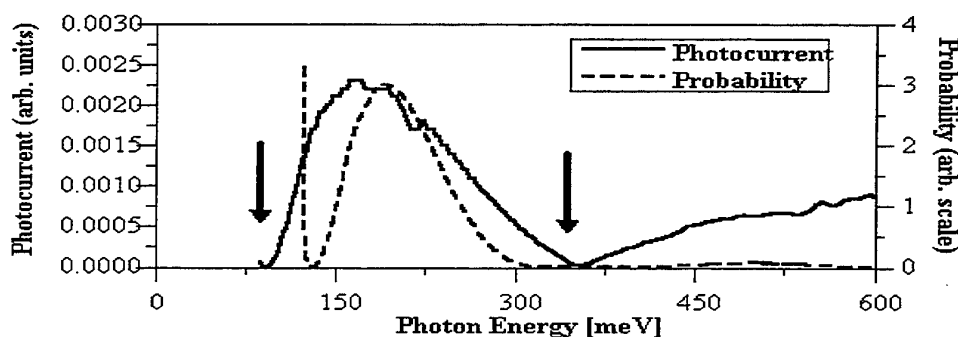


Figure – The photocurrent measured at T=20 K (solid line) and the calculated probability of intersubband transition from the ground state to the continuum states (broken line) versus photon energy (quantum dot: height 1 nm - radius 9 nm).

This feature has also been clearly demonstrated in a direct calculation of the intersubband transition probability from the bound state to the continuum. The photon-electron coupling is treated at the dipolar approximation. The shape of the dot is modeled by a flat cylinder. Within this approximation it becomes possible to calculate analytically both the energy spectrum and the associated probability of intersubband transition. The result is shown in the figure and displays a similar behavior with the experimental data: an enhancement of the probability of intersubband transition at 200 meV. Furthermore, with the same set of parameters, we found a good agreement with the photoluminescence experiment, indicating the accuracy of the present theoretical model.

To conclude we have presented clear experimental and theoretical evidence that the Fano resonances strongly modulate the intersubband transition spectra in the QDs and affect the sensitivity of quantum dot infrared photodetector. We emphasize that a better understanding of this effect is a *sine qua non* condition to improve the efficiency of the photodetection.

## ErAs islands in GaAs for THz applications

Christoph Kadow<sup>1)</sup>, Andrew W. Jackson<sup>1)</sup>, Arthur C. Gossard<sup>1), 2)</sup>, John E. Bowers<sup>2)</sup>  
Shuji Matsuura<sup>3)</sup>, and Geoffrey A. Blake<sup>3)</sup>

<sup>1)</sup> *Materials Department, University of California Santa Barbara, Santa Barbara, CA 93106*

<sup>2)</sup> *Department of Electrical and Computer Engineering, University of California Santa Barbara, Santa Barbara, CA 93106*

<sup>3)</sup> *Division of Geological and Planetary Science, California Institute of Technology, Pasadena, CA 91109*

This paper concerns ErAs islands in GaAs. We report on the growth, pump probe measurements, and sources of THz radiation made from this material.

The material is grown by molecular beam epitaxy (MBE). The initial stages of ErAs growth on GaAs occur in Volmer-Weber growth mode, which results in spontaneous island formation [1]. These islands have sizes on the order of a few nanometer. The samples investigated contain several layers of ErAs islands and thus form a superlattice of ErAs islands and GaAs.

Pump-probe measurements indicate subpicosecond relaxation times for photogenerated carriers in the GaAs as short as 200 fs. The relaxation time depends strongly on the microstructure. In particular the relaxation time increases monotonically with the superlattice period. This is consistent with the ErAs islands acting as capture sites for photogenerated carriers and the relaxation time being determined by the time the carriers need to reach the ErAs islands.

The subpicosecond relaxation times and the high resistivity of the material allows its use as a fast photoconductor. Photomixers [2] were fabricated from this material. These devices are sources of THz radiation, their operation is based on the mixing of two CW diode lasers. The frequency of the THz radiation is given by the difference frequency of the two lasers. Photomixers are therefore tunable THz sources with narrow line width. The photomixers fabricated on ErAs containing material show similar characteristics to devices fabricated on low temperature grown GaAs. They emit approximately 100 nW at 1 THz. The output power starts to roll off at approximately 0.8 THz with 6 dB/octave and with 12 dB/octave at approximately 1.6 THz. This is expected from the relaxation time of the material and the RC time constant of the devices.

The high level of control over the microstructure allows us to engineer the relaxation time and other relevant device parameters, which should lead to improved performance.

- [1] For a review on growth of rare earth arsenides see for example: T. Sands, C.J. Palmstrom, J.P. Harbison, V.G. Keramidis, N. Tabatabaie, T.L. Cheeks, R. Ramesh, and Y. Silverberg, *Mat. Sci. Rpts.* **5** (3), 99 (1990).
- [2] E.R. Brown, K.A. McIntosh, K.B. Nichols, M.J. Manfra, and C.L. Dennis, *Proceedings of the SPIE*, vol. **2145**, 200 (1994).

# Field-induced Delocalization and Zener Breakdown in Semiconductor Superlattices

B. Rosam<sup>\*</sup>, F. Löser, D. Meinhold, V.G. Lyssenko, and K. Leo

*Institut für Angewandte Photophysik, Technische Universität Dresden, 01062 Dresden, Germany*

S. Glutsch and F. Bechstedt

*Institut für Festkörpertheorie und Theoretische Optik, Friedrich-Schiller-Universität Jena,  
07743 Jena, Germany*

K. Köhler

*Fraunhofer-Institut für Angewandte Festkörperphysik, 79108 Freiburg, Germany*

The physics of electrical breakdown in solids has been investigated for many decades due to the basic interest in the physical phenomena involved and due to the important applications. A key contribution was made by Zener who showed that the onset of electrical breakdown is related to the transition of the carriers from one band to higher bands (Zener tunneling). The experimental investigation of these basic transport phenomena has flourished in the last decades by the invention and perfection of the semiconductor superlattices (SLs). Among these results are the observation of the resonant interaction of different bands, the theoretical investigation of Zener breakdown in SLs, and very recently, the observation of inter-valence-band Zener tunneling in transport [1].

Here, we present the first observation of Zener breakdown in the optical spectra of semiconductor superlattices and its detailed theoretical description: In a superlattice with several electron subbands, the Wannier-Stark-ladder breaks down at high bias fields due to coupling of the subband states to the continuum. We show that this is associated with a field-induced delocalization of the wave functions which follows the previously observed Stark localization regime at medium field. The breakdown is associated with a threshold-like increase of oscillator strengths, line widths and a distinct change of the field shift of the transitions.

By using shallow superlattices with only one below-barrier electron subband, we are able to directly address the Zener breakdown in a particularly simple model system: We directly observe effects of intersubband tunneling from a single electron subband to above-barrier subbands. For the same system, we have also investigated the dynamics of the Zener breakdown using time-resolved four-wave mixing. At the breakdown threshold, the dephasing times decrease strongly due to the escape into the continuum.

[1] A. Sibille *et al.*, Phys. Rev. Lett. **80**, 4506 (1998)

---

<sup>\*</sup> rosam@pppns1.phy.tu-dresden.de, Tel.: +49 351 4632464, Fax.: +49 351 4637065

# A Semiconductor Superlattice in Strong Magnetic Fields

T. Bauer, A. B. Hummel and H. G. Roskos

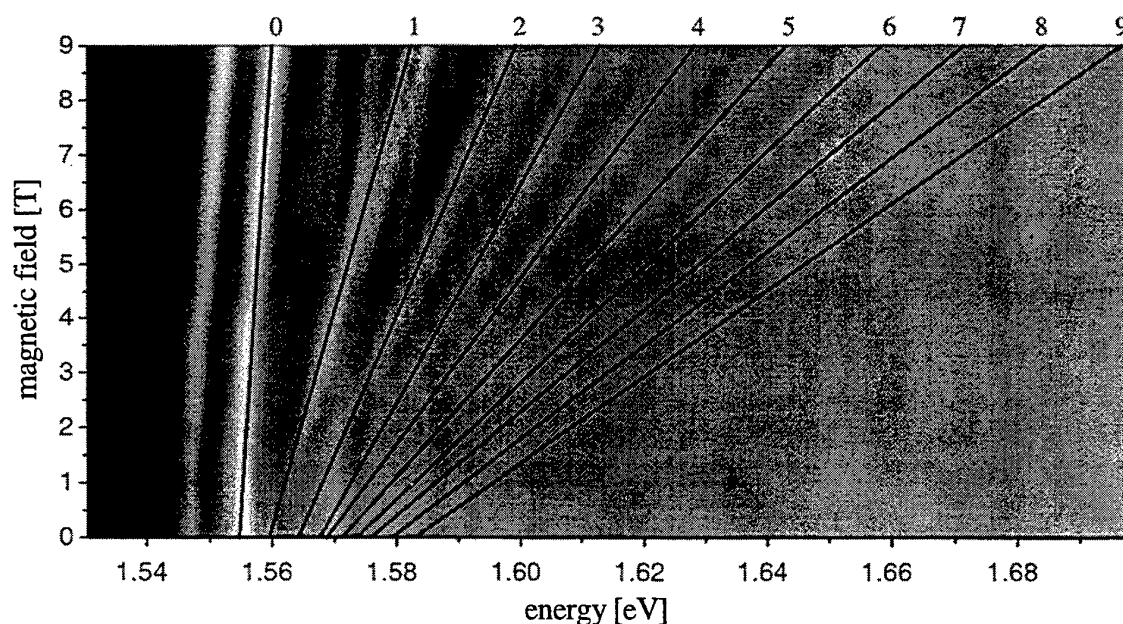
*Physikalisches Institut der J. W. Goethe-Universität, Robert-Mayer-Str. 2-4,  
D-60325 Frankfurt/Main, Germany, phone: +49 (0)69 798 23561, fax: +49 (0)69 798 28448*

K. Köhler

*Fraunhofer-Institut für Festkörperphysik, Tullastr. 72, D-79108 Freiburg, Germany*

The application of strong magnetic fields is known to reduce the dimensionality of the charge carriers in a semiconductor. This leads to the question whether magnetic confinement also reduces the dephasing rate of electronic wavepacket oscillations such as Bloch oscillations in superlattices. In preparation for time-resolved THz-emission measurements in magnetic fields we investigate the influence of a strong magnetic field on the energy levels of a GaAs/Al<sub>0.3</sub>Ga<sub>0.7</sub>As superlattice.

We present photocurrent spectra measured with a superlattice consisting of 35 periods of 17-Å barriers and 97-Å wells with applied magnetic fields in the range of 0 T to 9 T. Electric and magnetic field were chosen to be in the same direction in order to have orthogonal Landau and Wannier-Stark quantization directions. The figure shows the gray-scale encoded spectral structure for an internal electric field of 12 kV/cm. For zero magnetic field, one observes the well-known Wannier-Stark quantization with the spatially direct transition around 1.5531 eV and the spatially indirect -1- and -2-transition 7.7 meV and 6.1 meV below. The magnetic field leads to additional Landau quantization. The Landau fan evolving with increasing field is marked by straight lines. Surprisingly, the spectra are dominated by a single Landau fan instead of one fan for each Wannier-Stark transition. The quality of the spectra is so good that we can resolve many details such as a Landau fan of the second miniband, anticrossing behavior between Landau levels of the heavy-hole and light-hole transitions, and possibly the evolution of forbidden transitions.





## NEGATIVE DIFFERENTIAL RESISTANCE IN A SUPERLATTICE WITH OVERLAPPING MINIBANDS

R. A. Deutschmann, W. Wegscheider, M. Rother, M. Bichler and G. Abstreiter  
Walter Schottky Institute, TUM, Am Coulombwall, 85748 Garching, GERMANY

To date, the main tools for studying Bloch oscillations of electrons in semiconductors have either been nominally undoped superlattices for optical excitation experiments or weakly doped superlattices for transport experiments. We have developed a novel superlattice structure to study the transport of high mobility electrons in an undoped superlattice. In addition the Fermi energy within the superlattice miniband structure can continuously be controlled by a gate. Here we report on transport experiments on a superlattice where two minibands overlap, and compare our results to a superlattice with separate minibands.

Our samples are MBE grown undoped  $156 \times 76 \text{ \AA}$  GaAs /  $20 \text{ \AA}$  AlGaAs superlattices (SLs) sandwiched between two  $n^+$  GaAs contacts grown on a semi-insulating (001) GaAs substrate. After in situ cleavage an AlGaAs spacer and  $n^+$  GaAs gate are grown on the (110) plane, see Fig. 1. By applying a positive gate voltage with respect to the SL contacts a two dimensional electron gas (2DEG) can be induced which resides in the SL. A Kronig-Penney calculation yields a width for the first miniband of 23 meV, which overlaps with a second miniband caused by the first excited energy level in the triangular field effect potential.

In magnetotransport experiments performed in quasi four probe geometry at liquid Helium temperatures we observe clear Shubnikov-de Haas oscillations, with which we establish a relation between gate voltage and electron density in the SL. DC transport experiments reveal negative differential resistance (NDR) in the source-drain current at low electron densities, and a quenching and reappearance of NDR at medium and high densities, respectively, see Fig. 2. This is in clear contrast to a similar sample with a 4 meV miniband separated from the second miniband by about 10 meV, where no quenching of NDR is observed. Quenching of NDR occurs when the Fermi energy crosses both minibands simultaneously.

Fig. 1

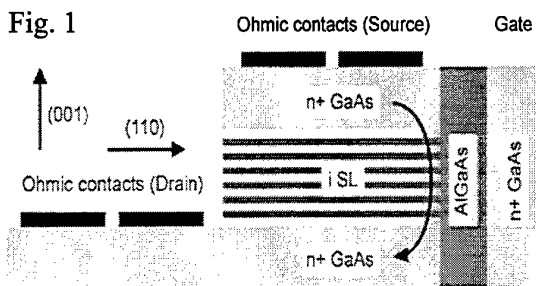


Fig. 1: Sample geometry (not to scale). Current is passed from source to drain in the undoped SL at the interface between the SL and the AlGaAs spacer layer. The electron density can be controlled by the gate voltage.

Fig. 2

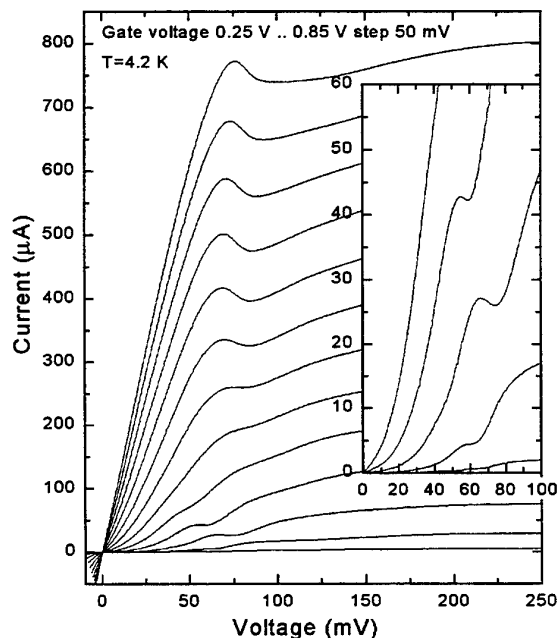


Fig. 2: Source-drain current vs. source-drain voltage relation for different electron densities in a sample with overlapping minibands. For gate voltages below 400 mV and above 600 mV negative differential resistance is observed, in between NDR is quenched.

## Dynamics of electric field domain walls in semiconductor superlattices

David Sánchez<sup>1</sup>, Miguel Moscoso<sup>2</sup>, Luis L. Bonilla<sup>2</sup>, Gloria Platero<sup>1</sup> and Ramón Aguado<sup>1</sup>

<sup>1</sup>*Instituto de Ciencia de Materiales (CSIC), Cantoblanco, 28049 Madrid, Spain*

<sup>2</sup>*Escuela Politécnica Superior, Universidad Carlos III de Madrid, Avenida de la Universidad 20,  
28911 Leganés, Spain.*

Vertical transport in weakly coupled semiconductor doped superlattices (SLs) has been shown to exhibit electric field domain formation, multistability, self-sustained current oscillations and driven and undriven chaos. Stationary electric field domains appear in voltage biased SLs if the doping is large enough. When the carrier density is below a critical value, self-sustained oscillations of the current may appear, due to the dynamics of the domain wall (which is a charge monopole accumulation layer) separating the electric field domains. This domain wall moves through the structure and is periodically recycled. The frequencies of the oscillations depend on the applied bias and range from the kHz to the GHz regime. We have studied the self-sustained oscillations of the current in SLs whose main mechanism is sequential tunneling. Our simulations show self-sustained oscillations of the current and current spikes reflecting the motion of the domain wall as observed experimentally. Furthermore, when contact doping is diminished, we predict a crossover from monopole to dipole self-oscillations resembling those in the Gunn effect. Experimentally, only the monopole oscillations have been observed, for the contacts doping is usually set to values which are too high. The dipole-like oscillations could be observed constructing samples with lower doping at the contacts. In fact, as the doping of the contacts is reduced, we predict current oscillations due to dipole charge waves. The crossover between both types of self-oscillations occurs. Indeed, our results show for first time that there is an intermediate range of contact doping and a certain interval of external dc voltage for which monopole and dipole self-oscillations with different frequencies are both stable. Hysteretic phenomena then exist.

## Mechanisms of Absolute Negative Conductivity of Semiconductor Superlattices.

Yu.A.Romanov, Ju.Yu.Romanova, E.V.Demidov

Institute for physics of microstructures of RAS,

603600 Nizni Novgorod GSP-105 Russia

fax: (8312)675553, tel.: (8312)675037, E-mail: romanov@ipm.sci-nnov.ru

Absolute negative conductivity (ANC) of semiconductor superlattices (SL) was predicted in [1] and studied in detail in [2]. It was only 20 years later that it was verified by experiment [3]. It became necessary to revise and clarify some statements in the theory of the effect. In [1,2] these issues have not been given due consideration. The ANC theory proposed in [3], which is based on the model of a sequential resonance tunneling of electrons between neighboring quantum wells and the "analogy" with the nonstationary Josephson effect, is unsatisfactory. It does not explain appearance of ANC in the region of weak static fields and its absence in strong fields, which was observed experimentally [3].

We have shown that ANC in small static fields arises with appearance of electron "super-excited" quasienergy states among which the nonradiative transitions are forbidden. In strong fields ANC arises through resonance scattering of an electron between the quasienergy states irrespective of the miniband collapse. The ANC regions are sensitive to the mechanisms of electron scattering. Therefore the study was carried out for both the one-dimensional and the three-dimensional models of SL, with an analysis of the role played by the optical phonons.

ANC destroy SL transparency. We showed:

1. SL turns into an opaque state without static current with the finite DC-voltage as a result of the destruction of transparency. The field dependence of DC-voltage has hysteresis. The states are resistant to quasi-static oscillations. The stability to high-frequency oscillations depends on the resonant properties of the external circuit.
2. New regions of transparency with nonvanishing static current arise at a given static voltage across the SL. These states are unstable, too.
3. The oscillations of DC-voltage arise in SL which is in a strong external harmonic field. Their frequency can be controlled by the external circuit parameters and electron concentration.
4. In a general case the states in which SL turns under harmonic field are characterized by DC-voltage and nonlinear plasma or relaxation oscillations. The dissipative chaos occurs in a very strong field.

This work was supported by the INTAS-RFBR (grant 95-615) and by Russian Scientific Program "Physics of Solid State Nanostructures" (grant 99-1129).

1. A.A.Ignatov, Yu.A.Romanov Phys.Stat.Sol.(B), **73**, 327 (1976).
  2. Yu.A.Romanov, V.P.Bovin, L.K.Orlov Fiz.Tekh.Poluprovodn., **12**, 1885 (1978).
  3. R.J.Keay, S.Zeuner at al. Phys.Rev.Lett., **75**, 4102 (1995).
- K. Unterrainer, R.J.Keay at al. Phys.Rev.Lett., **76**, 2973 (1996).



## **BRUKER FT-IR:**

### **The Complete Spectrometer Line**

#### **VECTOR 22/33**

Compact, robust and affordable FT-IR spectrometers for "routine" analytical applications without compromising performance and reliability. The intuitive OPUS/IR software package provides an easy "push-button" approach to FT-IR. VECTOR 33 offers easy range change.

#### **EQUINOX 55**

FT-IR spectrometers for demanding analytical applications with optional automatic sample changers, IR-microscope, and hyphenated techniques such as GC/LC/TGA-IR.

#### **IFS 66/S, IFS 66v/S**

For challenging problems in R+D. Ultra fast and step scanning techniques for kinetic experiments. Expandable to the far IR as well as to the UV regions. For optimized performance in the FIR available as a vacuum version.

#### **VECTOR 22/N**

A series of FT-NIR spectrometers for rapid and reliable QA/QC work and for process monitoring. A wide range of fibre optic probes and sampling accessories is available.

#### **IFS 120 HR**

Highest resolution (better than  $0.001 \text{ cm}^{-1}$ ) research spectrometer for the complete spectral range from the far-IR to the UV. The IFS 120 M is designed for mobile applications.

#### **RFS 100/S**

Stand-alone FT-Raman spectrometer for fluorescence-free Raman measurements. Ramanscope for micro-sample analysis additionally available. FRA 106/S FT-Raman module for BRUKER research line FT-IR spectrometers.



#### **BRUKER OPTIK GMBH**

Wikingenstr. 13, D-76189 Karlsruhe, Germany  
Tel. (0721) 95 28-0 - Fax (0721) 95 28-712  
E-mail: [optik@bruker.de](mailto:optik@bruker.de)